

ABSTRACT

DOERING, JONATHAN ADAM. Understanding Musculoskeletal Changes with Age: Stiffness in Muscle-Tendon Units and Cellular Crosstalk. (Under the direction of Drs. Gregory S. Sawicki and Jacqueline Cole-Husseini).

The overall goals of the four studies presented herein are 1) to identify how the stiffnesses that govern the mechanical behavior of the muscle-tendon unit (MTU) during locomotion shift during aging and 2) to investigate how these stiffness changes arise at the cellular level and how these cellular changes can be affected by crosstalk between muscle and bone. These studies were performed using computational and experimental models of vertical hopping, in conjunction with *in vitro* studies.

In Chapter 1, the current state of the literature describing the stiffness changes attributed to aging in bone, muscle, and tendon is addressed. In Chapter 2, we used a previously described Hill-type model to sweep a 2D parameter space of muscle and tendon stiffnesses centered on a “typical” stiffness for a healthy young human. Results from the study suggest that tendon stiffness governs more of the function of the entire muscle-tendon unit (MTU) than does muscle stiffness. We hypothesize that aging may induce the observed MTU changes seen in humans in one of two ways: (1) stiffer muscle and tendon, or (2) stiffer muscle but more compliant tendon.

Studies investigating the stiffness changes of muscle-tendon units across age have demonstrated conflicting findings. Therefore, in Chapter 3, we replaced the modeled MTU with a biological one from either a young or old FN344 x BN1 aging rat hybrid and simulated the inertial environments from Chapter 2. We characterized the stiffness utilizing isometric testing, determined the resonant frequency of the MTU, and drove muscle contraction by direct nerve stimulation across a range of frequencies centered on the resonant frequency. We found that, while neither overall MTU stiffness nor muscle and tendon stiffness was not significantly

different between young and old rats, older MTUs tended to have increased muscle stiffness and decreased tendon stiffness. This trade off led to small changes in force, length, velocity, and power output of the muscle. This concludes that the tradeoff of stiffnesses in the MTU provide a robustness of the system to function changes.

While higher-level structural changes are often reported in muscle functional studies, how these changes arise at the cellular level are rarely investigated. In Chapter 4, we optimized a cellular co-culture system to enable experiments that examine the age-related changes in the growth and function of muscle myoblasts and bone osteoblasts. We selected bone due to its proximity to muscle and role in muscle growth and repair. We used a Brown Norway rat model and isolated cells from hindlimb muscles and bones. We tested several growth conditions to determine the one best for promoting both muscle and bone cell growth. Our results demonstrated that, while cell plate coating did not alter cell growth, the culture media altered how the cells grew and differentiated, with muscle and bone cells both preferring their own cell-specific media.

We employed the optimized conditions from Chapter 4 to perform an aging muscle and bone cell co-culture study in Chapter 5, using cells isolated from young and old rat hindlimbs contralateral to the ones used in the muscle function studies in Chapter 3. By characterizing the proliferation, differentiation, and crosstalk between muscle and bone cells, we attempt to determine the source of stiffness changes in aged MTUs. We hypothesized that collagen deposition is altered in old vs. young muscle as a result of insulin-like growth factor 1 (IGF-1) changes that may contribute to the observed aging stiffness changes. However, the results showed little difference in collagen deposition between young and old muscle cells across age.

The outcome of this work provides a framework for more cross-disciplinary studies leading to designs of new clinical interventions.

© Copyright 2018 by Jonathan Adam Doering

All Rights Reserved

Understanding Musculoskeletal Changes with Aging: Stiffness in Muscle-Tendon Units and Cellular Crosstalk

by
Jonathan Adam Doering

A dissertation submitted to the Graduate Faculty of
North Carolina State University
in partial fulfillment of the
requirements for the degree of
Doctor of Philosophy

Biomedical Engineering

Raleigh, North Carolina
2018

APPROVED BY:

Dr. Gregory Sawicki
Committee Co-Chair

Dr. Jacqueline Cole
Committee Co-Chair

Dr. Katherine Saul

Dr. Jason Franz

Dr. Emanuel Azizi
External Member

DEDICATION

I would like to dedicate this work to my friends and family that have continued to support me throughout my graduate studies.

- To my parents, Mark and Gretta, my brothers, Andrew and Bradley, and my sister, Darci, thank you for all your love, support, and inspiration. I could not have walked down this path without you. I love you all so much.
- To Dr. Sawicki, Dr. Cole, the PoWeR lab, and OML lab, thank you for the boundless patience, encouragement, advice, and constructive criticism throughout my graduate studies.
- Finally, to my wife Nikki and son Isaac, the amount of thanks I could give you would fill up more than this document has space. You were the rock on which this project was built. Your love and encouragement has been more than I could have asked, and you continued to have faith in me even when I had none. I love you and cannot wait to see where our journey takes us next.

BIOGRAPHY

I was born in Toronto, Ontario, on August 6th, 1987, and graduated high school in the spring of 2005. For my undergraduate education, I attended Virginia Tech and received a B.S. in Biological Sciences in the spring of 2009. During my undergraduate education, I was driven by the need to help my brother Bradley and his condition of cerebral palsy and initially pursued a medical school path. However, in the summer of 2009 I realized that medicine was not right for me and took some time to find what professional path I should follow. In the summer of 2010 I realized I wanted to better understand muscle disorders which led me to the lab of Dr. Robert Grange at Virginia Tech, working on understanding Duchenne's muscular dystrophy.

In Dr. Grange's lab I had the opportunity to learn basic study design, molecular biology techniques, and small animal handling as I developed my Master's thesis. My work in the lab focused on providing dietary supplements to ameliorate the dystrophic response in Duchenne affected mice. I subsequently earned my Master's in the summer of 2013, and I continued to work in the lab as a research technician while honing my skills.

My work in muscle physiology and biochemistry lead me to the lab of Dr. Greg Sawicki, where I was able to apply these skills to investigate the functional response in young and aged muscle tissue. Furthermore, a joint opportunity to work Dr. Jacqueline Cole led me to investigate how these functional changes may arise at the cellular level, and how these changes could be altered by communication with bone tissue. This work is contained herein.

ACKNOWLEDGMENTS

I would like to acknowledge several individuals for their contributions to the work herein:

- Dr. Gregory Sawicki and Dr. Jacqueline Cole, without whom this work would not have been possible. Thank you for the personal, intellectual, and material support throughout this project.
- Carly Britt, for assisting on the majority of the cellular work presented here. Thank you for the hard work, effort, and support.
- Finally, I would like to thank the current and past members of the Human PoWeR lab and OML lab for their encouragement and advice. I look forward to seeing how your careers develop!

TABLE OF CONTENTS

LIST OF TABLES	vii
LIST OF FIGURES	ix
CHAPTER 1: Understanding Changes in Muscle, Tendon, and Bone Aging Across Scale and Species	1
1.1. Introduction	1
1.2. Bone	2
1.2.1. Bone Cell Differentiation, Communication, and Mechanotransduction	2
1.2.2. Protein and Matrix Changes in Bone	7
1.2.3. Bone Geometry and Functional Changes	9
1.2.4. Measuring Bone Metrics Across Scale and Species	12
1.2.5. Bone Summary	14
1.3. Tendon	15
1.3.1. Tendon Cell Differentiation and Mechanotransduction	15
1.3.2. Protein and Matrix Changes in Tendon	18
1.3.3. Tendon Geometry and Functional Changes	19
1.3.4. Measuring Tendon Metrics Across Scale and Species	22
1.3.5. Tendon Summary	24
1.4. Skeletal Muscle	24
1.4.1. Skeletal Muscle Differentiation, Communication, and Mechanotransduction	24
1.4.2. Protein and Matrix Changes in Muscle	29
1.4.3. Muscle Geometry and Passive Functional Changes	30
1.4.4. Measuring Passive Muscle Metrics Across Scale and Species	33
1.4.5. Muscle Summary	34
1.5. Summary, Conclusions, and Experimental Directions	35
1.6. References	40
CHAPTER 2: Modeling Structural Changes of the Aging Muscle-Tendon Unit During Resonance	51
2.1. Abstract	51
2.2. Introduction	51
2.3. Methods	54
2.3.1. Previous Model Development	54
2.3.2. Current Model Implementation	56
2.3.3. Model Analysis	58
2.4. Results	59
2.4.1. Passive Pluck	59
2.4.2. Flight Phase and Dynamic Responses	60
2.4.3. CE Operating Length and Velocity	61
2.4.4. Mechanical Positive Power Production	62
2.4.5. Metabolic Rate, MTU and CE Apparent Efficiency	64
2.5. Discussion	66
2.5.1. Natural Frequency	66
2.5.2. Force and Power During Dynamic Contractions	66
2.5.3. Metabolic Rate and Apparent Efficiency	67

2.5.4. Application to Aging.....	67
2.6. Conclusions/Future Directions.....	69
2.7. References.....	70

CHAPTER 3: Structural and Functional Changes of Aged Muscle-Tendon Units During Resonance Tuning.....	73
3.1. Abstract.....	73
3.2. Introduction.....	73
3.3. Methods.....	76
3.3.1. Animal Subjects.....	76
3.3.2. Surgical Protocol and Instrumentation.....	76
3.3.3. Determination of Muscle-Tendon Properties.....	77
3.3.4. Determination of Phase and Average Total Power.....	80
3.3.5. Statistical Analysis.....	81
3.4. Results.....	82
3.4.1. Active and Passive Parameters.....	82
3.4.2. Overall System Dynamics.....	83
3.4.3. MTU Peak Force, Phase Dynamics, and Mechanical Power Output.....	84
3.4.4. Operating Length and Velocity.....	85
3.5. Discussion.....	86
3.5.1. MTU Active and Passive Properties with Age.....	86
3.5.2. Overall System Dynamics.....	87
3.5.3. MTU Property Implications During Aging.....	89
3.6. Conclusions.....	92
3.7. References.....	93

CHAPTER 4: Optimizing a Cell Co-Culture System to Understand Bone-Muscle Interactions.....	98
4.1. Abstract.....	98
4.2. Introduction.....	98
4.3. Methods.....	101
4.3.1. Animals and Cell Isolation.....	101
4.3.2. Co-Culture Validation and Optimization.....	102
4.3.3. Viability Analysis.....	104
4.3.4. Differentiation Analysis.....	104
4.3.5. Statistical Analysis.....	104
4.4. Results.....	105
4.4.1. Viability Results.....	105
4.4.2. Differentiation Results.....	106
4.5. Discussion.....	108
4.6. References.....	112

CHAPTER 5: Changes in Cellular Crosstalk Between Skeletal Muscle Myoblasts and Bone Osteoblasts in Aging.....	116
5.1. Abstract.....	116
5.2. Introduction.....	117

5.3. Methods.....	119
5.3.1. Animals and Cell Isolation.....	119
5.3.2. Co-Culture Design	121
5.3.3. Cell Proliferation.....	122
5.3.4. Cell Differentiation	122
5.3.5. Cellular Crosstalk.....	124
5.3.6. Statistical Analysis.....	124
5.4. Results.....	124
5.4.1. Cell Viability.....	124
5.4.2. Collagen and Myosin Expression	124
5.4.3. Mineralization	130
5.4.4. Crosstalk	130
5.5. Discussion	131
5.5.1. Cellular Proliferation	132
5.5.2. Cellular Differentiation.....	132
5.5.3. Cellular Crosstalk.....	134
5.6. Conclusions.....	136
5.7. References.....	138
CHAPTER 6: General Conclusions and Future Directions	142
6.1. Introduction.....	142
6.2. Tissue-Level Functional Outcomes	142
6.3. Cellular Crosstalk Outcomes	144
6.4. Future Directions and Final Thoughts	145
6.5. References.....	147

LIST OF TABLES

CHAPTER 2: Modeling Structural Changes of the Aging Muscle-Tendon Unit During Resonance

Table 1.	Parameter values used in model.....	56
Table 2.	Equations and parameter values used in model implementation	57
Table 3.	Metrics and equations for model analysis.....	59

CHAPTER 3: Structural and Functional Changes of Aged Muscle-Tendon Units During Resonance Tuning

Table 1.	Experimentally derived parameters for young and old rat medial gastrocnemius muscle-tendon units	82
----------	--	----

LIST OF FIGURES

CHAPTER 1: Understanding Muscle, Tendon, and Bone Across Scale and Species

Figure 1. Signaling pathways in bone cells and the effects of aging	5
Figure 2. Structural (left) and material (right) characteristics of whole bone under tensile loading	12
Figure 3. MSC differentiation into tenocytes, and effects on tendon signaling	17
Figure 4. ECM changes between young and old (aged) tendon.....	18
Figure 5. Stress-strain (A), creep (B), stress-relaxation (C), and hysteresis (D) properties of tendon	20
Figure 6. Satellite cell differentiation and propagation in development/injury	26
Figure 7. Muscle hypertrophy pathways, atrophy pathways, and the effects of aging .	27
Figure 8. Stress-strain of skeletal muscle and potential effects of aging	32

CHAPTER 2: Modeling Structural Changes of the Aging Muscle-Tendon Unit During Resonance

Figure 1. Physiological basis (A) for our model and force displacement curves for the PEE (B) and SEE (C).....	55
Figure 2. Passive force response of representative simulations (A), and natural frequency contour (B).....	60
Figure 3. Periodic data for stiffness conditions of (A) Normal, (B) -20% K_{SEE} and K_{PEE} , (C) +20% K_{SEE} and K_{PEE} , (D) -20% K_{SEE} and +20% K_{PEE} , and (E) +20% K_{SEE} and -20% K_{PEE}	61
Figure 4. Normalized CE force length (F-L, A) and -velocity (F-V, B) operating points for representative K_{SEE} and K_{PEE}	62
Figure 5. Average positive power produced in the (A) MTU, (B) CE, and (C) SEE for all simulation stiffness sweeps	63
Figure 6. Average metabolic rate ($J/(s*kg)$)(A), and apparent efficiency of the MTU (B) and CE (C) (contours) versus PEE stiffness (x-axis) and SEE stiffness (y-axis).....	65

CHAPTER 3: Structural and Functional Changes of Aged Muscle-Tendon Units During Resonance Tuning

Figure 1. (A) Schematic of in situ stimulation, (B) Force (i) and displacement (ii) data from a passive pluck condition, and (C) full force (i) and displacement (ii) data representative of the ω_0 condition 80

Figure 2. Averaged dataset across all viable preparations showing (i) mean workloop, (ii) force, (iii) ΔL , (iv) velocity, and (v) mechanical power output for the (A) -20% ω_0 , (B) -10% ω_0 , (C) ω_0 , (D) +10% ω_0 , and (E) +20% ω_0 conditions 83

Figure 3. Mean \pm SE data for (A) normalized peak force, (B) peak force phase, and (A) MTU positive, negative, and net average mechanical power over a cycle of stimulation. 85

Figure 4. Operating length from (A) young and old (B), and operating velocity from young (C) and old (D) averaged across all viable experiments during stimulation..... 86

CHAPTER 4: Optimizing a Cell Co-Culture System to Understand Bone-Muscle Interactions

Figure 1. Experimental design..... 103

Figure 2. AlamarBlue percent reduction in MSCs..... 105

Figure 3. AlamarBlue percent reduction in SCs..... 106

Figure 4. Alizarin Red quantification..... 107

Figure 5. Representative Alizarin Red images of MSCs in mono-culture..... 108

Figure 6. Representative images of SCs..... 108

Figure 7. Preliminary crosstalk data..... 110

CHAPTER 5: Changes in Cellular Crosstalk Between Skeletal Muscle Myoblasts and Bone Osteoblasts in Aging

Figure 1. Study design..... 122

Figure 2. AlamarBlue reduction across differentiation days for different cultures..... 125

Figure 3. Immunocytochemistry analysis of cultured cells..... 128, 129

Figure 4. Alizarin Red solubilization data from fixed cells 130

Figure 5. IGF-1 expression from conditioned media on day 14 131

CHAPTER 1: Understanding Muscle, Tendon, and Bone Aging Across Scale and Species

1.1.Introduction

Aging is a universal, detrimental, and progressive process, characterized by a reduced ability to respond to internal and external stresses and leading to functional losses in tissues throughout the body¹. The rate of this progression is highly variable and may depend on numerous factors, including genetics, disease history, and lifestyle². While the appearance and rate of age-related losses may differ between individuals, all organ systems (nervous, muscular, skeletal, etc.) can be affected. In particular, the relationship between the muscular and skeletal systems in response to aging has been an emerging topic of interest³. In aging, the functions of muscle and bone (i.e., support, locomotion, posture, etc.) are reduced^{4,5}. The functional reductions in these tissues are directly influenced by changes in their structural components (e.g., muscle cross-sectional area, bone mineral density); however, the direct links between specific structural changes in bone, tendon, and muscle and corresponding functional declines are not well understood⁶⁻⁹. Understanding how structural changes arise in the parent tissues may begin to explain these reductions in functional outcomes.

Cellular and molecular events (e.g., signaling cascades, protein synthesis/degradation, etc.) in bone, tendon, and muscle are influenced by a variety of factors. Through mechanotransduction, mechanical loading of tissues induces cellular events¹⁰, such as activation/deactivation of tissue-specific cell types, altered expression of proteins, and tissue remodeling, which commonly effect structural changes in musculoskeletal tissues. In aging, decreased loading and subsequent alteration of mechanotransduction pathways in musculoskeletal tissues are common¹¹, but other factors, such as energy metabolism or diet, will also alter the structural properties of these tissues¹². Regardless of how these structural changes arise, musculoskeletal tissue function declines with aging.

Functional responses in musculoskeletal tissue include several important relationships. From mechanical testing, stress/strain curves in specific tissues highlight the values for important material properties, such as modulus, ultimate stress, and ultimate strain of the tissues^{13,14}. Testing to measure the viscoelastic properties of these tissues, particularly muscle and tendon, can also be performed¹³. In a whole body sense, these tissue-specific responses can have an additive effect, leading to altered ranges of motion or force outputs. Furthermore, altered ranges of motion and forces can lead to higher-level functional changes such as altered gait. In summary, changes at the tissue level can build to changes at the whole body. By understanding the tissue-specific functional changes in aging, researchers can better describe treatments to improve quality of life.

This review focuses on the structural and functional changes of musculoskeletal (bone, tendon, and muscle) tissues with aging, and how these changes may be measured in several human and animal models. First, the cellular changes in aging will be discussed for each tissue and how these cellular changes influence structural properties. Second, the functional characteristics of each tissue, and how they change with aging, will be described. Finally, we will discuss how understanding age-related functional and structural changes for these tissues may inform changes in the function of neighboring tissues.

1.2. Bone

1.2.1. Bone Cell Differentiation, Communication, and Mechanotransduction

Bone is the primary structural component of the body, providing protection to internal organs, storing essential minerals, and allowing for locomotion and load bearing¹⁵. To accomplish these functions, bone exists as a composite material, containing an organic matrix (mostly collagen type I, cells, and water) embedded with inorganic minerals (primarily hydroxyapatite)^{15,16}. The development of bone into this composite material is primarily driven by the cells native to bone: osteoblasts (bone forming cells), osteocytes (mature osteoblasts), and osteoclasts (bone resorbing

cells)¹⁶. Osteoblasts and osteocytes arise from a mesenchymal origin, and osteoblasts synthesize and deposit new matrix in the modeling and remodeling of bone¹⁶. Osteoblasts that become trapped within the matrix during modeling or remodeling become entombed in the bone and transition into osteocytes, responsible for mechanosensing and control of bone remodeling¹⁶. Osteoclasts, on the other hand, arise from a hematopoietic lineage, and are multinucleated cells responsible for removing old or damaged bone¹⁶. Like many cellular events, functions of these cells are highly regulated by a variety of signaling factors. With aging, both the number and function of these cells may be altered.

Like all cells, bone cells have a limited lifespan determined by a plethora of factors, including the number of replications, external signaling changes from other cells, and cellular damage. With increased cellular divisions, the ability of the cells to fully replicate genetic information is reduced, until eventually apoptosis is initiated¹⁷. With aging, many of these cell types progressively reach this apoptotic stage, and new cells are more difficult to produce^{18,19}. This reduces the bone's ability to remodel. In remodeling, osteoclasts resorb bone while osteoblasts place new bone, yet with a reduction in cell number, the amount of bone removed or placed diminishes. This reduction in remodeling ability can begin as early as age 30 in humans and progressively declines throughout the lifespan²⁰. While the number of cells may be restricted by replication cycles limiting subsequent divisions, the signaling events pertaining to these cells may also change, resulting in a compounding effect in bone.

The pathways that control the differentiation, remodeling, and communication between bone cells are wide-ranging and complex; highlighted here are the most-studied pathways pertaining to bone aging. Osteoblast differentiation is regulated by the wingless-type MMTV integration site (Wnt) pathway (Figure 1). For osteoblast differentiation to occur, the Wnt protein binds to protein

receptors on the cell surface, resulting in a signaling cascade that allows β -catenin to translocate to the nucleus and initiate differentiation²¹. In aging, two pathways have been hypothesized that inhibit the Wnt signaling pathway: oxidative stress and reduced Wnt ligand expression. With oxidative stress, reactive oxygen species (ROS) activate transcription factors that sequester β -catenin, thereby inhibiting differentiation²²⁻²⁵. Reduced Wnt expression may arise from a decreased number of Wnt genes, brought on by higher-level signaling changes, or mutations in the gene due to repeated cellular divisions^{26,27}. Reduced Wnt signaling leads to a diminished number of osteoblasts and osteocytes; therefore, the remodeling process is tilted in favor of bone resorption, resulting in the bone loss associated with aging. Animal studies have demonstrated that increased Wnt signaling leads to a protective effect, preventing bone loss^{28,29}.

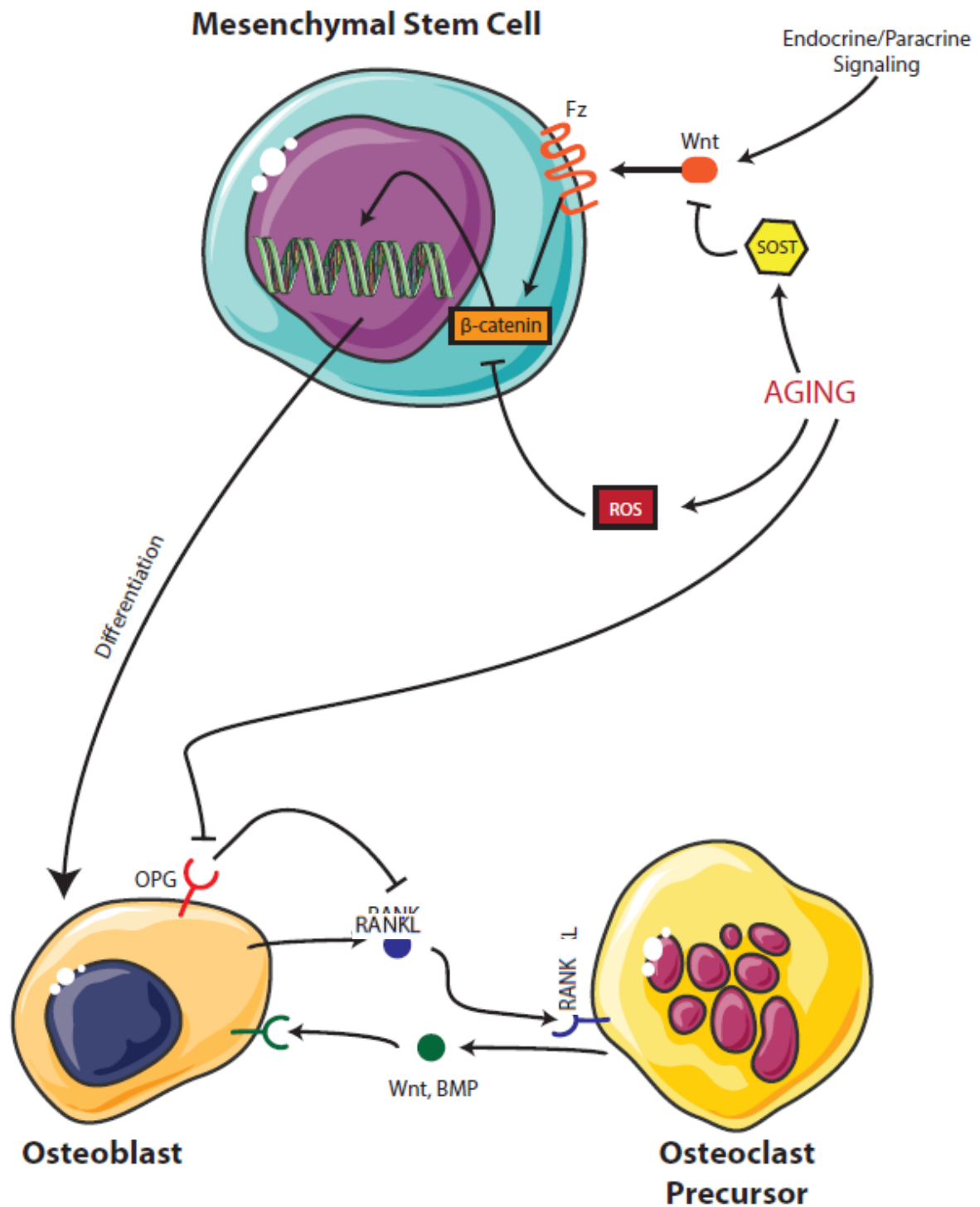


Figure 1. The effects of aging on bone cell signaling pathways. MSCs differentiate into osteoblasts based on binding of Wnt proteins via endocrine/paracrine pathways, which induces β -catenin to translocate to the nucleus and promotes differentiation. Aging hinders this process through increased ROS or sclerostin (SOST) signaling. Once differentiated, bone remodeling can occur through RANK signaling. Bone resorption can occur through expression of the OPG receptor that sequesters RANK. In aging, a decreased number of osteoblasts presents leading to decreased OPG receptors. Bone remodeling then demonstrates increased resorption and decreased new bone production.

The communication between bone cell types may also breakdown in aging. As stated previously, bone remodeling is a tightly coordinated effort between osteoblasts and osteoclasts, governed by communication between them and also with osteocytes, which is critical to the homeostasis and repair of bone. Three types of communication between these cells exist: direct contact, gap junctions, and paracrine signaling pathways^{30,31}. In direct contact (i.e., juxtacrine signaling), membrane-bound proteins between cells can interact with each other to start intracellular cascades. With gap junctions, the osteocytes can allow the passage of small water-soluble molecules between them. However, the most affected communication type with aging is paracrine signaling between osteoblasts and osteoclasts^{30,31}, which is complex and multi-faceted and has been described thoroughly elsewhere^{32,33}. Briefly, osteoblasts and osteocytes secrete receptor activator of nuclear factor kappa-B ligand (RANKL), a differentiation factor for osteoclasts that binds to RANK receptors on the osteoclast membrane³⁴. Osteoclasts are activated to resorb bone, and in turn secrete their own set of paracrine signaling factors that signal osteoblasts to create new bone. Control of this feedback may be accomplished by an antagonistic receptor on osteoblasts, osteoprotegerin (OPG), which also binds RANKL, reducing activation of osteoclasts³⁵. Studies have shown that the number of osteoblasts and osteoclasts is reduced in aging^{18,19}; however, osteocytes can also produce RANKL, further causing differentiation and activation of osteoclasts to break down bone. However, with less OPG available (due to fewer osteoblasts overall), the feedback to inhibit osteoclasts is reduced, and the remodeling process becomes further imbalanced, leaning towards increased bone resorption³⁶. If this is compounded with mechanotransduction pathways present, bone remodeling can be further affected.

Mechanotransduction pathways in bone represent a unique avenue for cellular changes that arise due to loading of the bone. In aging, reduced physical activity is common, reducing the loads

typically observed on the bone³⁷. As a consequence, after osteoclasts are activated by RANKL, the osteoblasts cannot return to normal level bone synthesis, and a reduction of bone mass occurs³³. Many different signaling pathways related to loading may explain this phenomenon, yet one of the most hypothesized explanations for this reduction in osteoblast-related bone synthesis is the sclerostin signaling pathway. Sclerostin is a Wnt antagonist in osteoblasts and is an inhibitor of bone development³⁸. Studies have demonstrated that mechanical loading of bone decreased sclerostin levels while increasing bone mass³⁹. With reduced loading, sclerostin levels are increased, and go on to inhibit the Wnt pathway for osteoblast differentiation and activation⁴⁰. In summary, aging can cause a reduction in the amount of bone-specific cell types while simultaneously reducing the communication effectiveness between these cell types. Furthermore, lifestyle choices (e.g., reduced activity) have a compounding effect on bone's ability to remodel. While cellular activation and communication is important for remodeling, the changes of the bone matrix with aging have not been discussed.

1.2.2. Protein and Matrix Changes in Bone

Bone is a composite material, containing both inorganic and organic components. The inorganic component of bone consists of minerals, primarily hydroxyapatite. The organic matrix component of bone contains primarily collagen type I with a small amount of non-collagenous proteins²⁰. The collagen provides flexibility and resistance to tensile forces of bone, while the mineral provides resistance to compression forces. With aging, the organic component and the production of its associated matrix changes the most. Collagen type I, the primary aspect of the organic matrix, is secreted by osteoblasts during bone remodeling²⁰. Collagen production by osteoblasts can be modified by a variety of different pathways; however, one pathway under intense investigation is the insulin-like growth factor 1 (IGF-1) pathway.

IGF-1 is an important growth and differentiation factor that is secreted and expressed by many tissues. In bone specifically, growth is modulated by IGF-1 through endocrine, paracrine, and autocrine signaling, and can be secreted by all bone cells⁴¹. IGF-1 binds to IGF-1 receptor (IGF-1R), which leads to a signaling cascade with a wide variety of end results including: alterations in Wnt signaling, increased glucose uptake, altered cellular metabolism, and increased bone growth^{41,42}. Knockout studies in mice have demonstrated that in osteoblasts, when IGF-1 is not produced, less collagen I is produced, reducing the amount of bone formation^{43,44}. Alternatively, increasing IGF-1 results in increased long bone growth and cortical bone width, suggesting increased activation of osteoblasts and collagen I secretion⁴⁴. IGF-1 effects on osteoclasts and osteocytes have not been well studied, yet those that have been performed suggest that IGF-1 knockout leads to decreased osteoclast numbers and a reduced ability of osteocytes to signal remodeling⁴⁵. In aging, IGF-1 levels are reduced⁴⁶, and therefore bone formation is reduced. Combined with cellular communication events discussed previously, the remodeling process is further pushed toward resorption. While IGF-1 plays an important role in collagen I synthesis and deposition, the aging process can also adversely affect the collagen structure within bone.

Collagen in bone is first synthesized within osteoblasts as pro-collagen fibrils, which are then secreted and further modified so that the collagen fibrils can aggregate into a triple-helical fibril⁴⁷. The triple-helical fibrils associate to form larger fibrils and then fibers⁴⁷. Collagen fibrils are further stabilized by the formation of crosslinks, which provide the greatest impact on the strength and toughness of the collagen. In aging, the number and type of collagen crosslinks change. Typical crosslinks are formed enzymatically, where the end regions (N- and C-terminus) of one collagen molecule binds to the helical region of another⁴⁸. As aging proceeds, crosslinks are then formed instead by connecting both terminal regions and a helical region, which increases the

stiffness of the collagen⁴⁸. Additionally, aging introduces nonenzymatic crosslinks, where advanced glycation end-products (AGEs) increase and allow the collagen to resist turnover and fibers to persist longer⁴⁷. Studies have demonstrated that nonenzymatic crosslinking increases with age, while enzymatic crosslinking decreases⁴⁹. Popular hypotheses suggest that this change in crosslink type may be a protective effect in response to decreased collagen production with aging⁴⁷. These nonenzymatic crosslinks would then allow collagen to remain longer without degrading (since new collagen production would be decreased); however, while the stiffness of collagen increases, the strength and toughness of bone may decrease. Collagen orientation can also change with aging, where the changes in crosslinking cause the orientation to become more aligned in a singular direction, which will also alter mineralization.

The primary mineral found in bone, hydroxyapatite, exists as a mineral crystal that can vary in size with age. Studies in humans have shown that bone mineral crystal size increases with age for the first few decades of life (20-30 years) and progressively decreases afterward⁵⁰. Additionally, the amount of carbonate (as a measure of substitution in hydroxyapatite) was increased after 30 years of age⁵⁰. Other studies have also established that due to the sizes of the mineralized crystals and collagen orientation, the mineral density of young bone is less dense than that of older bone, but these changes seem to vary across species and bone type²⁰. Nevertheless, signaling changes exist within bone in aging, and these signaling changes contribute to overall changes in the structural components of bone, such as collagen crosslinking, mineral deposition, and bone mass, that negatively impact the overall load-bearing function of bone.

1.2.3. Bone Geometry and Functional Changes

As the matrix of bone is laid down, and mineralization occurs, bone begins to take its characteristic geometric shape depending on the location in the body. In aging, larger bones such as the long bones are often investigated. The long bones have compact cortical bone along the

diaphysis and porous cancellous bone in the metaphysis and epiphysis. The morphology of bone can change in accordance with Wolff's law: as load is altered, the bone adapts to facilitate that load⁵¹. This functional adaptation occurs in many cases, including exercise, limb disuse, and spaceflight, as well as direct loading in animal models. During aging, both cortical and cancellous bone experience morphological changes in response to decreased loading. In mice, cortical bone size, trabecular bone volume, and bone strength declines after as early as 12 months of age⁵². In rat aging studies, the long bones experience cortical thinning, as well as decreased trabecular bone volume fraction, trabecular thickness, and mineral density in the metaphysis^{53,54}. Furthermore, murine hindlimb suspension models (as an analog of disuse) demonstrated similar age-related declines in bone metrics⁵⁵. In human studies, while more difficult to determine (see section 2.4), demonstrate patterns to those seen in animal models with cortical thinning and decreases in trabecular number and bone volume fraction⁵⁶. In general across studies, the cross-sectional area of the bone decreases, cortical bone mass decreases, and trabecular bone has a less robust architecture. Just as changes in the cellular response can lead to changes in the bone geometry, changes in the geometry can then alter the functional response of the bone.

Bone is typically characterized by the loads that are applied during activities of daily living (e.g., walking, running). These activities place loads on the bones that are complex in nature, and combinations of simpler loading modes: axial loading (tension or compression), bending, and torsion (twisting)¹⁴. For each of these loading types, specific mechanical testing can determine the bone strength and stiffness. When a monotonically increasing load is applied in one of the three loading modes until the bone breaks, the bone progressively deforms. This load-deformation behavior is characterized by an initial linear (elastic) region, followed by the yield point, a nonlinear post-yield region containing the ultimate load and displacement, and then the failure

point at which the bone breaks¹⁴. The slope of the elastic region is the stiffness of bone, and the area under the entire curve is the energy absorbed until failure¹⁴. Aging bone has a greater stiffness, undergoing smaller deformations at each load⁴⁹. In many cases, older bone has a smaller or nonexistent post-yield region and instead fractures at the yield point, demonstrating more brittle behavior. While the whole bone structural properties calculated from the load-displacement curves may change in aging, tissue-level apparent material properties can also demonstrate age-related changes.

The tissue-level material properties are independent of the bone size and shape and are based on mechanical testing of samples with known geometries. With these tests, the load-displacement data can be normalized by geometric measures to produce stress-strain curves. Stress is defined as the load per cross-sectional area, and strain is defined as the change in length (displacement) per initial length¹⁴. Instead of stiffness, the slope of the curve now represents the modulus of elasticity (i.e., Young's modulus)¹⁴. The area under the curve is again the energy absorbed until failure, yet with regards to tissue mechanics is referred to as toughness. In aging, bone experiences an increase in the modulus of elasticity and a decrease in toughness and ultimate stress⁵⁷. These declines contribute to the increased incidence of fracture in aging, particularly with osteoporosis. Understanding how these changes initially arise is of critical importance to developing new treatments. Experimentally determining the factors can be difficult and may require the use of animal models.

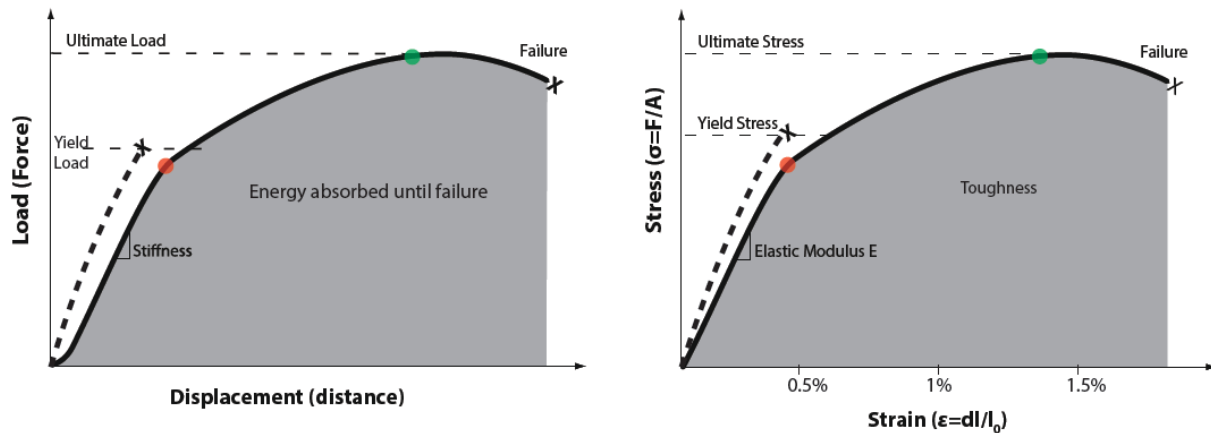


Figure 2. Structural (left) and material (right) characteristics of bone under tensile loading. The structural stiffness and Young's modulus are determined from the linear portion of each curve. The red dot indicates the end of the elastic region and begins the post-yield deformation region. The green dot indicates when the most amount of load or stress is reached. In normal bone, the ultimate stress can reach anywhere between 100 and 150 MPa, and can occur between 1 and 2% strain, with failure occurring shortly thereafter. Aging bone (indicated by the dotted curve in both plots) typically demonstrates increase stiffness and modulus, and can fail as early as the yield load. Very little post-yield deformation is often demonstrated, indicating more brittle bone.

1.2.4. Measuring Bone Metrics Across Scale and Species

Measuring cellular responses and mechanical properties from bone can be difficult to accomplish in humans. Many of the mechanical properties that can be measured in bone require the use of isolated whole bone samples (i.e. removed from the body), which may only be obtained from cadaveric samples. It is from these cadaveric samples that much of our understanding of the bone changes with aging arise. However, measuring changes *in vivo* in humans is more difficult. One measurement technique is the dual energy X-ray absorptiometry (DXA) scan, which is the clinical gold standard for measuring bone mineral density (BMD), the metric used to diagnose osteopenia and osteoporosis⁵⁸. However, DXA scans calculate an areal BMD using projected area in the plane of the scan^{58,59}. Other imaging modalities, such as quantitative computed tomography (QCT), can measure true volumetric BMD, yet the cost, extra radiation, and time required to complete these QCT scans have led to the DXA scan being the most widely used⁶⁰. While these imaging techniques can give insight to bone mass and density, many of the mechanical properties

of bone can only be performed on bone *ex vivo*. Therefore, mechanical properties are performed in cadaveric samples, bone biopsies, or animal models.

While animal bones do not directly represent human bones, high-resolution imaging and mechanical testing of these bone samples provides critical information about general trends for mechanical properties with aging or in response to treatments, and samples are much easier to obtain for a wide range of ages and disease states. Micro-computed tomography (micro-CT), and now even nano-CT, provide detailed volumetric information about bone microstructure and mineralization and their distribution within the bone⁶². However, the X-ray dosing for these systems is high, and scans can only be performed on *ex vivo* samples. *In vivo* micro-CT scanners have a slightly lower dosing (and thus a lower spatial resolution) and can be used for longitudinal measurements in live animals, but they can only accommodate small animals, such as rats and mice. High resolution peripheral computed tomography (HR-pQCT) is a recent technology that enables similar measurements *in vivo* humans, but it is limited to peripheral sites, such as the forearm and tibia, and has a spatial resolution that is about an order of magnitude lower than micro-CT. As imaging technology advances, perhaps clinical CT scanners will become more widely used and replace DXA as the gold standard for assessing bone health. However, much is still unknown about how these structural changes arise at the cellular level, which cannot be measured with these techniques.

Cellular techniques are wide-ranging and well developed. In bone, mesenchymal stem cells or hematopoietic stem cells can be harvested from bone marrow and cultured to maturation to give rise to osteoblasts and osteoclasts. From these cultured cells, morphology can be assessed using microscopy, with or without staining to aid visualization. Expression profiles for certain signaling and growth factors, such as Wnt, RANKL, or IGF-1⁶³, can be determined from cultured cells from

conditioned media using enzyme-linked immunosorbent assay (ELISA) techniques. Staining protocols on these cells can also demonstrate where signaling proteins may be localized or the amount of metabolic activity of the cells. Additionally, gene expression of the respective signaling proteins can be measured using quantitative real-time polymerase chain reaction (qRT-PCR). At the tissue level, bone can be demineralized, sectioned, and stained to examine how the cells organize in their native structure. Similarly, staining protocols can also be performed on these sections to determine similar metrics as described for cell cultures. These techniques are easily performed on patient bone biopsies or bone samples from animal models and have helped shape our current understanding of bone.

1.2.5. Bone Summary

Bone is an important tissue, performing the essential functions of protection, postural support, and mineral balance. Bone's ability to withstand and transmit loads make it critical when performing tasks of daily living, as is its ability to adapt in response to altered loading conditions. This functional adaptation is controlled by a variety of cellular processes involving all three cell types within bone: osteoblasts, osteocytes, and osteoclasts. Osteocytes sense mechanical changes within the bone and promote remodeling, and osteoclasts and osteoblasts work together in a tightly coordinated effort to resorb and rebuild bone, respectively, to facilitate both the metabolic and mechanical roles of the skeleton. In aging, many of the processes are negatively altered, leading to an imbalance between bone resorption and formation and resulting in an overall deficit in bone mass and structure. Aging also impacts the material properties of bone, including decreased modulus of elasticity, ultimate stress, and toughness, all which contribute to bone fragility. Bone mass, structure, and material properties all affect the functional ability of bone to bear load and resist fracture. Understanding how aging impacts all of these components is important for developing new treatments and therapies to mitigate fracture risk. Measuring both cellular and

mechanical metrics is more difficult to do *in vivo* in humans due to the invasive nature of many of the techniques. Use of animal models can facilitate these experiments, yet the models must be extensively validated to confirm that they adequately mimic human conditions and that the findings are translatable to humans. The structure-function relationships have been well characterized in bone, both in health and in aging and disease, but these relationships in other musculoskeletal tissues, namely tendon and muscle, have been less investigated and remain poorly understood. However, many of the approaches used to examine these structure-function relationships in bone can be applied to the other tissues.

1.3. Tendon

1.3.1. Tendon Cell Differentiation and Mechanotransduction

While bone provides structure and protection to the body, and muscle generates forces to stimulate movement, tendon transmits these muscle forces to the bone to produce joint moments and facilitate movement. Tendon is a connective tissue consisting of primarily extracellular matrix (ECM) with fibroblast-like cells referred to as tenocytes⁶⁴. Tenocytes arise from a mesenchymal lineage and are responsible for secreting the collagen component of the ECM⁶⁴, which is made primarily of collagen type I⁶⁵. Tenocytes also secrete repair proteins and matrix proteoglycans that control the collagen synthesis and degradation⁶⁴. Tenocyte differentiation is poorly understood, yet the best hypothesis suggests that the helix-loop-helix transcription factor, scleraxis (Scx), promotes tenocyte differentiation⁶⁶. Scx is primarily activated by a signaling cascade initiated by bone morphogenetic protein 12 (BMP-12). In both mesenchymal stem cells and mature tenocytes, secretion of BMP-12 and subsequent activation of Scx leads to the development of new tenocytes⁶⁶. Similar to bone, the ability of tenocytes to replicate is based on number of replications, external signaling, and damage exhibited throughout the lifespan. While the specifics of how

tenocytes respond to these factors remain poorly understood, in aging, the result is a decrease in the number of available tenocytes to remodel tendon tissue⁶⁷. Additionally, the metabolic function of the tenocytes and the ability to produce new proteins are reduced⁶⁷. These tenocyte-specific decreases lead to a decreased ability to respond to mechanical stimulation.

Tenocytes can sense mechanical signals (e.g., tension, compression, hydrostatic pressure) through their own cytoskeletal arrangement of actin molecules. In homeostasis, tenocytes exist at an initial length and orientation. Upon receiving mechanical stimuli, changes in the length and orientation of the tenocyte activates intracellular ion channels, thereby releasing intracellular calcium which enables the release of ATP⁶⁵. Release of ATP can lead to activation of several autocrine and paracrine signaling pathways⁶⁵. Depending on the nature of the mechanical signals (e.g., loading, unloading, voltage changes), the tenocytes can secrete either more collagen I or matrix metalloproteinases (MMPs) that degrade collagen I⁶⁵. This process is very similar to the adaptive response of bone described by Wolff's law. In aging, tenocytes are fewer, leading to less collagen I production and increased degradation of old collagen by MMPs, resulting in an overall decrease in collagen turnover⁴⁷. These changes in tenocytes can also lead to protein and ECM changes that must adapt to the aging environment.

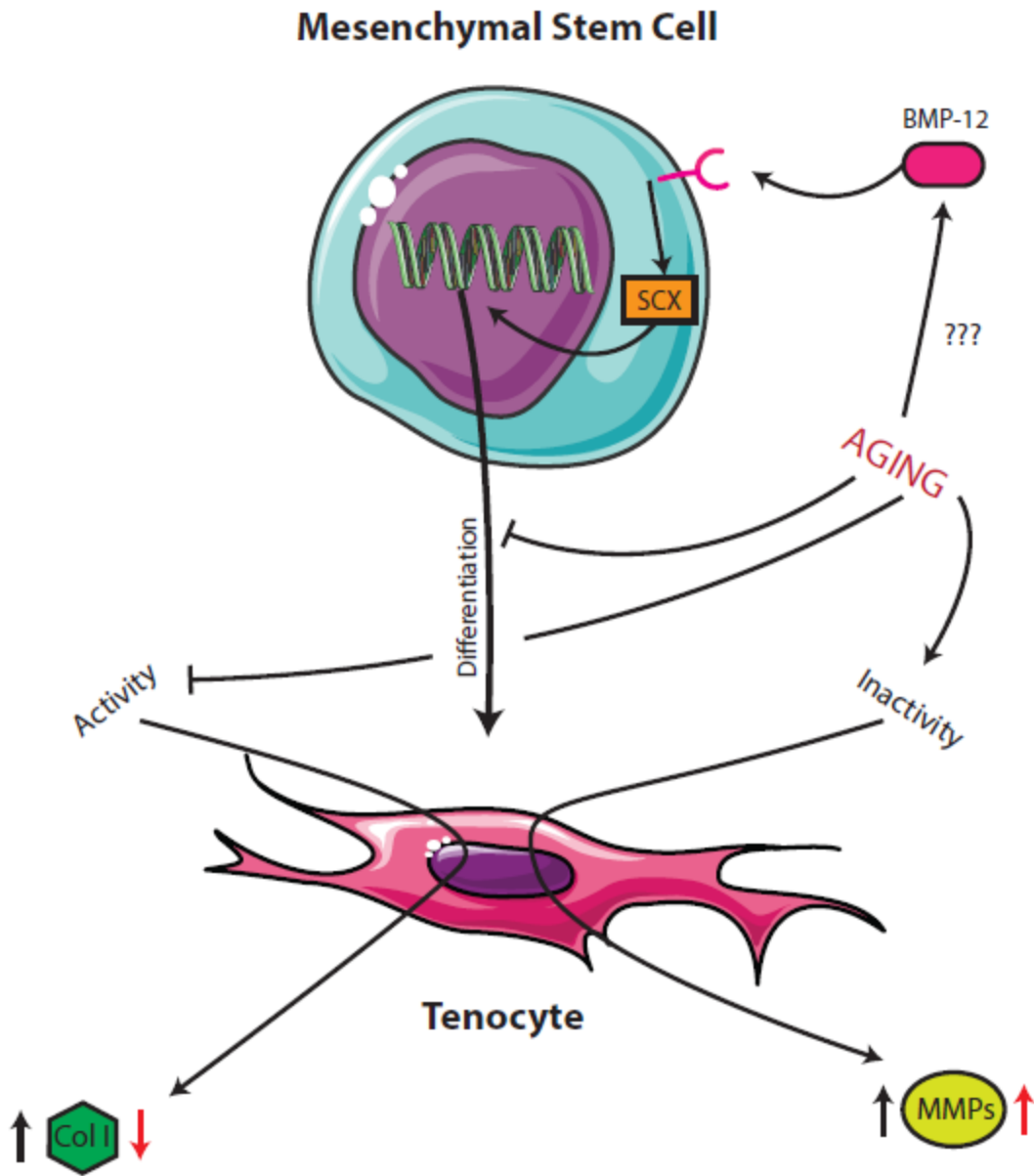


Figure 3. Aging effects on MSC differentiation into tenocytes and tendon signaling. MSCs are signaled by BMP-12 and other signaling molecules to make scleraxis (SCX), which translocates to the nucleus and promotes differentiation. With increased activity, various signaling events in the differentiated tenocyte promote increased expression of collagen I (Col I), while inactivity promotes increased matrix metalloproteinase (MMP) expression. In aging, it is unclear how differentiation is affected, yet the end result suggests a decreased number of differentiated tenocytes. Additionally, an aging lifestyle suggests an increase in inactivity and additional inflammatory pathways, inhibiting Col I expression and promoting further MMP expression (red arrows). Therefore, aged tendons may demonstrate decreased new collagen production and increased degradation of the collagen that is present.

1.3.2. Protein and Matrix Changes in Tendon

In addition to cellular changes, tendon undergoes changes to the ECM. Similar to bone, collagen content decreases with age in both human and animal model, but the type(s) of collagen affected remains unclear. Since tendon is composed primarily of collagen I (60-90%)⁶⁸, the predominant hypothesis suggests that a decrease in collagen I dominates. Aging also reduces the amount of proteoglycans present in tendons. Because proteoglycans bind water within the tendon ECM, this proteoglycan loss may explain the reduced water content observed in aging tendons⁶⁹. Similar to bone, tendon collagen has increased AGEs with aging, which promotes increased collagen crosslinking^{70,71}.

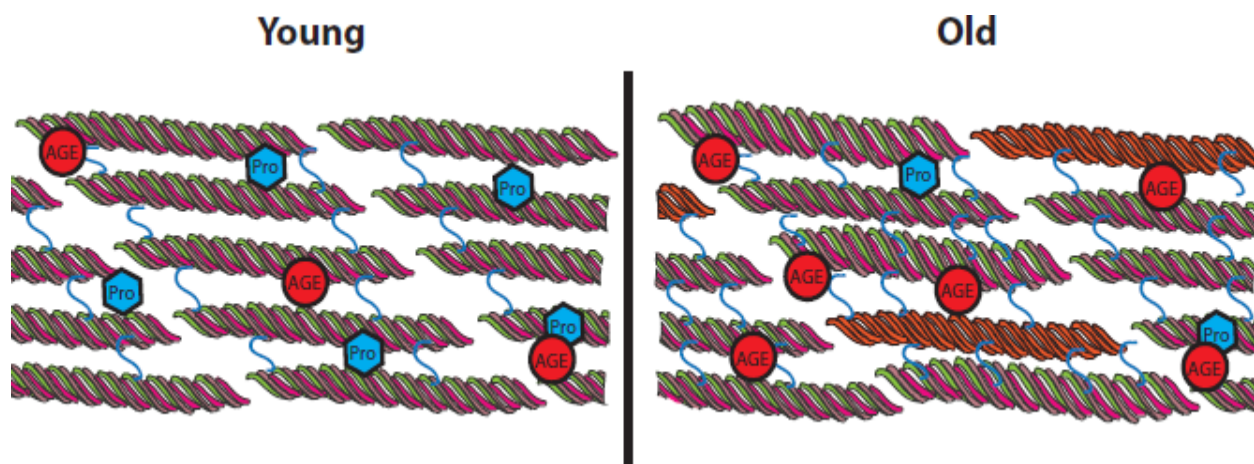


Figure 4. ECM changes between young and old (aged) tendon. In young tendon, collagen fibers (rainbow helices) have a limited number of crosslinks, typically with the terminus of one fiber linking to the mid-region of another. Young tendon also has a moderate amount of proteoglycans (Pros) that help sequester water and limited advanced glycation end products (AGEs) that promote crosslinking. In old tendon, Pros are greatly reduced, and AGEs are increased, leading to a less hydrated, more crosslinked ECM. The collagen itself may be replaced by other fiber types (i.e., elastin, orange helices). Interestingly, similar changes occur with aging in both bone and muscle ECM.

These crosslink changes lead to increased size of collagen molecules, and thus increase tissue stiffness, and greater crosslinking results in slower degradation by MMPs⁴⁷. Hypotheses suggest this may be a protective effect, since tenocytes can no longer produce new collagen as quickly⁴⁷. Perhaps to compensate for these collagen changes, animal studies have demonstrated that certain tendons have increased elastin content, which could reduce the tendon stiffness⁶⁹, although this claim is contentious (see discussion in section 3.3). In summary, these changes suggest that aging

tendon has larger collagen molecules and a less hydrated and more crosslinked ECM that may contain a higher contribution of elastin than ECM of younger tendons. Both the cellular and ECM components contribute to the overall geometry of tendon and dictate its functional response, which becomes negatively altered with aging.

1.3.3. Tendon Geometry and Functional Changes

Tendon geometry is highly dependent on the orientation of the collagen fibers that make up the majority of the tendon. Tendon collagen organizes in a hierarchical nature, resulting in a cross-sectional area (CSA) made up of numerous collagen fibrils⁷². Collagen arranges in a parallel longitudinal fashion, and thus its mechanical properties are much greater in the longitudinal direction than transversely. As with bone, the material properties of the tendon can be determined from a stress-strain curve based on a tensile test with monotonically increasing load until failure. The regions of the stress-strain curve can be divided into three parts: the toe region, the elastic (linear) region, and the plastic (nonlinear) region. In the toe region, the stress increases slowly with increasing strain, because the collagen fibrils are not taut but have a crimping pattern that must be straightened out before the overall structure can bear increasing loads⁷². In the elastic region, the crimping is extended and the collagen fibrils have aligned, and the stress increases linearly with strain, allowing measurement of the elastic modulus⁷². Stretching a tendon to the elastic region is reversible, although repeated loading can lead to fatigue effects in which the strain is reduced over time. In the plastic region after the yield point, the stress levels off and then decreases with increasing strain, as the tendon incurs irreversible damage, leading up to a complete rupture or break at failure⁷².

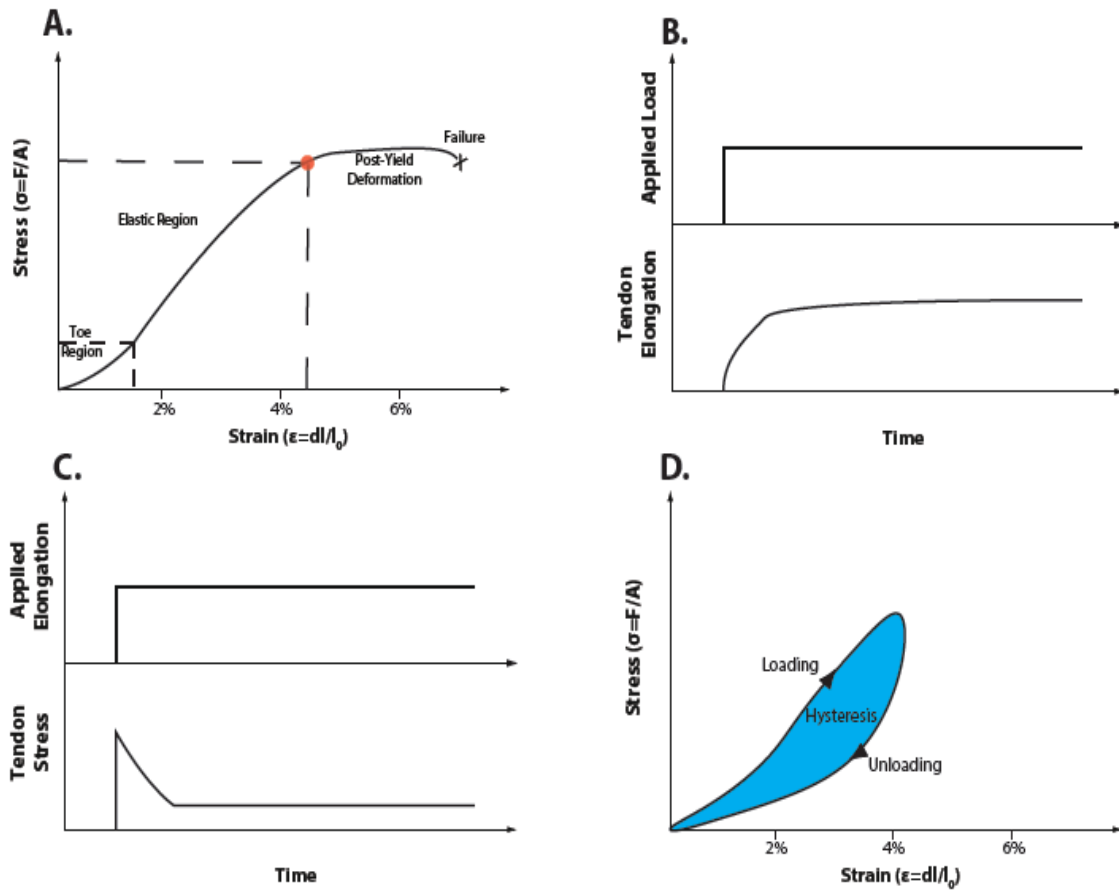


Figure 5. Tensile and viscoelastic properties of tendon. A) Tensile properties of tendon demonstrated in a nonlinear stress-strain curve, with an initial toe region where the collagen crimping straightens out, then the linear region where the elastic modulus is measured before the yield point (red dot), and finally the inelastic region where the tendon undergoes post-yield strain and ultimately failure. Typically, failure occurs between 5 and 10% strain, with maximum stresses between 60 and 120 MPa. B) Creep behavior. If held at a constant stress, the tendon will elongate to the equilibrium strain value. C) Stress relaxation behavior. If held at a constant strain, the tendon will relax until the stress reaches an equilibrium value. D) Hysteresis behavior. During cyclic loading, the unloading trajectory will be lower than the loading trajectory, with the change in area beneath the two (blue shading) representing the mechanical energy dissipated between loading and unloading. Unfortunately, age-related changes are not well defined. It has been suggested that aged tendon may have an increased modulus, take a longer amount of time to reach equilibrium in both creep and stress relaxation, and sweep larger hysteresis areas than young tendon, although the literature has not yet reached a consensus.

Tendon failure can be highly variable in age, either more ductile with substantial post-yield strain before rupture, or more brittle with failure occurring immediately after yield (similar to brittle bone). Tendon also demonstrates viscoelastic behavior, which means it experiences 1) creep (i.e., lengthening, or increasing strain, over time with a constant applied stress) and 2) stress relaxation (i.e., decreasing stress over time with a constant applied strain); and the response to loading is 3) rate-dependent (i.e., increasing modulus with increasing strain rate) and 4) history-

dependent (i.e., energy dissipation occurs during a loading-unloading cycle, manifesting as hysteresis on the stress-strain curve)⁷². These viscoelastic properties arise from the nature of the ECM, in particular the interaction between proteoglycans and bound water and are adversely affected by aging.

From a geometric perspective, aged tendon typically has an increased CSA due to the increased collagen crosslinking, while the overall length of the tendon remains relatively unchanged. However, the age-related changes in tendon mechanical properties remain unclear. Animal studies on tendons across several species have demonstrated that aged tendon has increased stiffness and modulus⁷³, decreased stiffness and modulus^{74,75}, or no change in stiffness and modulus^{76,77}. These discrepancies can arise due to the varied nature of tendon itself; tendon exists in a variety of sizes and locations and can function as energy-cycling springs (e.g., Achilles tendon)⁷⁸, or as a positional lever to off-load joints (e.g., tendons of the fingers)⁷⁹. Many of these studies also employ a variety of testing methods (see section 3.4), which muddles interpretation of the age-related changes. Careful consideration of animal species, age, and methodology must be made when determining age-related changes. In general, studies in animal models generally agree that the stiffness and modulus of tendon increase with age and then decrease with advanced age^{77,80}. A recent study demonstrated that tendon of aged rats (~32 months, corresponding to approximately 70 years of age in humans) had increased stiffness and modulus compared to young rats⁸¹. Older aged rats (i.e., over 32 months) were not tested, although we could speculate that this increased age could result in a decreased stiffness compared to the 32-month-old rats. Similar discrepancies are seen across human studies, yet the general consensus suggests that tendon stiffness is decreased or does not change with aging^{82,83}. However, human subjects experience a wider variation in confounding factors, such as genetics, physical activity, diet, and lifestyle, which contributes to more variability

in tissue properties and makes study results more incongruent. Numerous studies have investigated the viscoelastic properties with age. Hysteresis in both animal and human studies either showed no change, or an increase in energy dissipated^{75,84}. Increased energy loss can negatively impact cyclic loading (i.e., those seen in walking), reducing the tendon's ability to elastically return after being loaded. In animal studies, the stress-relaxation behavior decreases with age⁷⁴, yet human studies did not demonstrate this change. Additionally, due to proteoglycan loss and increased AGEs, thereby reducing the water content, tendons may become more brittle with age, and exhibit decreased viscoelastic properties. In summary, aging can negatively impact the mechanical properties of the tendon, which can directly affect a person's ability to walk. Measuring these changes has proven challenging, as discussed above, yet both animal and human studies have sought to optimize measurements to reach an agreement concerning these age-related changes.

1.3.4. Measuring Tendon Metrics Across Scale and Species

Measuring tendon mechanics *in vivo* has proven difficult, yet recent technologies have made these measurements more manageable. *In vivo* studies generally use a motion capture setup to determine a joint moment based on muscle forces (i.e., a load). This load is determined using inverse dynamics and is paired with imaging techniques (e.g., ultrasound or x-ray) used to capture the tendon stretch. Ultrasound is more frequently used due to its real-time and high-frequency capabilities compared to other imaging modalities. While these techniques are typically noninvasive, they introduce several issues that may be avoided with other testing methods. First, using inverse dynamics to calculate muscle forces introduces uncertainty in the moment arms through which the tendon acts⁸⁵. Additionally, the muscle forces that are generated may not be made by a single muscle or muscle group, with agonist/antagonist activation of other muscles impacting the calculated muscle force. Therefore, the force that a single tendon feels, versus what

is calculated, may not match. Secondly, *in vivo* testing methods do not allow tendons to be tested to failure, so critical components of the stress-strain relationship (e.g., late elastic region, yield, plastic region) may not be determined. Finally, using ultrasound (or any other imaging technique) may only capture a specific region of the tendon and not the entire tendon. Regions of tendon may stretch more or less than other regions, which may not be indicative of the entire stretch of the tendon⁸⁶. *In vitro* experimentation using human samples or animal models can overcome many of these issues, but they also present issues of their own.

As with bone, many *in vitro* methods involve the dissection of a tendon from an animal or cadaver, or taking a tendon biopsy. Tendon mechanical properties are determined by placing the tissue into a load frame, and loads are then applied most commonly in tension. One primary issue with testing is gripping the tendon sufficiently so that it does not slip out of the grips and is not damaged by them, both of which could impact measurements of stress and strain⁸⁷. Alternative gripping methods can alleviate some of these issues, such as leaving the bone-tendon interface intact during dissection and applying tension to the tendon, which then pulls on the bone instead of a clamp, simulating a more natural interaction⁸⁸. Strain gauges can also be placed along the tendon to determine region-specific stresses on the tendon, which may avoid problems with slippage⁸⁹, although this would likely only enable measurements at lower loads in the elastic region. Measurements at the collagen fibril level can be performed using atomic force microscopy, although these techniques are in their nascent stages⁹⁰. Finally, *in vitro* experiments can determine cell-level changes through methods as those described in section 2.4. Briefly, tenocytes can be cultured to determine signaling proteins, structural content/organization, genetic content, or cellular morphology. While *in vitro* experiments have been used for decades, many of the *in vivo*

methods have been developed quite recently, yet taken together, help inform how tendon changes with age.

1.3.5. Tendon Summary

Tendon plays an important role by transmitting loads from muscle to bone, as well as aiding muscle by storing and returning energy during movement. Tendon's ability to cycle energy make it critical when performing locomotor tasks, and similar to bone, altering loading conditions induces adaptations in tendon composition. Tendon remodeling is driven by the tendon-specific fibroblast, the tenocyte. Tenocytes sense changing load through mechanotransduction, where either more collagen I can be produced or MMPs secreted to degrade collagen I. In aging, many of the processes involved with remodeling tendon are negatively altered, leading to a decrease in collagen I turnover. Changes in the structural content of tendon can directly impact its function. Depending on several factors, including CSA, collagen crosslinking and AGEs, the tensile and viscoelastic properties can be described. Aging induces changes in tendon structural properties, such as increasing CSA, yet many mechanical responses remain unclear. A variety of testing methods both *in vivo* and *in vitro* exist to determine these mechanical changes across species. Therefore, developing experiments to determine these mechanical changes should carefully consider the animal, sex, tendon type, and testing method to better reach a consensus. While the structural changes of tendon with age are clearly defined, their impact on functional changes is not. This discrepancy continues with muscle, and suggests a need for further investigation.

1.4. Skeletal Muscle

1.4.1. Skeletal Muscle Cell Differentiation, Communication, and Mechanotransduction

Skeletal muscle, the most common muscle type in the body, plays an important role in the body by generating the force necessary to produce movement of the skeletal system. This ability to

generate force highlights an important characteristic: skeletal muscle has both passive and active components. For the purposes of this review, the passive properties will be summarized. The primary cell type, the muscle fiber, is a long, cylindrical cell comprised of filamentous proteins, actin, myosin, and titin, as well as cellular organelles common to other cell types. The pulling interaction of actin and myosin provides the active force necessary to produce movement, while titin provides a passive resistance to return actin and myosin to their initial positions⁹¹. Muscle fibers arise from a mesenchymal lineage, with skeletal muscle-specific stem cells referred to as satellite cells⁹². Similar to both bone and tendon, aging reduces the number of these satellite cells, as well as their ability to repair and build muscle fibers.

Satellite cells are located between the muscle fiber sarcolemma and the surrounding ECM, termed the basal lamina. In normal skeletal muscle, satellite cells remain quiescent and are characterized by the expression of the protein paired box 7 (Pax7)⁹³. Once stimulated (either by damage or signaling factors), satellite cells express regulatory proteins myogenic factor 5 (Myf5) and myoblast determination protein (MyoD), which cause rapid division and differentiation of other satellite cells. Once divided, satellite cells either self-renew (divide with one returning to a quiescent state) or differentiate into myoblasts and begin to downregulate Pax7 expression and instead upregulate skeletal muscle proteins such as myogenin and myogenic regulatory factor 4 (MRF4)⁹³. Once a sufficient amount of myoblasts are present, the myoblasts begin to fuse together to form new muscle fibers. In aging, activation of satellite cells (i.e., the internal signaling cascade initiated by damage or growth factors) takes a longer amount of time⁹⁴. Additionally, aged satellite

cells demonstrate a decreased ability to self-renew, leading to an exhausted pool of satellite cells⁹⁴.

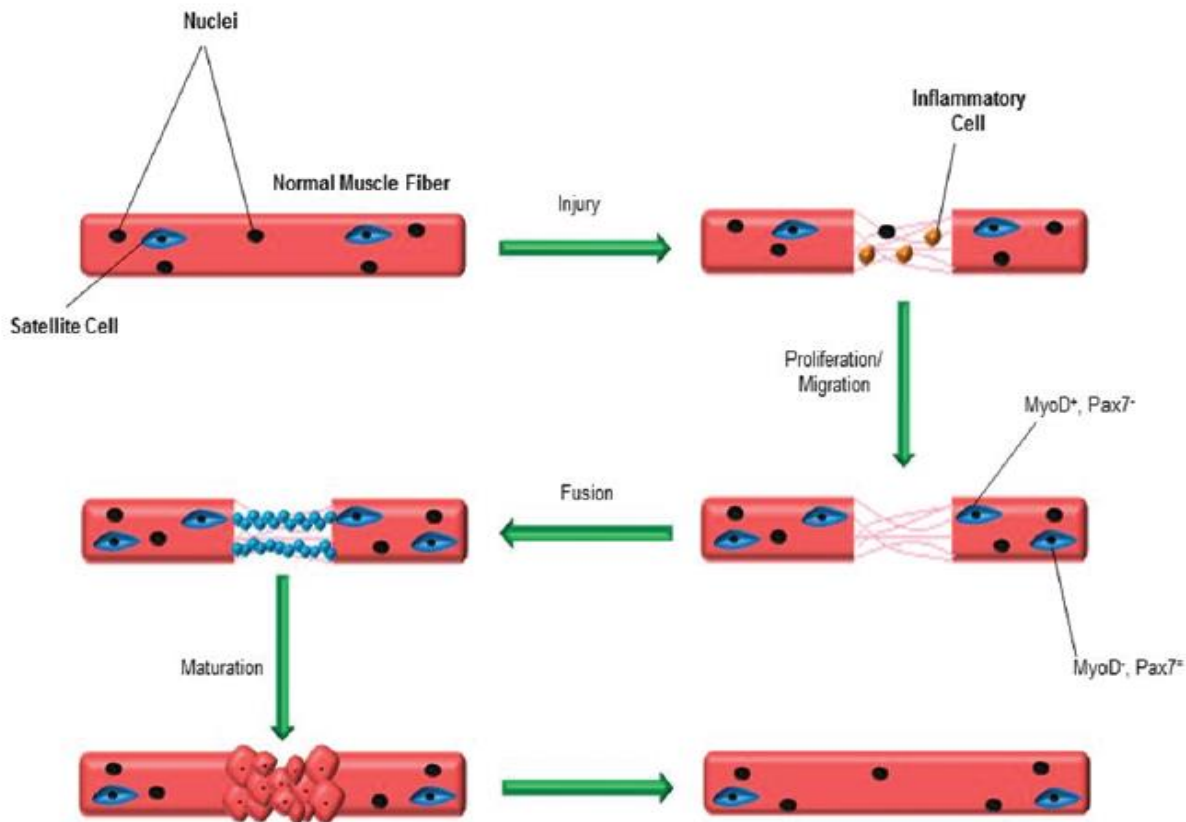


Figure 6. Satellite cell differentiation and propagation in development/injury. Satellite cells secrete Pax7 while in the quiescent state. In either development or injury, satellite cells are activated and begin expressing Myf5 and MyoD, beginning a rapid proliferation process. Additionally, Pax7 is downregulated during this time. Satellite cells then fuse and mature to create or repair new muscle. Some satellite cells will remain quiescent during proliferation, demonstrating their ability to self-renew. In aging, these process take a longer amount time, while satellite cells gradually lose their ability to self-renew. Unable to replace muscle fibers, muscle often uses fibrotic or connective fibers instead in repair.

The underlying cause of this reduced self-renewal is currently under investigation, with a variety of responsible signaling cascades hypothesized, including IL-6, JAK/STAT, and p38/MAPK⁹⁵.

The reduced number of satellite cells caused by impaired self-renewal, coupled with the reduced function of the satellite cells, lead to a reduced ability to repair and regenerate new muscle fibers in aged tissue. While satellite cells are primarily responsible for replacing damaged tissue, other signaling pathways present in mature skeletal muscle are also adversely affected by aging.

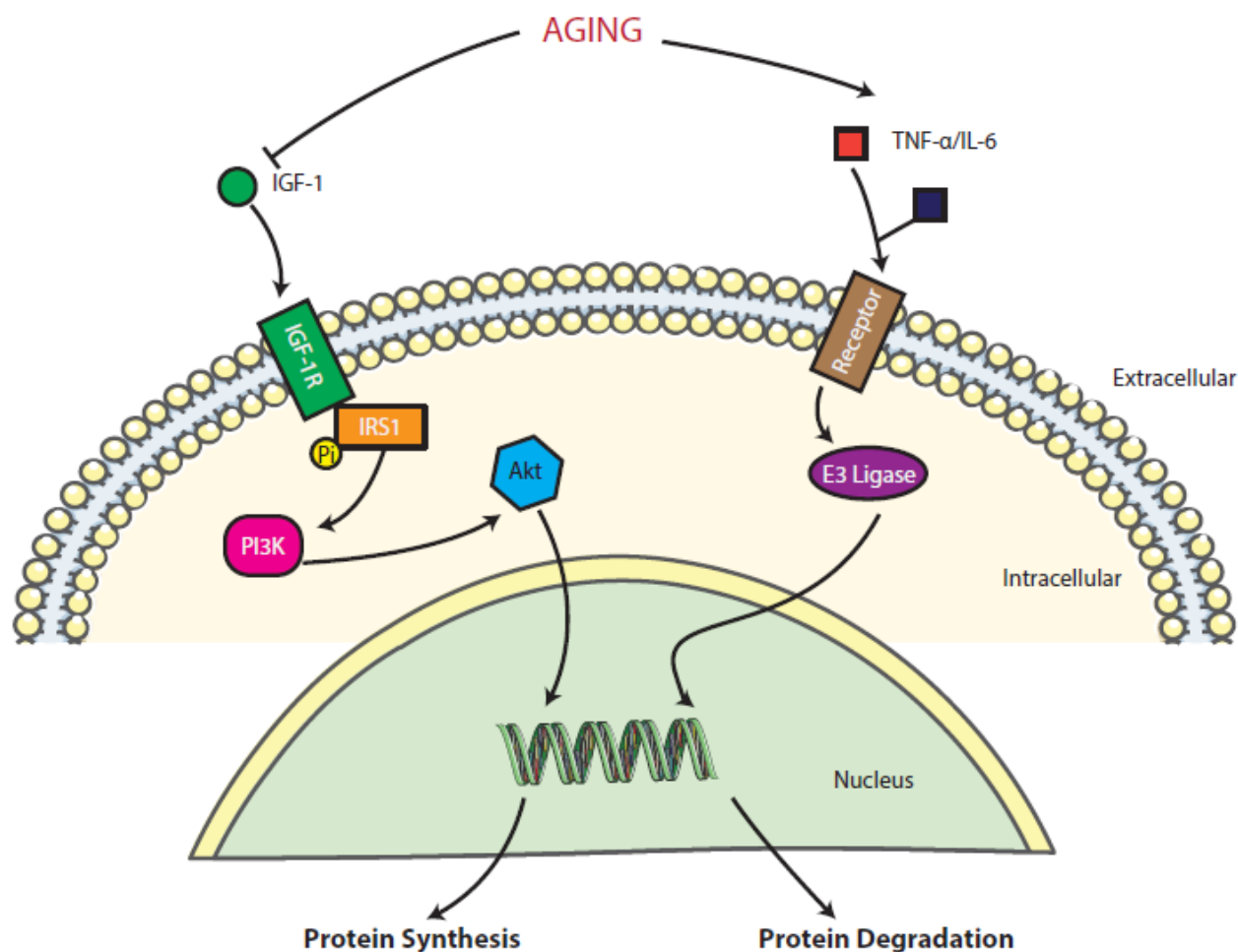


Figure 7. Muscle hypertrophy pathways, atrophy pathways, and the effects of aging. In muscle hypertrophy, IGF-1 binds to its receptor, leading to the phosphorylation of IRS1, subsequently leading to the activation of PI3K and Akt, ultimately resulting in increased protein synthesis. Alternatively, muscle atrophy begins with signaling from pro-inflammatory molecules, leading to subsequent signaling cascades that result in the activation of E3 ligases, which lead to protein degradation. In aging, hypertrophy pathways are often inhibited, while atrophy pathways are upregulated, leading to an overall decrease in muscle mass.

The ability of mature skeletal muscle to grow in size (i.e., hypertrophy), involves an increase in protein synthesis and a decrease in protein degradation. The most studied hypertrophic signaling pathway is the IGF-1 signaling pathway. Similar to bone, under increased activity (either loading or increased activation), IGF-1 binds to its associated receptor IGF-1R, and causes the phosphorylation of insulin receptor substrate 1 (IRS1) on the intracellular surface of the muscle

fiber cell membrane^{96,97}. IRS1 subsequently activates the phospho-inositol-3 kinase (PI3K), which through a few intermediates leads to the activation of protein kinase B (Akt), a potent secondary enzyme that has numerous downstream targets^{97,98}. Typically, activation of Akt leads to the protein synthesis and an increase in size of the muscle. In aging, however, both intra- and extracellular IGF-1 is reduced, leading to a decrease in new protein synthesis within the muscle⁹⁹. IGF-1 may be secreted by the muscle, or by other tissues that then signal the muscle through the blood stream; however, whether autocrine (secreted from the same tissue) or paracrine/endocrine (from neighboring tissue) IGF-1 contributes more to hypertrophy is poorly understood¹⁰⁰. Understanding how IGF-1 expression changes with aging may reveal new targets for intervention. While hypertrophy is associated with protein synthesis, muscle atrophy is associated with protein degradation and is also more pronounced with aging.

Muscle atrophy is characterized by an increase in protein degradation initiated by an increase in inflammatory signaling factors and glucocorticoids. While numerous atrophy signaling pathways exist, two of the most investigated include the NF- κ B and p38/Mitogen-activated protein kinase (MAPK) pathways¹⁰¹. Both signaling pathways are initiated by inflammatory signaling factors, such as tumor necrosis factor alpha (TNF- α) or interleukin 1 (IL-1), leading to activation and expression of ubiquitin ligases¹⁰¹. E3 ligases mediate the sarcomere breakdown by promoting degradation of myosin heavy chain. Additionally, these E3 ligases inhibit protein synthesis, making additional myosin production difficult¹⁰¹. In aging, muscle atrophy (*sarcopenia*) is common, and likely results from several factors, including inactivity, poor nutrition, and comorbidities such as arthritis and osteopenia^{102,103}. These lifestyle changes can lead to increased inflammatory responses, promoting these atrophy pathways¹⁰². In summary, muscle changes with aging are multi-faceted: satellite cells responsible for creating new muscle fibers are worn down,

muscle hypertrophy pathways are under-expressed, and muscle atrophy pathways are over-expressed. These changes all lead to protein changes within the muscle fiber, as well as in the ECM, that directly affect the passive properties of the whole muscle.

1.4.2. Protein and Matrix Changes in Muscle

Similar to both bone and tendon, skeletal muscle demonstrates altered collagen expression with aging. However, studies have demonstrated the difficulty in determining the type of collagen present. Skeletal muscle has 28 subtypes of collagen, with types I, III, IV, and VI being the most studied¹⁰⁴. Different isoforms of collagen have different strengths and lengths and may contribute to the functional decline in mechanical properties associated with aging (see section 4.3)¹⁰⁴. For instance, animal studies have demonstrated an increase in the amount of collagen type I, but a decrease in collagen type III, with aging¹⁰⁵. Additionally, the ECM was thicker, with an increased expression of collagen type IV¹⁰⁶. In general, however, measurement of collagen mRNA expression has been in contention. Numerous animal studies demonstrate that collagen expression is decreased with age in rats^{107,108}, but in human studies, collagen synthesis tends to be increased¹⁰⁹. This discrepancy may be explained by the differences between species, in that humans may experience other conditions or have confounding factors not seen in highly controlled laboratory animals. Furthermore, the collagen present in muscle may have increased crosslinking, as demonstrated in previous tissues, due to a decreased ability to renew collagen, leading to overall increased stiffness. Finally, as atrophy pathways become more active, space left open by myosin/muscle fiber degradation can be filled with new collagen instead of new muscle, leading to a larger ECM¹¹⁰. As the ECM becomes larger and satellite cells become worn out, altered signaling can lead to further activation of atrophic pathways and producing a positive feedback cycle that induces further collagen deposition.

Other ECM components that may change include the amount of fat infiltration and other elastic fibers. Fat infiltration, or myosteatorsis, can occur in response to inflammatory signals, although its exact role in muscle aging is poorly understood¹⁰⁴. The predominant hypothesis suggests that to promote inflammatory signaling, adipocytes invade and release additional inflammatory signals¹¹¹. Elderly individuals have increased myosteatorsis, yet it can be reversed with training exercises¹¹². The effect of myosteatorsis on the mechanical properties of skeletal muscle has not been investigated¹⁰⁴, and few studies have investigated changes in other ECM components, such as elastin or fibrinogen, with aging. In animal studies, elastin expression increased with age¹¹³. However, elastin promotes compliance in tissues and may provide a protective effect due to the increasing stiffness attributed to increased collagen production, although this point is in contention due to the low number of studies available.

1.4.3. Muscle Geometry and Passive Functional Changes

On the tissue level, skeletal muscle mass declines with age¹⁰⁴, and this sarcopenia is attributed to the decreased number and size of muscle fibers available. Specifically, type II fibers (i.e., fast fibers) degrade more quickly than type I fibers (i.e., slow fibers)^{114,115}. Studies also suggest that the type II fibers that are present are reduced in size with aging, while the type I fibers remain relatively unchanged^{116,117}. As the tissue loses fibers, the lengths of the muscle fascicles tend to shorten, and the pennation angle of the fibers begin to decrease¹¹⁸. Taken together, these results suggest that the muscle physiological cross sectional area (PCSA) decreases with age, which will reduce the amount of active force the muscle can produce⁹¹. In addition to the decreased CSA, the aged muscles have less contractile tissue, replaced with more ECM or fatty tissue¹¹⁰. While the fiber loss can be more attributed to active force production, the changes in the ECM (and to a lesser extent, titin) can affect the passive properties of the tissue.

Both the material and viscoelastic properties of aged skeletal muscle are rarely reported in the literature. However, these properties in normal tissue have been well established. The material properties of skeletal muscle, like bone and tendon, are described by the stress-strain relationship as the muscle is pulled to longer lengths, which is the passive behavior of the tissue. Since muscle has both active (with muscle electrically stimulated) and passive components, a single passive curve does not fully describe the tissue mechanics. Testing for muscle typically includes measurements when the muscle is electrically stimulated, and the resulting plots of interest are length-tension (i.e., force-length) curves for the active component, passive component, and the total⁹¹. The length of the muscle just before it starts to develop force when it is stretched is referred to as its optimal length or resting length (l_0). For the passive stress-strain relationship, as the muscle is stretched, force increases exponentially (Figure 8). As the muscle is elongated to strains greater than 40%, the muscle reaches its yield point and demonstrates very little post-yield deformation thereafter¹¹⁹. Muscle elastic modulus is the slope of the linear region of the stress-strain curve (and stiffness is the slope of the linear region of the length-tension curve). In the sparse literature that does exist, animal studies suggest that muscle stiffness increases with aging^{120,121}, while human studies suggest that muscle stiffness decreases with aging. This discrepancy, which may arise from the different testing methods used in each experiment (see Section 4.4), should be investigated with further studies.

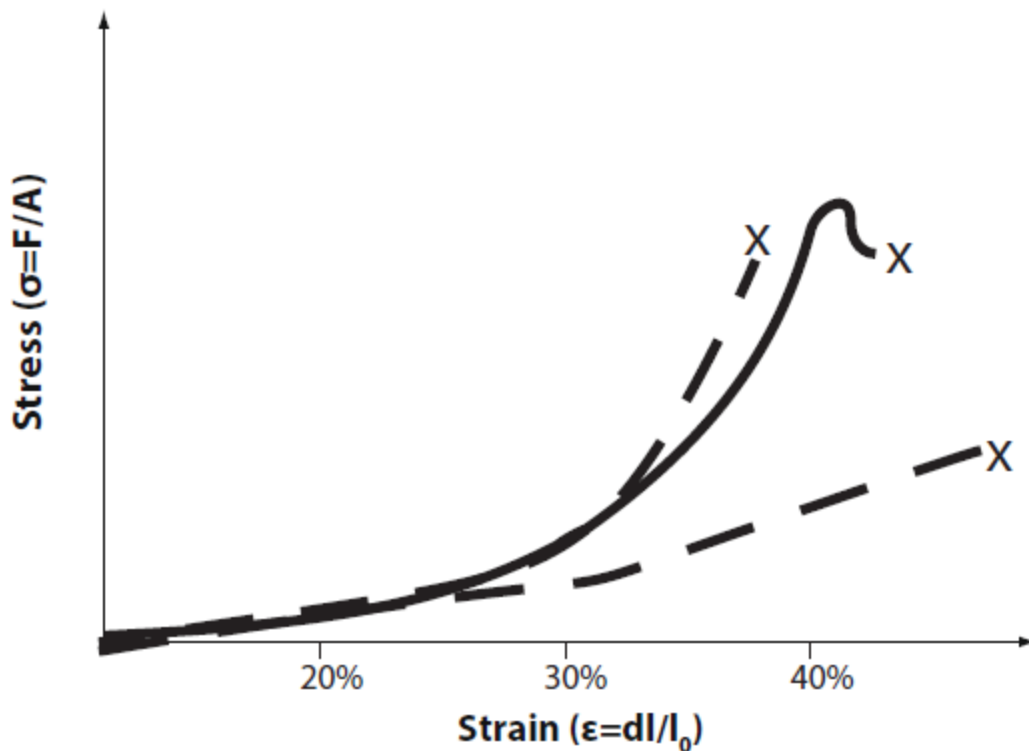


Figure 8. Passive tensile properties of skeletal muscle and potential effects of aging. Muscle loads increase exponentially when stretched, with very little post-yield behavior. Compared to bone and tendon, muscle can reach much higher strains, yet the stresses reached are similar (100-150 MPa). However, skeletal muscle rarely reaches these strains *in vivo* due to several, including the range of motion of the muscle, resistive proteins, and even stretch reflexes. In aging (dotted lines), the changes are unclear. Some literature suggests that the muscle becomes stiffer, while others suggest that muscle becomes more compliant. These discrepancies carry over to the viscoelastic properties, as well, and may arise from the different muscles, animal models, and testing methods used in experimentation.

The viscoelastic properties of normal skeletal muscle are also well defined. Muscle can be subjected to stress-relaxation tests, where the muscle is held at a constant stretched length, and the force that is produced decreases with time^{13,122}. Alternatively, the muscle also demonstrates creep characteristics, where if the muscle is held at a constant tension (i.e., load), the length of the muscle will increase over time until an equilibrium value is reached^{13,122}. Finally, if the muscle is repeatedly stretched, each resulting passive curve will be different, but if the muscle is allowed a period of rest, the original passive curve can be restored^{13,122}. Very few studies have reported the viscoelastic properties of aged muscle. A study investigating the viscoelastic properties of muscle-

tendon units (MTUs) in the lower leg of aging women demonstrated that an increase in absorbed passive elastic energy was present in aged MTUs¹²³, suggesting that aging may increase the viscoelastic properties of the aged MTU, with longer periods of time needed for the muscle to reach equilibrium¹²³. These changes were thought to have arisen from increases in the collagen content of the ECM¹²³. In summary, we have insufficient data from existing studies in the literature to make definitive conclusions about the mechanical properties of aged tissue, again highlighting the need for further studies.

1.4.4. Measuring Passive Muscle Metrics Across Scale and Species

As with bone and tendon, the mechanical properties of skeletal muscle can be determined both *in vivo* and *in vitro*. *In vivo* studies of skeletal muscle are quite similar to those performed on tendon. Muscle force and length changes are calculated from measured reaction forces and kinematic data across a muscle and joint. Unfortunately, most joints are highly complex, with multiple crossing muscles and complex ranges of motion. Additionally, anthropometric data (i.e., muscle origin and insertion) are often required to determine force-length relationships. During testing, a limb is constrained to allow only motion of the joint of interest¹²⁴. Resistance to the motion is measured by either a force plate, dynamometer, or torque sensor at the joint^{124,125}. The length changes can be calculated using anthropometric data and the movement about the joint. Fascicle length changes can be determined using ultrasound, as described previously, and can also help determine the viscoelastic properties, as the speed of the sound waves can be used to derive the tissue shear properties¹²⁶. Additionally, pennation angle can also be determined through the use of ultrasound¹²⁷. Altering the loading in a time-dependent manner can also be used to determine viscoelastic properties¹²⁷. Finally, electromyography can be used to determine the activation level (based on electric impulses detected) of the muscle of interest. Unfortunately, as with tendon, the

size, number, and complexity of muscles surrounding a joint may cause difficulty when determining exact muscle properties for a single muscle or muscle group, often requiring assumptions or estimation strategies. Furthermore, while these experiments can be performed on animals, it is often much easier and common to perform them in human studies.

Uniaxial tensile testing of a whole muscle is the most basic and common method for estimating the material properties of muscle. Similar to tendon, opposite ends of the muscle are fixed to a load frame using clamps. One end is fixed, and the other is elongated in one direction to produce passive length-tension curves. The active curves are produced by applying a fixed elongation, activating the muscle with an applied voltage, and then measuring the resulting force produced. In many cases, the length changes are normalized to the initial or resting length, and the force is normalized to the PCSA or the maximum force of the muscle¹¹⁹. In smaller animal models, such as the mouse, the entire muscle may be dissected out and attached to the MTS device with sutures at either end. Larger animal models may use complex dissection methods with a bone still intact to obtain more realistic loading conditions¹²⁸. Viscoelastic properties can also be determined on an isolated muscle by varying the loading or strain rate. For stress relaxation, several strain values are used, where the muscle is elongated to some strain and held there, while the force production is monitored. For creep, several loading values are chosen, and strain is measured over time.

1.4.5. Muscle Summary

Skeletal muscle plays an important role in the body by generating the forces that enable skeletal movement. Skeletal muscle is a unique tissue, because it has both active components (responsible for generating forces during contraction) and passive components (responsible for returning muscle to original lengths and protecting against damage). Similar to tendon and bone, the amount these components are utilized controls the amount of repair/remodeling that occurs in the tissue.

Skeletal muscle repair is driven by the muscle-specific stem cell, the satellite cell. Satellite cells sense inflammatory signals and help remove and replace damaged muscle. In aging, many of the processes involved with repairing muscle are negatively altered, leading to decrease satellite cell activation, new muscle cell synthesis, and increased fibrosis infiltration. Additionally, to remodel muscle, hypertrophy and atrophy signaling pathways are more activated with aging, demonstrating increased atrophy and decreased hypertrophy. Changes in the structural content of muscle can directly impact its function. Depending on several factors, including PCSA, collagen crosslinking, and fibrosis/fat deposition, the tensile and viscoelastic properties can be described. Aging will alter structural properties, such as decreasing the PCSA, yet changes in mechanical responses remain unclear. A variety of testing methods both *in vivo* and *in vitro* exist to determine these mechanical changes across species, but experimental variations across studies contribute to the insufficient understanding about age-related changes in muscle. As with tendon, developing experiments to determine these mechanical changes should carefully consider the animal, sex, muscle, and testing method to reach an agreement. In summary, both the structural and functional aspects of muscle are generally well understood individually, but how one informs the other is not. Furthermore, changes with aging also remain unclear. Bone, tendon, and muscle also interact extensively *in vivo* due to their close proximity, both from mechanical interactions and paracrine effects among the tissues. Therefore, understanding crosstalk between these tissues may enhance our understanding of their structural and functional properties, both in health and in aging, and may reveal new targets for intervention.

1.5. Summary, Conclusions, and Experimental Directions

Collectively, bone, tendon, and muscle are critical for enabling movement and performing daily tasks. During these tasks, loads are generated and placed on these tissues, and altered loading

conditions will induce adaptational responses in the various tissues. At the cellular level, this process is referred to as mechanotransduction and dictates how the cells react to different loading conditions. These mechanotransduction pathways rely on tightly controlled signaling pathways and can often lead to increased or decreased synthesis of proteins necessary in tissue remodeling. In aging, these processes are often adversely affected, as cells have a decreased ability to proliferate/self-renew, expression of signaling factors is altered, and the function of expressed proteins is reduced. However, while these signaling pathways are fairly well established in each tissue individually, how neighboring tissues can influence these pathways is an emerging area of interest. For instance, in both bone and muscle, IGF-1 plays a critical role in the remodeling process. IGF-1 can be secreted by muscle to affect itself (via autocrine signaling), can be secreted out to neighboring tissues (via paracrine signaling), or secreted into the bloodstream to affect distant tissues (via endocrine signaling)^{129,130}. Due to the close proximity of muscle and bone, IGF-1 secreted by muscle could have an additive effect on the autocrine signaling of IGF-1 within bone. Similarly, bone may send IGF-1 to muscle to augment signaling^{129,130}. IGF-1 is merely one example, as numerous studies have attempted to elucidate signaling effects between muscle and bone, demonstrating that numerous factors from both tissues can affect the other, such as inflammatory markers (e.g., TNF- α , IL-6), proliferation markers (e.g., myostatin), and markers of protein synthesis (e.g., prostaglandin, osteocalcin)¹³¹⁻¹³³. While these pathways have been implicated in the crosstalk between muscle and bone, few studies have investigated which pathways are influenced by aging. The studies presented herein highlight a novel approach using co-culture strategies to monitor and evaluate these pathways in young and aged rat cells. Furthermore, studies using parabiosis approaches have demonstrated that a shared vasculature with a young animal can mitigate known age-related detriments in an aged animal¹³⁴, supporting the

notion that circulating factors exist that impact aging. Use of these co-culture techniques could provide information as to which signaling factors are more important to reduce the degenerative processes of aging. Unfortunately, which signaling factors contribute most to the gross tissue and protein changes with aging is unclear; ultimately, these changes lead to increased loss of bone mass (osteopenia/osteoporosis) and skeletal muscle mass (sarcopenia).

In general, tissue can be described by its structure-function relationships. “Structure” here refers to the underlying organization of proteins, cells, and ECM, driven by signaling pathways. Tissue structure directly impacts its “function,” or the tensile (e.g., modulus from stress-strain curve) and viscoelastic (e.g., stress relaxation, creep) properties. In some tissues, these relationships are well established; for instance, in bone the osteoblasts and osteoclasts responsible for maintaining bone matrix can directly influence the bone mass, microstructure, and material properties, which subsequently affect the whole bone stiffness and strength. Unfortunately, in tissues such as tendon and skeletal muscle, the structure-function relationships remain poorly defined. In muscle, active and passive components make identifying which structural components influence specific functional aspects difficult. For instance, passive stretching studies may induce a stretch reflex, where the muscle sends its own action potential, causing the muscle to actively contract. Blocking action potential propagation with drug intervention (i.e., botox, curare) can mitigate these effects^{135,136} and allow investigators to determine passive properties, which are currently helping to define these structure-function relationships. Yet, how these structure-function relationships may be altered in clinical conditions still requires research. With aging, the processes in bone are more well defined; bone generally loses BMD and bone volume, becomes more brittle, and has increased tissue stiffness, and these changes tend to occur similarly across species. However, skeletal muscle relationships are less well defined. Both increased and decreased

stiffness (as a functional measure) have been reported in skeletal muscle across species, discrepancies that may arise due to differing testing methods, animal species, or the muscle type under investigation. These issues persist in tendon studies, yet the literature leans towards a decreasing stiffness with age. Together, a MTU is the primary unit responsible for movement. Studies from our lab have demonstrated that altered stiffness of both muscle and tendon can negatively impact the efficiency of the MTU. As aging alters the MTU stiffness, these negative effects would likely manifest in an aged MTU. The functional studies presented herein will seek to determine the stiffness changes of a single MTU in the hindlimb of young and aged rats. We plan to use a hopping model from previous experiments to demonstrate gait-like patterns not realized by other studies¹³⁷. Determining these stiffness changes in aged animals and how that impacts MTU function may inform new methods for ameliorating age-related declines.

Aging induces numerous changes from the cellular level to the tissue level, which manifest as functional changes at the musculoskeletal system level. Unfortunately many of these changes are not well defined. Using structure-function relationships can help bridge the gap between cellular and whole tissue changes. At the structural level, cellular changes induced by signaling are well defined in bone, yet are more unclear in muscle. Additionally, how one tissue may inform the other is also unclear. At the functional level, both muscle and bone in age undergo a decrease in mass, resulting in a decreased ability of muscle to generate force, and decreased ability of bone to withstand those forces. In aging bone, the tissue stiffness typically increases as a result of changes in collagen turnover and crosslinking, and the structure-function relationships in bone are fairly well defined with aging. However, in skeletal muscle and tendon, the stiffness changes are not well defined. Furthermore, what cellular changes more directly influence the stiffness changes are

not well defined. The experiments herein attempt to discover these relationships and hope to reveal new targets at either the structural or functional level to mitigate the effects of aging.

1.6. References

1. Tuite DJ, Renstrom PA, O'Brien M. The aging tendon. *Scand J Med Sci Sports*. 1997;7(2):72-77.
2. Belsky DW, Caspi A, Houts R, et al. Quantification of biological aging in young adults. *Proc Natl Acad Sci U S A*. 2015;112(30):E4104-10. doi: 10.1073/pnas.1506264112 [doi].
3. Reginster JY, Beudart C, Buckinx F, Bruyere O. Osteoporosis and sarcopenia: Two diseases or one? *Curr Opin Clin Nutr Metab Care*. 2016;19(1):31-36. doi: 10.1097/MCO.0000000000000230 [doi].
4. Freemont AJ, Hoyland JA. Morphology, mechanisms and pathology of musculoskeletal ageing. *J Pathol*. 2007;211(2):252-259. doi: 10.1002/path.2097 [doi].
5. Marcell TJ. Sarcopenia: Causes, consequences, and preventions. *J Gerontol A Biol Sci Med Sci*. 2003;58(10):M911-6.
6. Weiner S, Traub W, Wagner HD. Lamellar bone: Structure-function relations. *J Struct Biol*. 1999;126(3):241-255. doi: S1047-8477(99)94107-2 [pii].
7. Robertson BD, Sawicki GS. Unconstrained muscle-tendon workloops indicate resonance tuning as a mechanism for elastic limb behavior during terrestrial locomotion. *Proc Natl Acad Sci U S A*. 2015;112(43):E5891-8. doi: 10.1073/pnas.1500702112 [doi].
8. Russell B, Motlagh D, Ashley WW. Form follows function: How muscle shape is regulated by work. *J Appl Physiol (1985)*. 2000;88(3):1127-1132.
9. Narici M, Franchi M, Maganaris C. Muscle structural assembly and functional consequences. *J Exp Biol*. 2016;219(Pt 2):276-284. doi: 10.1242/jeb.128017 [doi].
10. Suki B, Parameswaran H, Imsirovic J, Bartolak-Suki E. Regulatory roles of fluctuation-driven mechanotransduction in cell function. *Physiology (Bethesda)*. 2016;31(5):346-358. doi: 10.1152/physiol.00051.2015 [doi].
11. Wu M, Fannin J, Rice KM, Wang B, Blough ER. Effect of aging on cellular mechanotransduction. *Ageing Res Rev*. 2011;10(1):1-15. doi: 10.1016/j.arr.2009.11.002 [doi].
12. Anderson AS, Roberts PC, Frisard MI, et al. Metabolic changes during ovarian cancer progression as targets for sphingosine treatment. *Exp Cell Res*. 2013;319(10):1431-1442. doi: 10.1016/j.yexcr.2013.02.017 [doi].
13. Fung YC. **Structure and stress-strain relationship of soft tissues**. *American Zoologist*. 1984;24(1):13-22.

14. Cole JH, van der Meulen MC. Whole bone mechanics and bone quality. *Clin Orthop Relat Res.* 2011;469(8):2139-2149. doi: 10.1007/s11999-011-1784-3 [doi].
15. Clarke B. Normal bone anatomy and physiology. *Clin J Am Soc Nephrol.* 2008;3 Suppl 3:S131-9. doi: 10.2215/CJN.04151206 [doi].
16. Mohamed AM. An overview of bone cells and their regulating factors of differentiation. *Malays J Med Sci.* 2008;15(1):4-12.
17. Sharpe WD. Age changes in human bone: An overview. *Bull N Y Acad Med.* 1979;55(8):757-773.
18. Klein-Nulend J, Sterck JG, Semeins CM, et al. Donor age and mechanosensitivity of human bone cells. *Osteoporos Int.* 2002;13(2):137-146. doi: 10.1007/s001980200005 [doi].
19. Stenderup K, Justesen J, Clausen C, Kassem M. Aging is associated with decreased maximal life span and accelerated senescence of bone marrow stromal cells. *Bone.* 2003;33(6):919-926. doi: S8756328203002679 [pii].
20. Boskey AL, Coleman R. Aging and bone. *J Dent Res.* 2010;89(12):1333-1348. doi: 10.1177/0022034510377791 [doi].
21. Kim JH, Liu X, Wang J, et al. Wnt signaling in bone formation and its therapeutic potential for bone diseases. *Ther Adv Musculoskelet Dis.* 2013;5(1):13-31. doi: 10.1177/1759720X12466608 [doi].
22. Almeida M, Han L, Martin-Millan M, et al. Skeletal involution by age-associated oxidative stress and its acceleration by loss of sex steroids. *J Biol Chem.* 2007;282(37):27285-27297. doi: M702810200 [pii].
23. Almeida M, Han L, Martin-Millan M, O'Brien CA, Manolagas SC. Oxidative stress antagonizes wnt signaling in osteoblast precursors by diverting beta-catenin from T cell factor- to forkhead box O-mediated transcription. *J Biol Chem.* 2007;282(37):27298-27305. doi: M702811200 [pii].
24. Manolagas SC. From estrogen-centric to aging and oxidative stress: A revised perspective of the pathogenesis of osteoporosis. *Endocr Rev.* 2010;31(3):266-300. doi: 10.1210/er.2009-0024 [doi].
25. Almeida M, O'Brien CA. Basic biology of skeletal aging: Role of stress response pathways. *J Gerontol A Biol Sci Med Sci.* 2013;68(10):1197-1208. doi: 10.1093/gerona/glt079 [doi].
26. Rauner M, Sipos W, Pietschmann P. Age-dependent wnt gene expression in bone and during the course of osteoblast differentiation. *Age (Dordr).* 2008;30(4):273-282. doi: 10.1007/s11357-008-9069-9 [doi].

27. Liu H, Fergusson MM, Castilho RM, et al. Augmented wnt signaling in a mammalian model of accelerated aging. *Science*. 2007;317(5839):803-806. doi: 317/5839/803 [pii].
28. Bennett CN, Longo KA, Wright WS, et al. Regulation of osteoblastogenesis and bone mass by Wnt10b. *Proc Natl Acad Sci U S A*. 2005;102(9):3324-3329. doi: 0408742102 [pii].
29. Bennett CN, Ouyang H, Ma YL, et al. Wnt10b increases postnatal bone formation by enhancing osteoblast differentiation. *J Bone Miner Res*. 2007;22(12):1924-1932. doi: 10.1359/jbmr.070810 [doi].
30. Matsuo K. Cross-talk among bone cells. *Curr Opin Nephrol Hypertens*. 2009;18(4):292-297. doi: 10.1097/MNH.0b013e32832b75f1 [doi].
31. Matsuo K, Irie N. Osteoclast-osteoblast communication. *Arch Biochem Biophys*. 2008;473(2):201-209. doi: 10.1016/j.abb.2008.03.027 [doi].
32. Bonewald LF, Johnson ML. Osteocytes, mechanosensing and wnt signaling. *Bone*. 2008;42(4):606-615. doi: 10.1016/j.bone.2007.12.224 [doi].
33. Chen JH, Liu C, You L, Simmons CA. Boning up on wolff's law: Mechanical regulation of the cells that make and maintain bone. *J Biomech*. 2010;43(1):108-118. doi: 10.1016/j.jbiomech.2009.09.016 [doi].
34. Wada T, Nakashima T, Hiroshi N, Penninger JM. RANKL-RANK signaling in osteoclastogenesis and bone disease. *Trends Mol Med*. 2006;12(1):17-25. doi: S1471-4914(05)00267-4 [pii].
35. Boyce BF, Xing L. Functions of RANKL/RANK/OPG in bone modeling and remodeling. *Arch Biochem Biophys*. 2008;473(2):139-146. doi: 10.1016/j.abb.2008.03.018 [doi].
36. Demontiero O, Vidal C, Duque G. Aging and bone loss: New insights for the clinician. *Ther Adv Musculoskelet Dis*. 2012;4(2):61-76. doi: 10.1177/1759720X11430858 [doi].
37. Forwood MR, Burr DB. Physical activity and bone mass: Exercises in futility? *Bone Miner*. 1993;21(2):89-112.
38. Hay E, Bouaziz W, Funck-Brentano T, Cohen-Solal M. Sclerostin and bone aging: A mini-review. *Gerontology*. 2016;62(6):618-623. doi: 000446278 [pii].
39. Robling AG, Niziolek PJ, Baldrige LA, et al. Mechanical stimulation of bone in vivo reduces osteocyte expression of sost/sclerostin. *J Biol Chem*. 2008;283(9):5866-5875. doi: M705092200 [pii].
40. Spatz JM, Ellman R, Cloutier AM, et al. Sclerostin antibody inhibits skeletal deterioration due to reduced mechanical loading. *J Bone Miner Res*. 2013;28(4):865-874. doi: 10.1002/jbmr.1807 [doi].

41. Guntur AR, Rosen CJ. IGF-1 regulation of key signaling pathways in bone. *Bonekey Rep.* 2013;2:437. doi: 10.1038/bonekey.2013.171 [doi].
42. Fowlkes JL, Bunn RC, Thraillkill KM. Contributions of the insulin/insulin-like growth factor-1 axis to diabetic osteopathy. *J Diabetes Metab.* 2011;1(3):S1-003. doi: S1-003 [pii].
43. Zhang M, Xuan S, Bouxsein ML, et al. Osteoblast-specific knockout of the insulin-like growth factor (IGF) receptor gene reveals an essential role of IGF signaling in bone matrix mineralization. *J Biol Chem.* 2002;277(46):44005-44012. doi: 10.1074/jbc.M208265200 [doi].
44. Yakar S, Courtland HW, Clemmons D. IGF-1 and bone: New discoveries from mouse models. *J Bone Miner Res.* 2010;25(12):2543-2552. doi: 10.1002/jbmr.234 [doi].
45. Wang Y, Nishida S, Elalieh HZ, Long RK, Halloran BP, Bikle DD. Role of IGF-I signaling in regulating osteoclastogenesis. *J Bone Miner Res.* 2006;21(9):1350-1358. doi: 10.1359/jbmr.060610 [doi].
46. Liu JM, Zhao HY, Ning G, et al. IGF-1 as an early marker for low bone mass or osteoporosis in premenopausal and postmenopausal women. *J Bone Miner Res.* 2008;26(2):159-164. doi: 10.1007/s00774-007-0799-z [doi].
47. Kjaer M. Role of extracellular matrix in adaptation of tendon and skeletal muscle to mechanical loading. *Physiol Rev.* 2004;84(2):649-698. doi: 10.1152/physrev.00031.2003 [doi].
48. Vashishth D, Gibson GJ, Khry JJ, Schaffler MB, Kimura J, Fyhrie DP. Influence of nonenzymatic glycation on biomechanical properties of cortical bone. *Bone.* 2001;28(2):195-201. doi: S8756-3282(00)00434-8 [pii].
49. Bailey AJ, Sims TJ, Ebbesen EN, Mansell JP, Thomsen JS, Mosekilde L. Age-related changes in the biochemical properties of human cancellous bone collagen: Relationship to bone strength. *Calcif Tissue Int.* 1999;65(3):203-210. doi: CT224-98 [pii].
50. Hanschin RG, Stern WB. X-ray diffraction studies on the lattice perfection of human bone apatite (crista iliaca). *Bone.* 1995;16(4 Suppl):355S-363S. doi: 875632829400051Z [pii].
51. Frost HM. Wolff's law and bone's structural adaptations to mechanical usage: An overview for clinicians. *Angle Orthod.* 1994;64(3):175-188. doi: 10.1043/0003-3219(1994)0642.0.CO;2 [doi].
52. Weiss A, Arbell I, Steinhagen-Thiessen E, Silbermann M. Structural changes in aging bone: Osteopenia in the proximal femurs of female mice. *Bone.* 1991;12(3):165-172.
53. Jiang Y, Zhao J, Genant HK, Dequeker J, Geusens P. Long-term changes in bone mineral and biomechanical properties of vertebrae and femur in aging, dietary calcium restricted,

- and/or estrogen-deprived/-replaced rats. *J Bone Miner Res.* 1997;12(5):820-831. doi: 10.1359/jbmr.1997.12.5.820 [doi].
54. Mosekilde L, Danielsen CC, Knudsen UB. The effect of aging and ovariectomy on the vertebral bone mass and biomechanical properties of mature rats. *Bone.* 1993;14(1):1-6.
55. Aguirre JI, Plotkin LI, Stewart SA, et al. Osteocyte apoptosis is induced by weightlessness in mice and precedes osteoclast recruitment and bone loss. *J Bone Miner Res.* 2006;21(4):605-615. doi: 10.1359/jbmr.060107 [doi].
56. Kiebzak GM. Age-related bone changes. *Exp Gerontol.* 1991;26(2-3):171-187.
57. Zimmermann EA, Schaible E, Bale H, et al. Age-related changes in the plasticity and toughness of human cortical bone at multiple length scales. *Proc Natl Acad Sci U S A.* 2011;108(35):14416-14421. doi: 10.1073/pnas.1107966108 [doi].
58. Genant HK, Engelke K, Fuerst T, et al. Noninvasive assessment of bone mineral and structure: State of the art. *J Bone Miner Res.* 1996;11(6):707-730. doi: 10.1002/jbmr.5650110602 [doi].
59. Blake GM, Fogelman I. The role of DXA bone density scans in the diagnosis and treatment of osteoporosis. *Postgrad Med J.* 2007;83(982):509-517. doi: 83/982/509 [pii].
60. Damilakis J, Adams JE, Guglielmi G, Link TM. Radiation exposure in X-ray-based imaging techniques used in osteoporosis. *Eur Radiol.* 2010;20(11):2707-2714. doi: 10.1007/s00330-010-1845-0 [doi].
61. Turner CH, Burr DB. Basic biomechanical measurements of bone: A tutorial. *Bone.* 1993;14(4):595-608.
62. Bouxsein ML, Boyd SK, Christiansen BA, Guldberg RE, Jepsen KJ, Muller R. Guidelines for assessment of bone microstructure in rodents using micro-computed tomography. *J Bone Miner Res.* 2010;25(7):1468-1486. doi: 10.1002/jbmr.141 [doi].
63. Seibel MJ. Biochemical markers of bone turnover: Part I: Biochemistry and variability. *Clin Biochem Rev.* 2005;26(4):97-122.
64. Benjamin M, Kaiser E, Milz S. Structure-function relationships in tendons: A review. *J Anat.* 2008;212(3):211-228. doi: 10.1111/j.1469-7580.2008.00864.x [doi].
65. Lavagnino M, Wall ME, Little D, Banes AJ, Guilak F, Arnoczky SP. Tendon mechanobiology: Current knowledge and future research opportunities. *J Orthop Res.* 2015;33(6):813-822. doi: 10.1002/jor.22871 [doi].

66. Li Y, Ramcharan M, Zhou Z, et al. The role of scleraxis in fate determination of mesenchymal stem cells for tenocyte differentiation. *Sci Rep*. 2015;5:13149. doi: 10.1038/srep13149 [doi].
67. Tsai WC, Chang HN, Yu TY, et al. Decreased proliferation of aging tenocytes is associated with down-regulation of cellular senescence-inhibited gene and up-regulation of p27. *J Orthop Res*. 2011;29(10):1598-1603. doi: 10.1002/jor.21418 [doi].
68. Koob TJ, Vogel KG. Site-related variations in glycosaminoglycan content and swelling properties of bovine flexor tendon. *J Orthop Res*. 1987;5(3):414-424. doi: 10.1002/jor.1100050314 [doi].
69. Ippolito E, Natali PG, Postacchini F, Accinni L, De Martino C. Morphological, immunochemical, and biochemical study of rabbit achilles tendon at various ages. *J Bone Joint Surg Am*. 1980;62(4):583-598.
70. James VJ, Delbridge L, McLennan SV, Yue DK. Use of X-ray diffraction in study of human diabetic and aging collagen. *Diabetes*. 1991;40(3):391-394.
71. Tanaka S, Avigad G, Brodsky B, Eikenberry EF. Glycation induces expansion of the molecular packing of collagen. *J Mol Biol*. 1988;203(2):495-505. doi: 0022-2836(88)90015-0 [pii].
72. Martin B, Burr D, Sharkey N, Fyhrie D. Mechanical properties of ligament and tendon. In: *Skeletal tissue mechanics*. Springer; 2015:175-225.
73. Nielsen HM, Skalicky M, Viidik A. Influence of physical exercise on aging rats. III. life-long exercise modifies the aging changes of the mechanical properties of limb muscle tendons. *Mech Ageing Dev*. 1998;100(3):243-260. doi: S0047637497001474 [pii].
74. LaCroix AS, Duenwald-Kuehl SE, Brickson S, et al. Effect of age and exercise on the viscoelastic properties of rat tail tendon. *Ann Biomed Eng*. 2013;41(6):1120-1128. doi: 10.1007/s10439-013-0796-4 [doi].
75. Dunkman AA, Buckley MR, Mienaltowski MJ, et al. Decorin expression is important for age-related changes in tendon structure and mechanical properties. *Matrix Biol*. 2013;32(1):3-13. doi: 10.1016/j.matbio.2012.11.005 [doi].
76. Connizzo BK, Sarver JJ, Birk DE, Soslowsky LJ, Iozzo RV. Effect of age and proteoglycan deficiency on collagen fiber re-alignment and mechanical properties in mouse supraspinatus tendon. *J Biomech Eng*. 2013;135(2):021019. doi: 10.1115/1.4023234 [doi].
77. Haut RC. Age-dependent influence of strain rate on the tensile failure of rat-tail tendon. *J Biomech Eng*. 1983;105(3):296-299.

78. Roberts TJ, Azizi E. Flexible mechanisms: The diverse roles of biological springs in vertebrate movement. *J Exp Biol.* 2011;214(Pt 3):353-361. doi: 10.1242/jeb.038588 [doi].
79. Thorpe CT, Karunaseelan KJ, Ng Chieng Hin J, et al. Distribution of proteins within different compartments of tendon varies according to tendon type. *J Anat.* 2016;229(3):450-458. doi: 10.1111/joa.12485 [doi].
80. Nakagawa Y, Hayashi K, Yamamoto N, Nagashima K. Age-related changes in biomechanical properties of the achilles tendon in rabbits. *Eur J Appl Physiol Occup Physiol.* 1996;73(1-2):7-10.
81. Danos N, Holt NC, Sawicki GS, Azizi E. Modeling age-related changes in muscle-tendon dynamics during cyclical contractions in the rat gastrocnemius. *J Appl Physiol (1985).* 2016;jap.00396.2016. doi: 10.1152/japphysiol.00396.2016 [doi].
82. Flahiff CM, Brooks AT, Hollis JM, Vander Schilden JL, Nicholas RW. Biomechanical analysis of patellar tendon allografts as a function of donor age. *Am J Sports Med.* 1995;23(3):354-358.
83. Hubbard RP, Soutas-Little RW. Mechanical properties of human tendon and their age dependence. *J Biomech Eng.* 1984;106(2):144-150.
84. Kubo K, Kanehisa H, Miyatani M, Tachi M, Fukunaga T. Effect of low-load resistance training on the tendon properties in middle-aged and elderly women. *Acta Physiol Scand.* 2003;178(1):25-32. doi: 1097 [pii].
85. An KN, Takahashi K, Harrigan TP, Chao EY. Determination of muscle orientations and moment arms. *J Biomech Eng.* 1984;106(3):280-282.
86. Franz JR, Thelen DG. Depth-dependent variations in achilles tendon deformations with age are associated with reduced plantarflexor performance during walking. *J Appl Physiol (1985).* 2015;119(3):242-249. doi: 10.1152/japphysiol.00114.2015 [doi].
87. Ng BH, Chou SM, Krishna V. The influence of gripping techniques on the tensile properties of tendons. *Proc Inst Mech Eng H.* 2005;219(5):349-354.
88. Lu HH, Thomopoulos S. Functional attachment of soft tissues to bone: Development, healing, and tissue engineering. *Annu Rev Biomed Eng.* 2013;15:201-226. doi: 10.1146/annurev-bioeng-071910-124656 [doi].
89. Fleming BC, Beynon BD. In vivo measurement of ligament/tendon strains and forces: A review. *Ann Biomed Eng.* 2004;32(3):318-328.

90. Graham JS, Vomund AN, Phillips CL, Grandbois M. Structural changes in human type I collagen fibrils investigated by force spectroscopy. *Exp Cell Res.* 2004;299(2):335-342. doi: 10.1016/j.yexcr.2004.05.022 [doi].
91. Zajac FE. Muscle and tendon: Properties, models, scaling, and application to biomechanics and motor control. *Crit Rev Biomed Eng.* 1989;17(4):359-411.
92. Yin H, Price F, Rudnicki MA. Satellite cells and the muscle stem cell niche. *Physiol Rev.* 2013;93(1):23-67. doi: 10.1152/physrev.00043.2011 [doi].
93. Zammit PS, Relaix F, Nagata Y, et al. Pax7 and myogenic progression in skeletal muscle satellite cells. *J Cell Sci.* 2006;119(Pt 9):1824-1832. doi: jcs.02908 [pii].
94. Tajbakhsh S. Losing stem cells in the aged skeletal muscle niche. *Cell Res.* 2013;23(4):455-457. doi: 10.1038/cr.2013.3 [doi].
95. Motohashi N, Asakura A. Muscle satellite cell heterogeneity and self-renewal. *Front Cell Dev Biol.* 2014;2:1. doi: 10.3389/fcell.2014.00001 [doi].
96. Stitt TN, Drujan D, Clarke BA, et al. The IGF-1/PI3K/akt pathway prevents expression of muscle atrophy-induced ubiquitin ligases by inhibiting FOXO transcription factors. *Mol Cell.* 2004;14(3):395-403. doi: S1097276504002114 [pii].
97. Schiaffino S, Mammucari C. Regulation of skeletal muscle growth by the IGF1-akt/PKB pathway: Insights from genetic models. *Skelet Muscle.* 2011;1(1):4-5040-1-4. doi: 10.1186/2044-5040-1-4 [doi].
98. Bodine SC, Stitt TN, Gonzalez M, et al. Akt/mTOR pathway is a crucial regulator of skeletal muscle hypertrophy and can prevent muscle atrophy in vivo. *Nat Cell Biol.* 2001;3(11):1014-1019. doi: 10.1038/ncb1101-1014 [doi].
99. Sharples AP, Hughes DC, Deane CS, Saini A, Selman C, Stewart CE. Longevity and skeletal muscle mass: The role of IGF signalling, the sirtuins, dietary restriction and protein intake. *Aging Cell.* 2015;14(4):511-523. doi: 10.1111/acel.12342 [doi].
100. Adams GR. Invited review: Autocrine/paracrine IGF-I and skeletal muscle adaptation. *J Appl Physiol (1985).* 2002;93(3):1159-1167. doi: 10.1152/jappphysiol.01264.2001 [doi].
101. Glass DJ. Skeletal muscle hypertrophy and atrophy signaling pathways. *Int J Biochem Cell Biol.* 2005;37(10):1974-1984. doi: S1357-2725(05)00131-7 [pii].
102. Bonaldo P, Sandri M. Cellular and molecular mechanisms of muscle atrophy. *Dis Model Mech.* 2013;6(1):25-39. doi: 10.1242/dmm.010389 [doi].

103. Rom O, Kaisari S, Aizenbud D, Reznick AZ. Lifestyle and sarcopenia-etiology, prevention, and treatment. *Rambam Maimonides Med J*. 2012;3(4):e0024. doi: 10.5041/RMMJ.10091 [doi].
104. Kragstrup TW, Kjaer M, Mackey AL. Structural, biochemical, cellular, and functional changes in skeletal muscle extracellular matrix with aging. *Scand J Med Sci Sports*. 2011;21(6):749-757. doi: 10.1111/j.1600-0838.2011.01377.x [doi].
105. Kovanen V, Suominen H. Age- and training-related changes in the collagen metabolism of rat skeletal muscle. *Eur J Appl Physiol Occup Physiol*. 1989;58(7):765-771.
106. Ramaswamy KS, Palmer ML, van der Meulen JH, et al. Lateral transmission of force is impaired in skeletal muscles of dystrophic mice and very old rats. *J Physiol*. 2011;589(Pt 5):1195-1208. doi: 10.1113/jphysiol.2010.201921 [doi].
107. Goldspink G, Fernandes K, Williams PE, Wells DJ. Age-related changes in collagen gene expression in the muscles of mdx dystrophic and normal mice. *Neuromuscul Disord*. 1994;4(3):183-191.
108. Mays PK, McAnulty RJ, Campa JS, Laurent GJ. Age-related changes in collagen synthesis and degradation in rat tissues. importance of degradation of newly synthesized collagen in regulating collagen production. *Biochem J*. 1991;276 (Pt 2)(Pt 2):307-313.
109. Babraj JA, Cuthbertson DJ, Smith K, et al. Collagen synthesis in human musculoskeletal tissues and skin. *Am J Physiol Endocrinol Metab*. 2005;289(5):E864-9. doi: 00243.2005 [pii].
110. Mann CJ, Perdiguero E, Kharraz Y, et al. Aberrant repair and fibrosis development in skeletal muscle. *Skelet Muscle*. 2011;1(1):21-5040-1-21. doi: 10.1186/2044-5040-1-21 [doi].
111. Neels JG, Olefsky JM. Inflamed fat: What starts the fire? *J Clin Invest*. 2006;116(1):33-35. doi: 10.1172/JCI27280 [doi].
112. Taaffe DR, Henwood TR, Nalls MA, Walker DG, Lang TF, Harris TB. Alterations in muscle attenuation following detraining and retraining in resistance-trained older adults. *Gerontology*. 2009;55(2):217-223. doi: 10.1159/000182084 [doi].
113. Rodrigues CJ, Rodrigues Junior AJ. A comparative study of aging of the elastic fiber system of the diaphragm and the rectus abdominis muscles in rats. *Braz J Med Biol Res*. 2000;33(12):1449-1454. doi: S0100-879X2000001200008 [pii].
114. Klitgaard H, Bergman O, Betto R, et al. Co-existence of myosin heavy chain I and IIa isoforms in human skeletal muscle fibres with endurance training. *Pflugers Arch*. 1990;416(4):470-472.

115. Klitgaard H, Mantoni M, Schiaffino S, et al. Function, morphology and protein expression of ageing skeletal muscle: A cross-sectional study of elderly men with different training backgrounds. *Acta Physiol Scand*. 1990;140(1):41-54. doi: 10.1111/j.1748-1716.1990.tb08974.x [doi].
116. Larsson L. Morphological and functional characteristics of the ageing skeletal muscle in man. A cross-sectional study. *Acta Physiol Scand Suppl*. 1978;457:1-36.
117. Lexell J, Taylor CC, Sjoström M. What is the cause of the ageing atrophy? total number, size and proportion of different fiber types studied in whole vastus lateralis muscle from 15- to 83-year-old men. *J Neurol Sci*. 1988;84(2-3):275-294.
118. Narici MV, Maganaris CN, Reeves ND, Capodaglio P. Effect of aging on human muscle architecture. *J Appl Physiol (1985)*. 2003;95(6):2229-2234. doi: 10.1152/jappphysiol.00433.2003 [doi].
119. Morrow DA, Haut Donahue TL, Odegard GM, Kaufman KR. Transversely isotropic tensile material properties of skeletal muscle tissue. *J Mech Behav Biomed Mater*. 2010;3(1):124-129. doi: 10.1016/j.jmbbm.2009.03.004 [doi].
120. Danos N, Holt NC, Sawicki GS, Azizi E. Modeling age-related changes in muscle-tendon dynamics during cyclical contractions in the rat gastrocnemius. *J Appl Physiol (1985)*. 2016;121(4):1004-1012. doi: 10.1152/jappphysiol.00396.2016 [doi].
121. Rosant C, Nagel MD, Perot C. Aging affects passive stiffness and spindle function of the rat soleus muscle. *Exp Gerontol*. 2007;42(4):301-308. doi: S0531-5565(06)00327-5 [pii].
122. Fung YC. Elasticity of soft tissues in simple elongation. *Am J Physiol*. 1967;213(6):1532-1544.
123. Gajdosik RL, Vander Linden DW, McNair PJ, et al. Viscoelastic properties of short calf muscle-tendon units of older women: Effects of slow and fast passive dorsiflexion stretches in vivo. *Eur J Appl Physiol*. 2005;95(2-3):131-139. doi: 10.1007/s00421-005-1394-4 [doi].
124. Muraoka T, Chino K, Muramatsu T, Fukunaga T, Kanehisa H. In vivo passive mechanical properties of the human gastrocnemius muscle belly. *J Biomech*. 2005;38(6):1213-1219. doi: S0021-9290(04)00325-2 [pii].
125. Tian M, Hoang PD, Gandevia SC, Bilston LE, Herbert RD. Stress relaxation of human ankles is only minimally affected by knee and ankle angle. *J Biomech*. 2010;43(5):990-993. doi: 10.1016/j.jbiomech.2009.11.017 [doi].
126. Nordez A, Hug F. Muscle shear elastic modulus measured using supersonic shear imaging is highly related to muscle activity level. *J Appl Physiol (1985)*. 2010;108(5):1389-1394. doi: 10.1152/jappphysiol.01323.2009 [doi].

127. Strasser EM, Draskovits T, Praschak M, Quittan M, Graf A. Association between ultrasound measurements of muscle thickness, pennation angle, echogenicity and skeletal muscle strength in the elderly. *Age (Dordr)*. 2013;35(6):2377-2388. doi: 10.1007/s11357-013-9517-z [doi].
128. Moss RL, Halpern W. Elastic and viscous properties of resting frog skeletal muscle. *Biophys J*. 1977;17(3):213-228. doi: S0006-3495(77)85651-8 [pii].
129. Goodman CA, Hornberger TA, Robling AG. Bone and skeletal muscle: Key players in mechanotransduction and potential overlapping mechanisms. *Bone*. 2015;80:24-36. doi: 10.1016/j.bone.2015.04.014 [doi].
130. Bikle DD, Tahimic C, Chang W, Wang Y, Philippou A, Barton ER. Role of IGF-I signaling in muscle bone interactions. *Bone*. 2015;80:79-88. doi: 10.1016/j.bone.2015.04.036 [doi].
131. Brotto M, Bonewald L. Bone and muscle: Interactions beyond mechanical. *Bone*. 2015;80:109-114. doi: 10.1016/j.bone.2015.02.010 [doi].
132. Rudnicki MA, Williams BO. Wnt signaling in bone and muscle. *Bone*. 2015;80:60-66. doi: 10.1016/j.bone.2015.02.009 [doi].
133. Edwards MH, Dennison EM, Aihie Sayer A, Fielding R, Cooper C. Osteoporosis and sarcopenia in older age. *Bone*. 2015;80:126-130. doi: <http://dx.doi.org/10.1016/j.bone.2015.04.016>.
134. Conboy MJ, Conboy IM, Rando TA. Heterochronic parabiosis: Historical perspective and methodological considerations for studies of aging and longevity. *Aging Cell*. 2013;12(3):525-530. doi: 10.1111/ace1.12065 [doi].
135. Haubruck P, Mannava S, Plate J, et al. Botulinum neurotoxin A injections influence stretching of the gastrocnemius muscle-tendon unit in an animal model. *Toxins*. 2012;4(8):605-619.
136. Frank E, Mendelson B. Specification of synaptic connections mediating the simple stretch reflex. *J Exp Biol*. 1990;153:71-84.
137. Robertson BD, Sawicki GS. Unconstrained muscle-tendon workloops indicate resonance tuning as a mechanism for elastic limb behavior during terrestrial locomotion. *Proc Natl Acad Sci U S A*. 2015;112(43):E5891-8. doi: 10.1073/pnas.1500702112 [doi].

CHAPTER 2: Modeling Structural Changes of the Aging Muscle-Tendon Unit During Resonance

2.1. Abstract

Understanding and beneficially altering the structural changes that occur within a muscle-tendon unit (MTU) as individuals age could lead to less trips and falls. Here, we utilize a previously established simplified Hill-type model of the human triceps surae-Achilles tendon complex working on a gravitational inertial load during cyclic contractions. Our goal was to determine how stiffness changes of the muscle, or contractile element (CE), and tendon, or series elastic element (SEE), alter the mechanics and energetics within a MTU. We constructed a 2D parameter space consisting of a variety of combinations of SEE and passive elastic element (PEE) stiffness. We compared the performance of each combination by evaluating peak force, average positive mechanical power of the MTU and components, the operating point of the force-length (F-L) and –velocity (F-V) of the CE during active force production, average metabolic rate of the CE, and the apparent efficiency of the MTU and CE. Our results suggest that tendon stiffness play a larger role than muscle stiffness in governing MTU behavior. Increased tendon stiffness lead to greater shifts in operating F-L and F-V curves, as well as increased the amount of passive force generated by the CE. In aging, increased tendon stiffness may result in similar responses in humans. Future work should seek to target tendon stiffness to reduce age-related injury.

2.2. Introduction

In human locomotion, the primary structure providing the forces required for movement is the muscle-tendon unit (MTU). The MTU contains a muscle and tendon in series, where the role of tendon as an elastic tissue has proven to be important for elastic energy storage and return.^{1,2} The structure of both the muscle and tendon (e.g. pennation angle, physiological cross sectional area-

PCSA, collagen composition, etc.) directly influences the function (e.g. force, energy cycling, etc.) of the MTU.³ While there is a very good understanding of the structure or function of MTUs⁴, relatively little is known about how muscle or tendon structure orchestrates MTU function.

Different clinical populations demonstrate different structural relationships that can negatively influence MTU function. For instance, aging populations demonstrate an increase of the metabolic cost of locomotion⁵ and decrease in the overall efficiency⁶ yet the underlying causes of these changes remain poorly understood. In young individuals, the tendon serves to cycle energy, reducing metabolic cost; therefore age related structural changes to tendon may account for metabolic and efficiency changes in older individuals. Changes in collagen content of tendons in older individuals typically contribute to the development of more compliant tendons, leading to less efficient gait.⁷⁻⁹ However, the mechanism by which performance is altered is not known. Additionally, aging changes the structure of muscle. For example, aged muscles often exhibit reductions in PCSA¹⁰, maximum force¹¹, proportion of fast-twitch fibers^{12,13}, as well as an increase in passive stiffness.¹⁴ Lack of usage may result in many of these changes, as well as changes to microstructure. In regards to passive stiffness, myosatellite cells, responsible for repairing and producing new muscle, can no longer function, and muscle is instead replaced by fibrotic tissue.^{15,16} Increased fibrosis can lead to an increase of passive stiffness, but the effect of passive stiffness during functional movements has not been investigated. While aging is merely one example, other clinical conditions can demonstrate similar muscle-tendon stiffness changes, highlighting the need to understand the stiffness properties (i.e. structure) and the downstream functional changes that may occur.

Ideally, an MTU will exhibit the capacity for high forces and energy cycling in the tendon, thereby reducing muscle length changes and thus metabolically expensive muscle work.^{17,18} This

ideal behavior can be realized when the stiffnesses of the muscle and tendon are appropriately ‘tuned’.¹⁷ MTUs, when treated like a mechanical system, exhibit oscillatory behavior during locomotion.¹⁹ This oscillatory behavior can be described by the natural frequency, where, when stimulated at the natural frequency, the MTU reaches a ‘tuned’ state.²⁰ The natural frequency of any system is determined by the mass of the system and the stiffness of the system; therefore, in the case of MTUs, changing the stiffness can alter the natural frequency. However, while the natural frequency may change, the stimulation frequency may not match this new natural frequency leading to a de-tuned MTU. Therefore, understanding stiffness changes and the effect on natural frequency and MTU performance should be investigated.

While highly relevant to MTU performance, evaluating muscle and tendon stiffness in humans is difficult. Ultrasound imaging provides indirect insight into muscle and tendon stiffnesses^{7,21}, however, physically isolating MTUs *in vivo*(?) has been difficult. Reliance on animal models have been unable to reach a consensus on stiffness changes due to age: muscle stiffness remained unchanged²², or demonstrated a stiffer muscle²³, while tendon stiffness was unchanged.²⁴ Unfortunately, without an agreement between studies, it is difficult to determine what changes may occur in human MTUs. Additionally, changes in stiffness that do occur has no good guidance on correcting or improving the structure-function relationship. Therefore, computational models could have a role in identifying these structure-function relationships.

Our previous studies using computational models have demonstrated the importance of neural activation on regulating MTU function.²⁰ However, we have not yet explored the effects of structural changes within the MTU. In this study, we have modified our existing model to investigate the effects of stiffness changes of the passive properties of muscle (parallel elastic element- PEE) and tendon (series elastic element- SEE) on MTU mechanical performance. We

hypothesized that changing stiffness of the SEE or PEE away from a “normal” state (taken from the literature, see below) would: (1) reduce MTU force, (2) increase positive power performed by the muscle (contractile element- CE), and thus (3) decrease apparent MTU efficiency. We started our investigation by finding the natural frequency (ω_0) of the passive mechanical system under a load of the body with no CE activation. We then proceeded to determine dynamic properties of the system by adding CE activation to the system based on natural frequency of the “normal” case.

2.3. Methods

2.3.1. Previous Model Development

To investigate the effect that SEE and PEE stiffness has on the mechanics and energetics of gait, we modified our existing model of a cyclically stimulated MTU.²⁰ Briefly, the model included a mass-less hill-type model and PEE, in series with a non-linear SEE, operating with a fixed mechanical advantage on a point mass experiencing gravitational forces. The triceps-surae muscle group was lumped into a single non-pennate monoarticular muscle with no antagonistic muscles present. Additionally, the mass was modeled as half body mass to approximate loads during two leg hopping, and no assumptions were made regarding the flight phase (Figure 1A). Initial model parameters and equations are shown in tables 1 and 2, respectively.

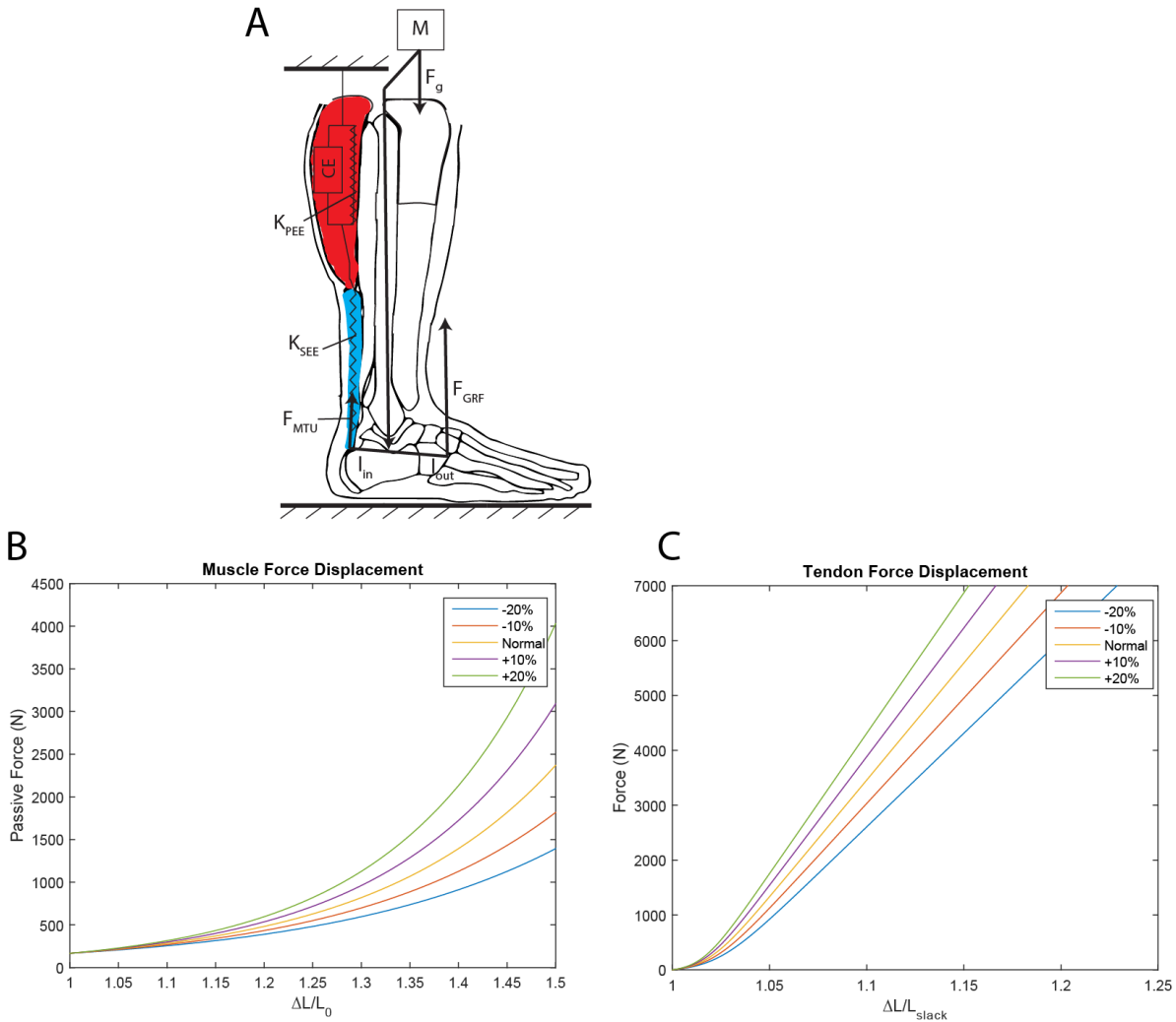


Figure 1. Physiological basis (A) for our model and force displacement curves for the PEE (B) and SEE (C). A lumped monoarticular triceps surae-Achilles tendon group interacts with a mass in gravity. System parameters and equations are shown in Tables 1 and 2.

Stimulation was modeled as a square wave pulse with a duty of 10% relative to the cycle period T_{stim} (where $T_{stim} = \omega_{stim}^{-1}$, stimulation duty = $0.1 \times T_{stim}$). Stimulation was also subject to a first order excitation-activation coupling dynamics to generate the activation function $a(t)$ to drive muscular contraction. Force generated by the muscle was modeled by:

$$F_{CE} = F_{max} \times a(u(t), \tau_{act}, \tau_{deact}) \times F_{l\ active}(l_{ce}, l_0) \times F_v(v_{CE}, v_{max}) + F_{l\ passive}(l_{CE}, l_0)$$

Where F_{CE} is total muscle force, F_{max} was maximum active isometric muscle force, $a(u(t), \tau_{act}, \tau_{deact})$ was normalized activation in terms of stimulation ($u(t)$), muscle activation (τ_{act}) and deactivation (τ_{deact}) time constants. Time constants were determined as described previously.²⁰ $F_{l\ active}$ and $F_{l\ passive}$ were instantaneous normalized force-length trajectories as a function of muscle and optimal lengths (l_{ce}, l_0 , respectively). F_v was instantaneous normalized force-velocity trajectories in terms of muscle velocity and maximum shortening velocity (v_{CE}, v_{max} , respectively).^{4,20}

Table 1. Parameter values used in model

Parameter	Value
Muscle Parameters	
F_{max}	7000 N
v_{max}	-0.45 m/s
l_0	0.055 m
Tendon Parameters	
l_{slack}	0.237 m
k_t (initial)	180,000 N/m
Activation Parameters	
τ_{act}	0.033 s
τ_{deact}	0.091 s
Pulse duty	10.0 %
Environment Parameters	
Gravity	9.8 m/s ²
EMA (l_{in}/l_{out})	0.33
Mass (Half body)	35 kg

2.3.2. Current Model Implementation

The triceps-surae MTU was modeled for a range of stiffnesses in both SEE and PEE components about a “normal” human condition (discussed below). All simulations were run for 15s with a fixed time step ($dt=0.0005$ s) and used the 4th order Runge-Kutta method to solve for system dynamics (MATLAB 2014b, MathWorks, Inc.) The final two cycles of stimulation were used in all analyses to ensure the system had reached a steady-state.

The SEE in the model contained a non-linear “toe” region at operating lengths just above the slack length, after which the stiffness was approximated as linear. Forces were generated in the SEE by the following:

$$F_{SEE} = \begin{cases} 0 & l_{SEE} \leq l_{slack} \\ k_{SEE}(k_t, F_{CE}) \times (l_{SEE} - l_{slack}) & l_{SEE} > l_{slack} \end{cases}$$

Where k_{SEE} was the stiffness function of the tendon (table 2), l_{SEE} was the length of the SEE, and l_{slack} was the slack length of the SEE. To vary the stiffness of the SEE, k_t of the stiffness function (table 2) was changed to $\pm 20\%$ at 10% increments of the “normal” condition (Normal= 180,000 N/m, range= 144,000 162,000 180,000 198,000 and 216,000 N/m). We believe these to be reasonable stiffness associated with other clinical conditions. The SEE stiffness functions for varying k_t are shown in Figure 1B.

Table 2. Equations and parameter values used in model implementation.

Parameter	Equation	Values
Muscle Force-Length		
$F_{l \text{ active}}$	$e^{- ((l_m/l_0)^b - 1)/s ^a}$	b=0.8698, s=0.3914, a=3.1108
$F_{l \text{ passive}}$	$A \times e^{(b \times ((l_m/l_0) - 1))}$	A=2.38 x 10 ⁻² , b=5.31 (initial)
Muscle Force-Velocity		
F_v when $v_m > 0$	$(1 - (v_{CE}/v_{max}))/((1 + (v_{CE}/(k \times v_{max})))$	k=0.17
F_v when $v_m < 0$	$1.8 - 0.8 \times ((1 + v_{CE}/v_{max})/(1 - 7.56 \times (v_{ce}/(k \times v_{max}))))$	k=0.17
Tendon Stiffness		
k_{SEE}	$k_t \times (1 + (0.9 / -e^{((Q \times F_{CE})/F_{max})}))$	Q=20
Activation Dynamics		
$\alpha(t)$	$\int [(u(t)/\tau_{act}) - (1/\tau_{act}) \times (\beta + (1 - \beta) \times u(t))] dt$	$\beta = \tau_{act}/\tau_{deact}$

Similarly, the PEE was modeled as non-linear with slack length and relationships based on equations from Azizi et al.²⁵ Passive forces were generated in the PEE by the following:

$$F_{l_{passive}} = A \times e^{(b \times ((\frac{l_m}{l_0}) - 1))}$$

Where $F_{l_{passive}}$ is the force generated by the PEE, A and b are constants, l_m is the length of the muscle, and l_0 is the optimal muscle length. To vary the stiffness of the PEE, the b constant was changed to $\pm 20\%$ at 10% increments of the “normal” condition (Normal= 5.31, range= 4.248 4.779 5.31 5.841 6.372). Varying the b constant $\pm 20\%$ is a reasonable approximation for passive forces demonstrated in muscles of clinical populations. The PEE force responses for varying b are shown in Figure 1.

By having a range of stiffnesses for both SEE and PEE, a 5 by 5 parameter space is generated. Each point of the space represented one condition from the model, at a specific SEE and PEE stiffness. For each condition, two simulations were performed: 1) a “passive pluck”, where the model contained no neural activation (i.e. $\omega_{stim}=0$) and instead oscillated against the mass to determine the natural frequency (discussed below), and 2) a dynamic contraction, where neural activation was supplied at a frequency equal to the natural frequency the normal case ($k_t=180,000$ N/m, $b= 5.31$, $T_{stim} = \omega_{stim}^{-1} = (\omega_{stim}^{norm})^{-1}$).

2.3.3. Model Analysis

The natural frequency of the system, ω_0 was of fundamental interest in the study. ω_0 was determined by finding the inverse of the period:

$$\omega_0 = T_0^{-1} = (x_2 - x_1)^{-1}$$

where T_0 is the period, and $x_{1,2}$ are the times (first and second, respectively) in which the model reaches peak forces during a passive pluck. ω_0 was calculated for each condition.

Operating length, operating velocity, average positive mechanical power, instantaneous metabolic power, average metabolic rate, and apparent efficiency were calculated the same as previously reported for each condition.²⁰ For simplicity, relevant formulas for calculation are shown in table 3.

Table 3. Metrics and Equations for model analyses

Metric	Equation
Metabolic Rate	
$p(v_{CE})$ for $v_{CE} < 0$	$0.01 - 0.11(v_{CE}/v_{max}) + 0.06e^{(23v_{CE}/v_{max})}$
$p(v_{CE})$ for $v_{CE} > 0$	$0.23 - 0.16e^{(-8v_{CE}/v_{max})}$
Average Positive Mechanical Power (MTU, CE, or SEE)	$\bar{P}_{mech}^+ = \left[\int_{t=0}^{T_{stim}} P_{mech}^+(t) dt \right] \times \omega_{stim}$
Metabolic Power	$P_{met}(t) = p(v_{CE}(t)) \times \alpha(t) \times F_{max} \times v_{max} $
Average Metabolic Rate*	$\dot{\bar{P}}_{met} = \left[\int_{t=0}^{T_{stim}} P_{met}(t) dt \right] \times (\omega_{stim}/M)$
Apparent Efficiency	$\bar{e}_{met} = \left(\int_0^{T_{stim}} P_{mech}^+(t) dt \right) / \left(\int_0^{T_{stim}} P_{met}(t) dt \right)$

*M=body mass

2.4. Results

2.4.1. Passive Pluck

For all modeled conditions, stable cyclic contractions were observed in the simulation time allotted. All SEE-PEE stiffness combinations resulted in natural frequencies that differed from the normal condition (i.e., 2.0 Hz) (Fig. 2). For example, compared to normal, decreasing or increasing SEE and PEE stiffness by 20% changed the MTU natural frequency to 1.8 Hz or 2.2 Hz, respectively. Different combinations of SEE and PEE stiffness resulted in curved contours, with the bottom right corner of a stiff SEE and compliant PEE demonstrating a similar natural frequency to that of the normal condition.

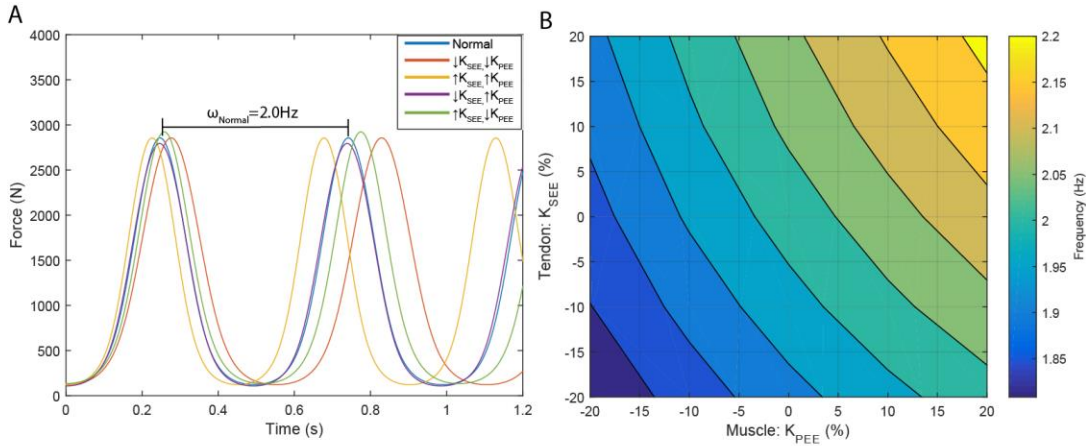


Figure 2. Passive force response of representative simulations (A), and natural frequency contour (B). The normal case (A, blue) demonstrates a natural frequency of 2.0 Hz (or a period of approximately 0.5s). Other conditions demonstrated in (A) are the $\pm 20\%$ combinations of SEE and PEE stiffness. Natural frequencies from all SEE-PEE stiffness combinations are demonstrated in the contour, with the normal condition at the center (B). Natural frequencies increase with increasing stiffness and decrease with decreasing stiffnesses

2.4.2. Flight Phase and Dynamic Response

Results from the active (i.e. muscle stimulated) simulations are shown in figure 3. A flight phase was attained in all conditions, with shorter flight phases as K_{SEE} decreased. The stiffest condition (i.e., +20% K_{SEE} and K_{PEE}) elicited the largest force response, but also increased passive force. Additionally, the time over which force developed increased in more compliant (i.e. -20% K_{SEE} and K_{PEE} relative to normal) cases. Changes in the force were more dependent on K_{SEE} changes than K_{PEE} changes. Length changes in the MTU, CE and SEE remained similar across simulations. Greater length changes of the MTU were seen in conditions where K_{SEE} was increased. Velocity and overall power responses in the MTU, CE, and SEE were also similar across the parameter space. However, in conditions where the K_{SEE} was increased, both velocities and power were increased. With regards to power, the CE also produced more power in stiffer conditions than compliant.

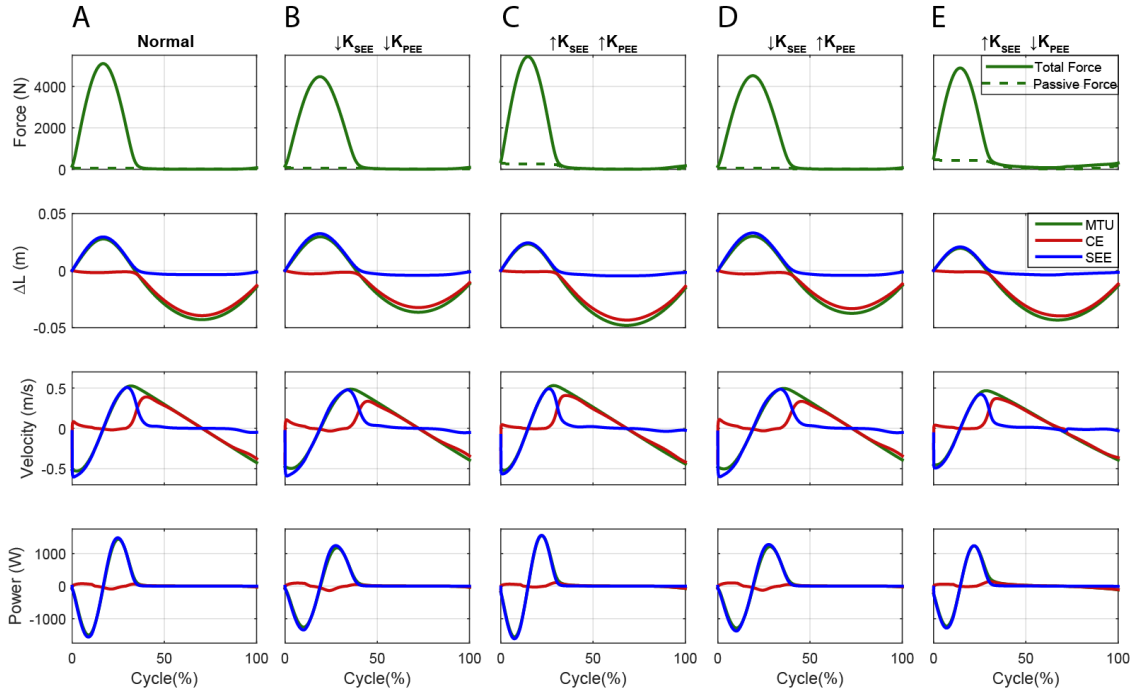


Figure 3. Periodic data for stiffness conditions of (A) Normal, (B) -20% K_{SEE} and K_{PEE} , (C) +20% K_{SEE} and K_{PEE} , (D) -20% K_{SEE} and +20% K_{PEE} , and (E) +20% K_{SEE} and -20% K_{PEE} . Each data set contains force dynamics (top), length change (first from top, $\Delta L_{CE} = l_{CE} - l_0^C$, $\Delta L_{SEE} = l_{SEE} - l_0^C$, $\Delta L_{MTU} = l_{MTU} - l_0^C$, l_0^C = length of component at start of cycle), velocity (second from top), and power (bottom). Each data set is plotted for a single period of stimulation relative to stimulation onset (0% of cycle).

2.4.3. CE Operating Length and Velocity

CE operating length and velocity was more influenced by SEE stiffness than PEE stiffness (Fig 4). Generally, increasing SEE stiffness increases the CE operating length, driving it towards longer lengths, while simultaneously increasing the range of the CE operating velocity. When K_{PEE} is increased, K_{SEE} effects are diminished and the CE operating length is driven closer to the optimum length, while the range in the operating velocity is reduced relative to the stiff case. More compliant K_{SEE} cases demonstrate little change in either operating point or range in force-length, but operating ranges are reduced in force-velocity. Changes seen in both operating length and velocity are more dependent on SEE stiffness changes than PEE stiffness changes.

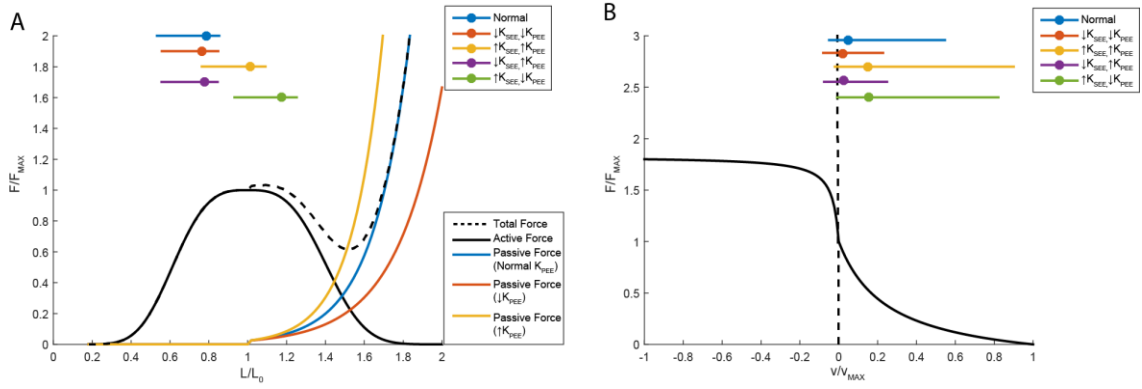


Figure 4. Normalized CE force-length (F-L, A) and -velocity (F-V, B) operating points for representative K_{SEE} and K_{PEE} . The range of F-L and F-V operating conditions occurring through active force production is indicated by colored bars, and the average operating point is marked on each bar. Passive curves for the different K_{PEE} values are shown on the F-L curve. Note that K_{SEE} and K_{PEE} modulate the F-L operating point and F-V operating point and range in stiffer conditions. Complaint cases have a smaller effect on F-L operating point, but reduce the operating range in F-V.

2.4.4. Mechanical Positive Power Production

Greatest average positive MTU power output was observed in the +15-20% range for both K_{SEE} and K_{PEE} (Fig 5A). CE average positive power was minimized when operating at K_{SEE} less than 7% of normal and K_{PEE} less than 3% of normal (Fig 5B). SEE average positive power was maximized at a K_{SEE} range of -5-+15% and K_{PEE} range of +11-20%. In general, increasing SEE and PEE stiffness served to increase SEE and MTU positive power, while having a minimal effect on the CE positive power.

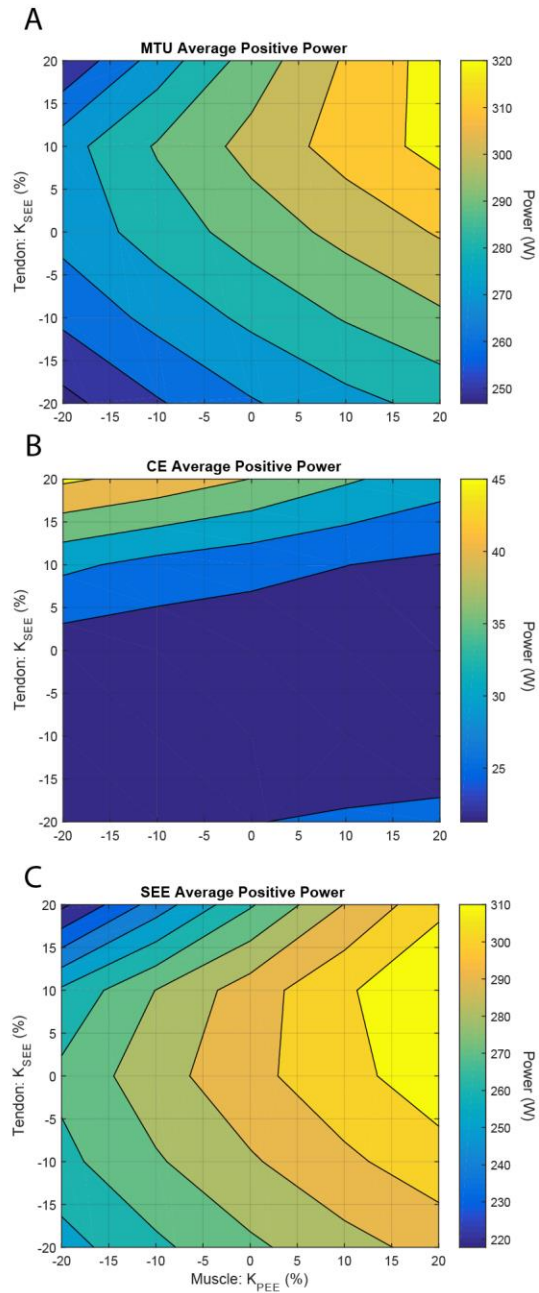


Figure 5. Average positive power produced in the (A) MTU, (B) CE, and (C) SEE for all simulation stiffness sweeps (contours). In all cases, average positive power trends with increases in K_{SEE} . CE remains relatively constant, while both MTU and SEE demonstrate larger changes overall. SEE also has a stronger dependence on K_{PEE} contributions.

2.4.5. Metabolic Rate, MTU and CE Apparent efficiency

Average metabolic rate was equally dependent on K_{SEE} and K_{PEE} , indicated by the curved contours during very compliant or very stiff cases (Fig. 6A). Cases closer to normal were more influenced by K_{SEE} than K_{PEE} demonstrated by the nearly horizontal contours in the ranges of 0-5% for K_{SEE} , and -5-5% for K_{PEE} (Fig 6A).

MTU apparent efficiency reached a maximum value of ~ 2.2 at normal K_{SEE} and 0-20% K_{PEE} (Fig 6B), and declined with either increasing or decreasing K_{SEE} to values of ~ 2.1 in the compliant cases, and ~ 1.8 in stiffer cases. MTU apparent efficiency was more dependent on K_{SEE} , indicated by nearly horizontal contours throughout.

CE apparent efficient demonstrated similar relationships to the MTU apparent efficiency (Fig 6C), although the apparent efficiency trends were flipped (i.e. high efficiencies in stiffer conditions, low efficiencies in normal and compliant cases). CE apparent efficiency ranged from a low of ~ 0.16 in the compliant cases, to a high of ~ 0.32 at high K_{SEE} and low K_{PEE} .

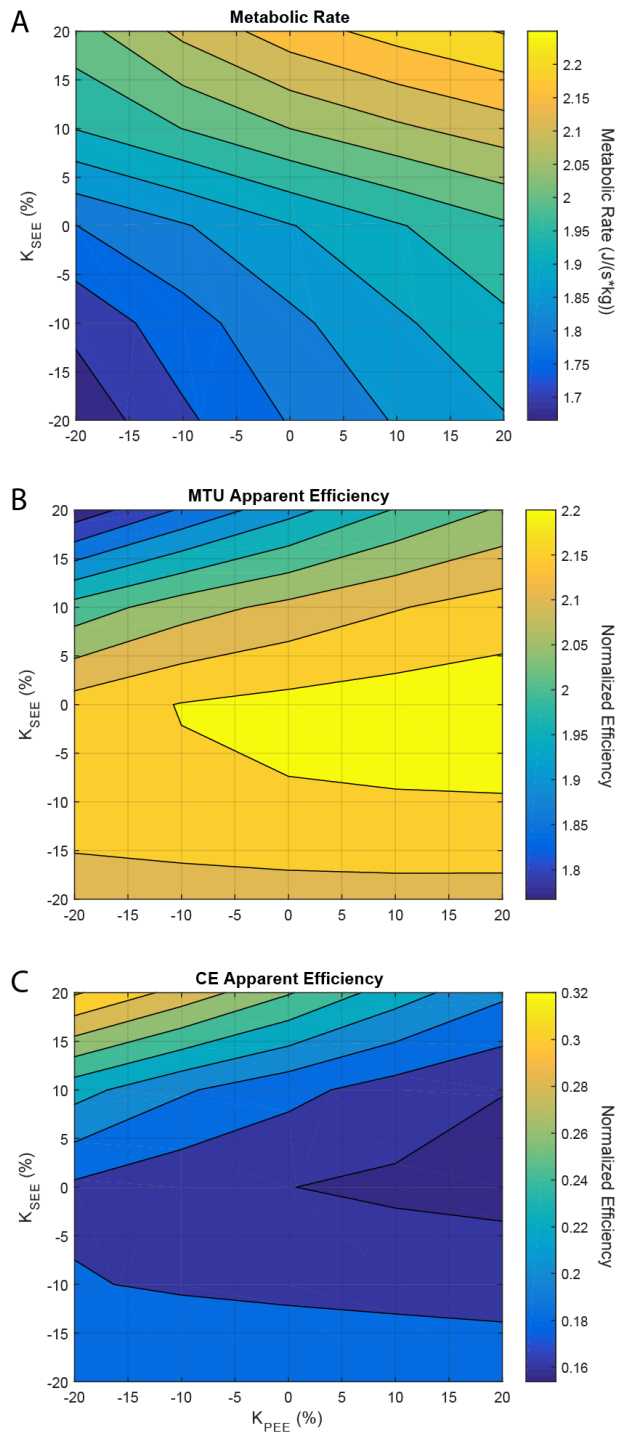


Figure 6. Average metabolic rate ($J/(s \cdot kg)$)(A), and apparent efficiency of the MTU (B) and CE (C) (contours) versus PEE stiffness (x-axis) and SEE stiffness (y-axis). Metabolic rate was K_{SEE} dependent in more normal cases (i.e. horizontal contours) (A), MTU apparent efficiency was dependent on K_{SEE} in complaint cases, and equally dependent on K_{SEE} and K_{PEE} in stiff cases (B), and CE apparent efficiency demonstrated similar dependencies as the MTU, although the efficiency trends are flipped (C).

2.5. Discussion

We conducted a simulation experiment investigating the effects of muscle and tendon stiffness on the performance of the triceps surae during cyclic movements. Our results demonstrate that triceps surae MTU dynamics are more influenced by tendon stiffness than by muscle stiffness.

2.5.1. Natural Frequency

MTU natural frequency was highly dependent on SEE and PEE structural properties, increasing with increased SEE or PEE stiffness and vice versa. Qualitatively, this matches our predicted outcome, and in outcomes shown in other similar mechanical systems.^{3,25} However, this relationship is not linear; that is, linear increases of stiffness do not lead to linear increases of natural frequency. Additionally, stiffness changes in the SEE lead to greater changes of the natural frequency than stiffness changes in the PEE. Differences between SEE and PEE stiffness responses may likely arise from material property differences, demonstrated by the force-displacement curves (fig 1). The modeled tendon is much more sensitive to changes in stiffness (table 2), which would have a greater impact on the natural frequency. These changes in natural frequency may be an underlying cause for changes seen elsewhere in the dynamic responses.

2.5.2. Force and Power During Dynamic Contractions

In partial support of hypothesis (1) the force responses from the dynamic contractions (Fig. 3, top row) were either increased or reduced. In cases where the SEE is more compliant the forces are reduced; however, in more stiff SEE cases, the forces are increased. Additionally, PEE stiffness had little effect on the force response. Increased MTU forces in the presence of increased SEE stiffness can be attributed to increased passive forces. Since the length changes by the MTU remained relatively constant across simulations, the presence of a stiff tendon does not allow for the normal tendon stretch.

While the stiffer tendon does not stretch as much, the muscle is forced to undergo greater length excursions, resulting in a greater force contributions from passive structures.²⁶ Indeed, this can be confirmed from the operating force-length curve (Fig. 4A), where the stiffer tendon cases force the muscle to operate at longer lengths. At longer lengths, the muscle acts closer to the descending limb of the active force-length curve, where passive contributions become more prominent. These passive contributions increase the overall force response which may not necessarily be beneficial.

In previous studies, increased passive force contribution can be indicative of increased muscle strain and reduced contributions from the SEE.²⁷⁻²⁹ In addition, while the model here describes the triceps surae MTU, these increased forces could have unforeseen consequences higher up the limb, leading to altered forces and moments in the knee and hip.³⁰⁻³²

In partial agreement with hypothesis (2), positive power of the CE increased for SEE stiffness greater than normal (fig 5B). However, there was little effect of PEE stiffness on CE positive power, again demonstrating the prevailing SEE stiffness effect on MTU dynamics. This is further demonstrated in SEE positive power, which increased with increasing SEE and PEE stiffnesses.

2.5.3. Metabolic Rate and Apparent Efficiency

In agreement with hypothesis (3), the apparent efficiency of the MTU decreased as stiffnesses are increased to more extreme stiff or complaint cases (fig 6B). Similar to changes in MTU mechanics, both metabolic rate and apparent efficiency of the MTU and CE were more sensitive to changes in SEE stiffness than to changes in PEE stiffness.

2.5.4. Application to Aging

Studies investigating the effects of aging on tendon properties have been unable to come to a consensus regarding their stiffness changes. Skeletal muscle changes tend to be consistent: muscle

mass declines with aging, and an infiltration of fibrotic connective tissue increases the muscle's passive stiffness. Tendon on the other hand is more undefined. Ultrasound studies in humans have demonstrated that the tendon of aged adults becomes more compliant⁷, unchanged³³, or stiffer³⁴ when compared to younger controls; additionally animal models have demonstrated that tendon can become more compliant²⁴, unchanged³⁵ or stiff.^{36,37} Using the animal model as a basis, our results demonstrate how dynamics may change in a stiff muscle-stiff tendon condition.

For instance, in a stiff-stiff condition (i.e. aged, top right corner of all contours), metabolic rate is increased, with CE apparent efficiency increased, and MTU apparent efficiency decreased compared to the normal (i.e. young) condition. Metabolic rate was modeled using CE velocity as inputs (table 2), thus operating velocity of an aged muscle should be higher than younger muscle. This is indeed the case, as the operating force-velocity curve for a stiff-stiff case (fig 4B, yellow), with the CE operating at a much larger range than younger (fig 4B, blue) cases. Therefore, CE are shortening faster at longer lengths (fig 4A), which may be detrimental to an aged gait.²⁷

In addition, force responses from the stiff-stiff condition demonstrate an increase in passive force (Fig 3C). Increased tendon stiffness would cause shorter length excursions during a contraction. As such, the muscle is forced to stretch further, leading to increased passive force contributions. Increased passive force contributions may be detrimental and lead muscle injury.²⁷ Length changes (Fig 3C) of the stiff-stiff condition further demonstrate this, as the overall muscle length change is greater than in any of the other conditions. Additionally, with increased length changes in the same period of time, the velocities are also increased. Thus, combined with the metabolic analyses described previously, in an aged condition where both muscle and tendon stiffnesses are increased, force is increased, muscle length excursion is greater, velocities are

increased, and operate less efficiently. Older individuals may overcome these detriments by adopting a “shuffled” gait characteristic of the aging population.

2.6. Conclusions/Future Directions

Using a simplified hopping model, we demonstrated the important influence of muscle-tendon stiffness in shaping triceps surae MTU mechanics and energetics. Of note, the SEE stiffness has a greater influence on MTU mechanics and energetics than PEE stiffness. This model is meant to provide support for *in vivo* experiments to understand structure-function changes with aging during human gaits. Future research will apply these findings to (1) explore stiffness in aging animal models and (2) determine ways to ameliorate stiffness changes in clinical populations, particularly aging.

2.7. References

1. Roberts TJ, Azizi E. Flexible mechanisms: the diverse roles of biological springs in vertebrate movement. *The Journal of experimental biology*. 2011;214(Pt 3):353-361.
2. Farris DJ, Sawicki GS. Human medial gastrocnemius force-velocity behavior shifts with locomotion speed and gait. *Proceedings of the National Academy of Sciences of the United States of America*. 2012;109(3):977-982.
3. Robertson BD, Sawicki GS. Unconstrained muscle-tendon workloops indicate resonance tuning as a mechanism for elastic limb behavior during terrestrial locomotion. *Proceedings of the National Academy of Sciences of the United States of America*. 2015;112(43):E5891-E5898.
4. Zajac FE. Muscle and tendon: properties, models, scaling, and application to biomechanics and motor control. *Critical reviews in biomedical engineering*. 1989;17(4):359-411.
5. Ortega JD, Fehلمان LA, Farley CT. Effects of aging and arm swing on the metabolic cost of stability in human walking. *J Biomech*. 2008;41(16):3303-3308.
6. Mian OS, Thom JM, Ardigo LP, Narici MV, Minetti AE. Metabolic cost, mechanical work, and efficiency during walking in young and older men. *Acta Physiol*. 2006;186(2):127-139.
7. Onambele GL, Narici MV, Maganaris CN. Calf muscle-tendon properties and postural balance in old age. *Journal of applied physiology*. 2006;100(6):2048-2056.
8. Coupe C, Hansen P, Kongsgaard M, et al. Mechanical properties and collagen cross-linking of the patellar tendon in old and young men. *Journal of applied physiology*. 2009;107(3):880-886.
9. Shadwick RE. Elastic Energy-Storage in Tendons - Mechanical Differences Related to Function and Age. *Journal of applied physiology*. 1990;68(3):1033-1040.
10. Buford TW, Lott DJ, Marzetti E, et al. Age-related differences in lower extremity tissue compartments and associations with physical function in older adults. *Exp Gerontol*. 2012;47(1):38-44.
11. Doherty TJ. Invited review: Aging and sarcopenia. *Journal of applied physiology*. 2003;95(4):1717-1727.
12. Deschenes MR. Effects of aging on muscle fibre type and size. *Sports medicine*. 2004;34(12):809-824.
13. Frontera WR, Reid KF, Phillips EM, et al. Muscle fiber size and function in elderly humans: a longitudinal study. *Journal of applied physiology*. 2008;105(2):637-642.

14. Gajdosik RL, Vander Linden DW, Williams AK. Influence of age on length and passive elastic stiffness characteristics of the calf muscle-tendon unit of women. *Physical therapy*. 1999;79(9):827-838.
15. Schultz E, Lipton BH. Skeletal-Muscle Satellite Cells - Changes in Proliferation Potential as a Function of Age. *Mech Ageing Dev*. 1982;20(4):377-383.
16. Brack AS, Conboy MJ, Roy S, et al. Increased Wnt signaling during aging alters muscle stem cell fate and increases fibrosis. *Science*. 2007;317(5839):807-810.
17. Dean JC, Kuo AD. Energetic costs of producing muscle work and force in a cyclical human bouncing task. *Journal of applied physiology*. 2011;110(4):873-880.
18. Farris DJ, Robertson BD, Sawicki GS. Elastic ankle exoskeletons reduce soleus muscle force but not work in human hopping. *Journal of applied physiology*. 2013;115(5):579-585.
19. Takeshita D, Shibayama A, Muraoka T, et al. Resonance in the human medial gastrocnemius muscle during cyclic ankle bending exercise. *Journal of applied physiology*. 2006;101(1):111-118.
20. Robertson BD, Sawicki GS. Exploiting elasticity: Modeling the influence of neural control on mechanics and energetics of ankle muscle-tendons during human hopping. *Journal of theoretical biology*. 2014;353:121-132.
21. Kubo K, Kanehisa H, Kawakami Y, Fukunaga T. Elastic properties of muscle-tendon complex in long-distance runners. *European journal of applied physiology*. 2000;81(3):181-187.
22. Brown M, Fisher JS, Salsich G. Stiffness and muscle function with age and reduced muscle use. *J Orthopaed Res*. 1999;17(3):409-414.
23. Rosant C, Nagel MD, Perot C. Aging affects passive stiffness and spindle function of the rat soleus muscle. *Exp Gerontol*. 2007;42(4):301-308.
24. Nakagawa Y, Hayashi K, Yamamoto N, Nagashima K. Age-related changes in biomechanical properties of the Achilles tendon in rabbits. *Eur J Appl Physiol O*. 1996;73(1-2):7-10.
25. Azizi E, Roberts TJ. Muscle performance during frog jumping: influence of elasticity on muscle operating lengths. *Proceedings Biological sciences / The Royal Society*. 2010;277(1687):1523-1530.
26. Wilson A, Lichtwark G. The anatomical arrangement of muscle and tendon enhances limb versatility and locomotor performance. *Philos Trans R Soc Lond B Biol Sci*. 2011;366(1570):1540-1553.
27. Proske U, Morgan DL. Muscle damage from eccentric exercise: mechanism, mechanical signs, adaptation and clinical applications. *J Physiol*. 2001;537(Pt 2):333-345.

28. Rassier DE, Lee EJ, Herzog W. Modulation of passive force in single skeletal muscle fibres. *Biol Lett.* 2005;1(3):342-345.
29. Koh TJ, Peterson JM, Pizza FX, Brooks SV. Passive stretches protect skeletal muscle of adult and old mice from lengthening contraction-induced injury. *J Gerontol A Biol Sci Med Sci.* 2003;58(7):592-597.
30. Fukui T, Ueda Y, Kamijo F. Ankle, knee, and hip joint contribution to body support during gait. *J Phys Ther Sci.* 2016;28(10):2834-2837.
31. Svoboda Z, Janura M, Kutilek P, Janurova E. Relationships between movements of the lower limb joints and the pelvis in open and closed kinematic chains during a gait cycle. *J Hum Kinet.* 2016;51:37-43.
32. D'Lima DD, Fregly BJ, Patil S, Steklov N, Colwell CW, Jr. Knee joint forces: prediction, measurement, and significance. *Proc Inst Mech Eng H.* 2012;226(2):95-102.
33. Lewis G, Shaw KM. Tensile properties of human tendo Achillis: effect of donor age and strain rate. *J Foot Ankle Surg.* 1997;36(6):435-445.
34. Waugh CM, Blazeovich AJ, Fath F, Korff T. Age-related changes in mechanical properties of the Achilles tendon. *J Anat.* 2012;220(2):144-155.
35. Pardes AM, Beach ZM, Raja H, Rodriguez AB, Freedman BR, Soslowsky LJ. Aging leads to inferior Achilles tendon mechanics and altered ankle function in rodents. *J Biomech.* 2017;60:30-38.
36. Elliott DH. Structure and Function of Mammalian Tendon. *Biol Rev Camb Philos Soc.* 1965;40:392-421.
37. Kjaer M. Role of extracellular matrix in adaptation of tendon and skeletal muscle to mechanical loading. *Physiol Rev.* 2004;84(2):649-698.

CHAPTER 3: Structural and Functional Changes of Aged Muscle-Tendon Units During Resonance Tuning

3.1. Abstract

In aging, there are changes in structure and function of muscle and tendon that can result in declined locomotion behavior. However, the causes for these changes are not well understood, with potential experiments being too invasive for human studies. Here we utilize an animal model to investigate the age-related changes in the structure-function properties of muscle-tendon units (MTUs). We quantified the passive and active properties of the medial gastrocnemius muscle and the passive properties of the Achilles tendon in young (~6 month) and old (~32 month) rats. Using these properties, we used our previously established motor controller to simulate hopping locomotion at a variety of stimulation driving frequencies. The changes observed between the age groups were small, yet old MTUs demonstrated increased muscle stiffness, decreased tendon stiffness, and decreased force output, decreased length change, and increased power outputs at slower driving frequencies. These results suggest that the higher metabolic cost associated with aging is in part due to the altered stiffnesses of MTUs. Furthermore, these changes in the stiffnesses can lead to shifts in the force-length and force-velocity operating range that can effect mechanical performance, yet remains on marginally affect by the driving frequency. Our study demonstrates the changes of elastic MTU behavior during cyclic contractions in aging.

3.2. Introduction

The conserved process of aging can result in declining mobility for older populations. Studies have demonstrated that older individuals exhibit an increase in metabolic cost of walking¹, decreased efficiency while running^{2,3}, and decreased force production within the muscle.⁴ This loss of function associated with age may be the result of several factors including: decreased

efficiency of muscle contraction⁵, decreased muscle mass or cross sectional area of the muscle⁴, increased deposition of non-contractile proteins (e.g. collagen)⁶⁻⁸, or other changes in muscle architecture that leads to an altered stiffness of the muscle-tendon unit. Understanding these underlying geometric or structural changes to the muscle tendon unit during aging could lead to new therapies reducing the severity of the functional decline.

Unfortunately, how specific structural changes lead to altered functioned outcomes are not well understood. Furthermore, studies investigating these relationships in the triceps surae muscle group have demonstrated different responses in different mammalian models. For instance, in humans, the muscle becomes stiffer, with the tendon becoming more compliant.^{9,10} Meanwhile rat model studies have demonstrated that both the muscle and tendon become stiffer.¹¹ The discrepancy between these two findings may be explained by the experimental methods used to acquire data of this nature. For instance, human studies often utilize less invasive techniques such as ultrasound to estimate length changes of a given muscle^{12,13}, while forces have to be estimated utilizing force plates and inverse dynamics¹⁴, or more invasive strain gauges.¹⁵ Animal studies can use these same whole body metrics^{16,17}, or more invasive surgical techniques where entire muscle can be isolated.^{11,18}

Another issue for determining appropriate structure-function relationships arises when considering the individual properties of muscle tendon units. Each skeletal muscle exhibits a non-linear excitation-contraction coupling and a non-linear stress-strain relationship.¹⁹ Both the tendon and muscle exhibit non-linear force displacement dynamics¹⁹, as well as variable gearing in muscle²⁰, and variable stiffness of the aponeurosis between the muscle and tendon.²¹ The history-dependent nature of muscle tendon units also plays a role in the potential response.^{22,23} Furthermore, across the lower limb, muscle tendon units can exhibit different origin and

attachment sites, geometries, wrapping, and biological moment arms that can further influence its function.²⁴ Therefore, experiments designed to solve some of the structure function relationships require simple approaches to isolate one or more of these variables.

Previous work performed by our lab sought to study mechanically simple behaviors such as hopping or bouncing to better understand elastic muscle tendon interactions at the ankle joint.^{25,26} The stationary behavior of hopping preserves the spring-like effects of walking, but minimizes involvement at other joints. Our work and those of the others have demonstrated that bouncing behavior of the muscle-tendon unit can be “tuned” to a resonant frequency such that the movement cycles large energy amounts in the tendon and aponeurosis.²⁵⁻²⁸ Tuned muscle-tendon mechanics results in spring-like joint behavior with mechanical power and efficiency beyond what is possible with muscle alone. Furthermore, neural control during these experiments cannot be overlooked. Using isolated muscles in workloop based experiments have demonstrated that influence of neural control on muscle function. In our previous experiments, a custom controller utilizing a simple harmonic model was used to simulate a natural hopping gait and was applied by an ergometer, with the timing of muscle activation varied in a controlled manner with respect to the phase of the movement cycle.²⁶ Our results showed that these experiments can lead to the identification of a neural stimulation pattern appropriate for net zero work and large amounts of energy storage and return.²⁶ However, this approach has not been utilized to study the effects of aging. Previous *in situ* studies drove an MTU at a constant sine wave¹¹, which may underestimate the behavior of the MTU during locomotion.

The purpose of this study was to examine the age-related changes in a MTU during hopping locomotion. We use an animal model of aging, the F33xBN rat (developed by the National Institute on Aging), to establish a more controlled environment that avoids the problems of human studies.¹¹

Furthermore, this strain is well suited for aging since it avoids confounding pathologies common in other systems. Our general hypothesis was that changes in the structure of the MTU due to age would drive subsequent changes in the function of the MTU. More specifically, we hypothesized that old MTU would demonstrate and increased stiffness, comparable to other studies, which would in turn lead to an increased resonant frequency when compared to young. We also expected the old MTU would have lower forces, decreased length changes, and decreased power outputs when compared to young. Finally, as each age MTU was driven at frequencies away from the resonant frequency, the behavior would change MTU trajectories such that they are no longer ideal for elastic energy storage and return.

3.3. Methods

3.3.1. Animal Subjects

All experiments performed were approved by the North Carolina State University Institutional Animal Care and Use Committee. Young (n=12, age 5-9 mo, body mass:) and old (n=10, age 33-34 mo, body mass:) male Brown Norway x F344 F1 hybrid rats, *Rattus norvegicus*, were obtained from the National Institute on Aging (F344BN; Bethesda, MD) and housed in the NC State University Biological Resources Facility. On arrival, there was a 1-wk adaptation period before use in experiments. Animals were fed standard chow and water ad libitum.

3.3.2. Surgical Protocol and Instrumentation

Before use in experiments, animals were anesthetized using 2% isoflurane, and maintained on a closed-system anesthesia machine (Kent Scientific, Torrington, CT). The animal was placed prone on a heated surgical stage (Aurora Scientific, Aurora, ON, Canada). The sciatic nerve was exposed via a small incision running from the caudal midline of the hind limb toward the base of the tail. A bipolar nerve cuff (Microprobes for Life Science, Gaithersburg, MD) was placed around

the nerve, and the nerve was severed proximally. The area around the cuff was filled with mineral oil and covered with a saline-moistened gauze. The Achilles tendon and gastrocnemius muscle were identified and exposed. Sonomicrometry transducers (1 mm diameter; Sonometrics Inc., London, ON, Canada) were implanted along a fascicle of the medial gastrocnemius (MG). This allowed for measurement of the muscle fiber length and velocity. All tendons, except that of the MG were severed and the calcaneus was cut leaving a bone chip attached to the MG tendon. This chip and tendon were secured in a custom-made clamp, maintaining as much free tendon unclamped as possible. An incision was made on the lateral side of the thigh and the femur was clamped into a stereotaxic frame. The tendon clamp was connected to the lever arm of an ergometer (310 C-LR; Aurora Scientific) using a steel cable (3 cm). The muscle was wrapped in a saline-moistened gauze and Saran wrap, and muscle temperature was maintained at 37°C using a heat lamp.

3.3.3. Determination of Muscle-Tendon Properties

Isometric fixed end tetanic contractions were elicited by a supramaximal 0.2-ms pulses at a pulse rate of 100 Hz for 400 ms (701 C stimulator, Aurora Scientific) under various amount of passive tension to produce a force-length curve. This allowed the quantification of both the optimal length (L_0) and maximal isometric force (F_{max}) of the MTU. After-loaded isotonic tetanic contractions were used to determine the force-velocity relationship of the muscle with the same stimulation protocol used for force-length determinations. Force was allowed to rise to a defined level of F_{max} (10, 30, 50, 70, or 90%), and the muscle was allowed to shorten to ensure a constant force. The order of passive forces (in force-length stimulations) and force level (in force-velocity stimulations) were randomized and a 3-min rest period was allowed for recovery between

stimulations. Maximum shortening velocity (v_{max}) was obtained by fitting the Hill equation to the pooled data for each age group.

To determine the system passive resonant frequency (ω_0) of the simulated environment, we allowed the MTU to oscillate against our simulated inertial system²⁶ until steady state behavior was reached. This approach also estimated linear MTU stiffness for the selected environment parameters (mass= 0.008 kg, length in= 54 , length out= 1). Using these parameters, the equilibrium force with which the system tended to oscillate around could be calculated:

$$F_{eq} = mg\left(\frac{l_{out}}{l_{in}}\right)$$

$$F_{eq} = 4.23 N$$

Linear MTU stiffness was calculated by finding the slope of the force rise during a passive oscillation around the equilibrium force. Passive stiffness of tendon (k_{SEE}) was calculated by estimating the slope of the force rise during a fixed end contraction around the equilibrium force. Passive stiffness of the contractile element (k_{CE}) was estimated by assuming that k_{CE} and k_{SEE} acted as a spring in series and solving for k_{CE} :

$$k_{MTU} = \frac{k_{CE}k_{SEE}}{k_{CE} + k_{SEE}}$$

$$k_{CE} = \frac{k_{MTU}k_{SEE}}{k_{MTU} - k_{SEE}}$$

All stimulation frequencies in dynamic conditions were centered on the resonant frequency value. Before dynamic conditions, eight fixed end contractions were performed at the resonant frequency and a stimulation duty of 10% as a means of determining a baseline force for estimating muscle fatigue. This pattern of stimulus was also applied to dynamic conditions.

For conditions where the active MTU performed a dynamic interaction with the simulated inertial load, the driving frequency was varied $\pm 40\%$ ω_0 in 20% intervals. Driving frequencies were

randomized to hinder fatigue effects, and each frequency conditions consisted of eight cycles of stimulation. Simulation specifics for dynamic contractions are reported in Robertson et al. Briefly, each trial began with the MTU under optimal passive tension and the inertial load resting on a virtual table. The table would disengage when the MTU force exceeded that of the gravitational load. Once the condition was satisfied, the table is removed and the MTU is allowed to oscillate against the load with no constraint placed on the system. The system was allowed 3-4 cycles to reach steady state behavior and the following 3 cycles were used in the subsequent analysis. MTU component mechanical power (P_{mech}) was calculated for these experiments by:

$$P_{mech}(t) = F(t) \times \frac{d}{dt}L(t)$$

Where $F(t)$ and $L(t)$ were recorded force vs. time and length vs. time, respectively. Additionally, operating length and velocity were calculated as described previously.

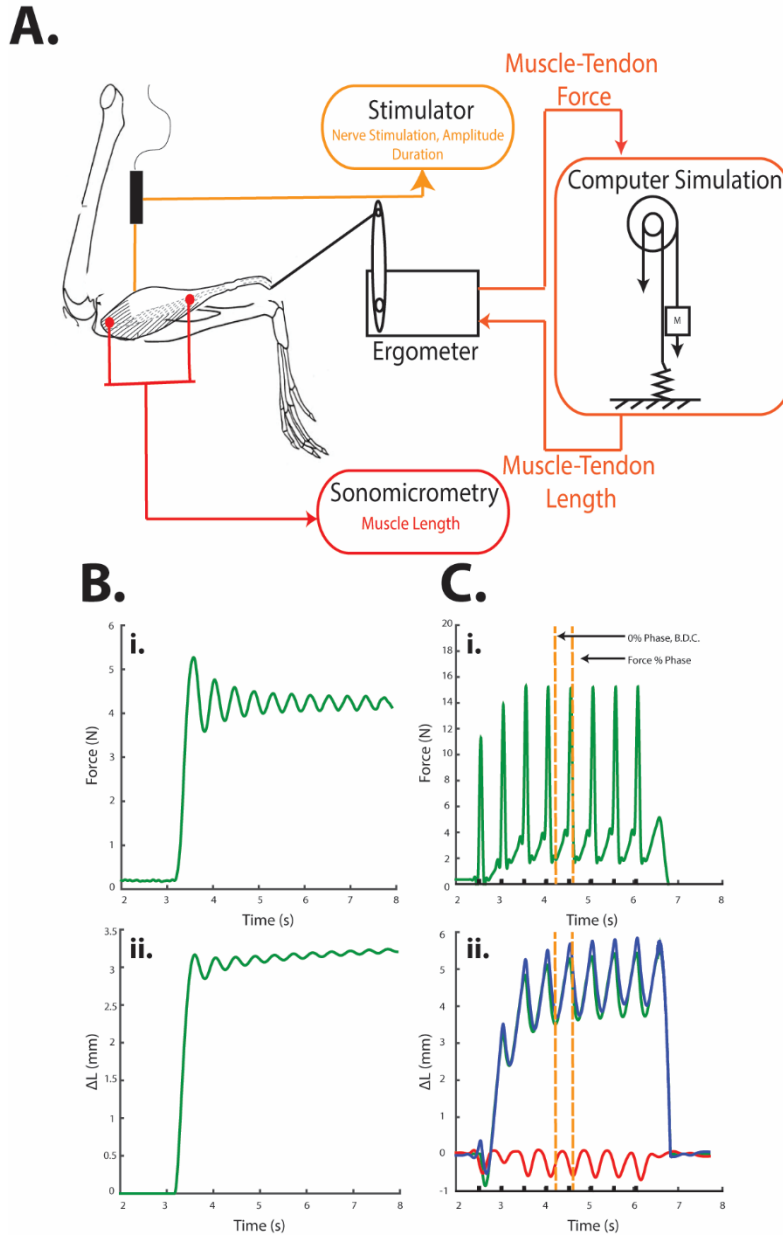


Figure 1. (A) Schematic of *in situ* stimulation, (B) Force (i) and displacement (ii) data from a passive pluck condition, and (C) full force (i) and displacement (ii) data representative of the ω_0 condition. Note that patterns are cyclic. Notice that the system stabilizes and reach steady state quickly. The convention used to define muscle phase is annotated between C, i and ii.

3.3.4. Determination of Phase and Average Total Power

Phase data were calculated relative to the minimum MTU length observed for each stretch-shortening cycle and normalized to stimulation onset for each conditions. A schematic of these

measured values is shown in Figure 1C. Phase values from other workloops studies are reported in this manner where wave-like trajectories are applied; experiments performed herein are comparable to these previous studies.

Average positive-mechanical power (\bar{P}_{mech}) for the MTU was computed by integrating instantaneous mechanical power over a cycle and dividing by the stimulation cycle period ($T_{Drive} = \omega_{Drive}^{-1}$) by the following:

$$\bar{P}_{mech} = \frac{1}{T_{Drive}} \int_{t=0}^{t=T_{Drive}} P_{mech}(t) dt$$

In order to calculate average positive and negative powers (\bar{P}_{mech}^+ and \bar{P}_{mech}^- , respectively), the same calculation was made for only the regions of either positive or negative instantaneous power.

3.3.5. Statistical Analysis

Due to the difficulty of the surgical preparation, not all animal subjects could complete a full data set. We therefore compiled the data for each dependent variable based on the animals where data was collected, and the results shown indicate the different number of subjects for each table or plot. We conducted a two-factor repeated measures ANOVA (factors: muscle stimulation frequency and animal age) to test for an effect of either factor on a number of key dependent measures of muscle-tendon mechanics and energetics during dynamic contractions ($\alpha=0.05$, Graphpad Prism, GraphPad Software, San Diego, CA). For dependent measures where two-factor ANOVA main effects or interactions were significant ($p<0.05$), we performed Tukey's post-hoc analysis for multiple comparisons.

3.4. Results

3.4.1. Active and Passive Parameters

Our active and passive parameters differ from other studies describing age-related changes in the muscle tendon unit. We found that while there was no significant differences between age groups, aged animals tended towards a decrease in the maximum isometric force (F_{\max}) and an increase in the maximum shortening velocity (v_{\max})(Table 1). We observed no differences in the optimal lengths of the MTU, SEE, or CE between age groups. However, we found that at longer lengths, the aged MTU was slightly stiffer compared to young. Furthermore, we also found that the stiffness of the series elastic tendon tended toward a decrease in aged MTU, resulting in increase of the stiffness of the CE, contrary to previous studies.²⁹ Due to this alternating trade-off in stiffness, we observed no difference in the resonant frequency (ω_0) between age groups.

Table 1. Experimentally derived parameters for young and old rat medial gastrocnemius muscle-tendon unit

	Young (n=6)	Old (n=6)
Mass		
Body mass,* g	371.45 ± 7.18	559.66 ± 31.22
MTU mass, g	1.75 ± 0.19	2.27 ± 0.20
Active Parameters		
F_{\max} , N	18.83 ± 3.74	13.87 ± 2.45
v_{\max} , ^a m/s	0.128	0.179
Passive Parameters		
L_0 MTU, m	0.028 ± 0.001	0.027 ± 0.002
L_0 SEE, m	0.017 ± 0.003	0.016 ± 0.002
L_0 CE, m	0.011 ± 0.001	0.012 ± 0.001
k_{MTU} , ^b N/m	3683 ± 307.1	5867 ± 1960
k_{SEE} , ^c N/m	6102 ± 1303	5423 ± 1069
k_{CE} , ^d N/m	8641 ± 4237	9686 ± 6439
ω_0 , ^e Hz	2.14 ± 0.08	2.11 ± 0.09

Values are mean ± SEM

*Values are significantly different between young and old ($p < 0.05$)

^aValue was estimated by fitting a single curve to the complied data for each age group

^bValue was estimated by determining the slope of force rise during passive oscillation through the equilibrium force within a passive pluck

^cValue was estimated by determining the slope of force rise as the length passes through the equilibrium force

^dValue was estimated by rearranging the spring series stiffness equation and solving for k_{CE}

^eCalculated by averaging the period over 5 cycles and determining the inverse

3.4.2. Overall System Dynamics

In general, the system dynamics were observed to be cycle and self-stabilizing (Fig 1C, i and ii). A representative dataset showing the mean of three cycles of muscle stimulation across all available animals and driving frequency (ω_{drive}) conditions are shown in Fig 2 (normalized data shown in Fig S2). We assumed that the pennation effects were small. Observations demonstrate that there are alternating phases of energy storage and return within the MTU over a stretch-shorten cycle. All data are plotted against relative axes (Absolute ΔL , and mean behavior in force, length changes, and power output were small within a single animal, further demonstrating steady and periodic behavior.

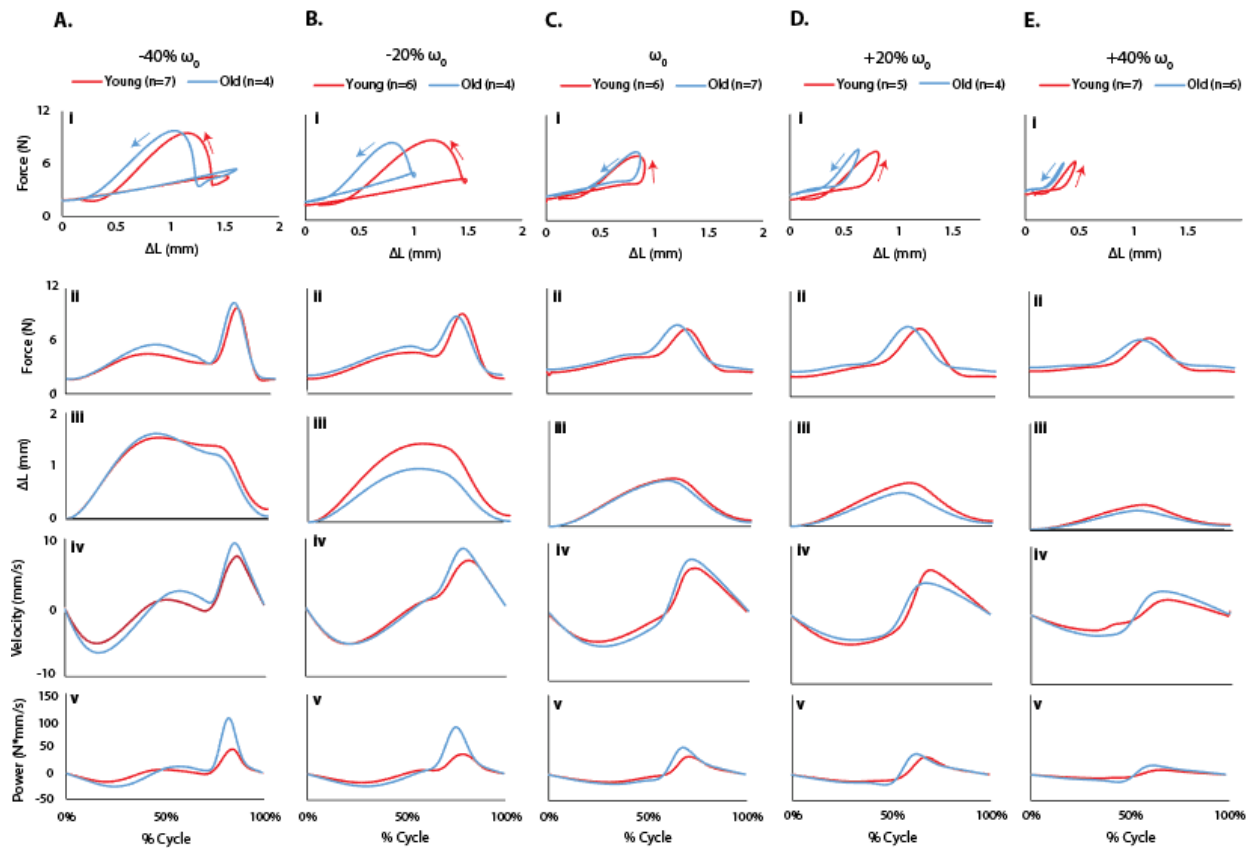


Figure 2. Averaged dataset across all viable preparations showing (i) mean workloop, (ii) force, (iii) ΔL , (iv) velocity, and (v) mechanical power output for the (A) $-20\% \omega_0$, (B) $-10\% \omega_0$, (C) ω_0 , (D) $+10\% \omega_0$, and (E) $+20\% \omega_0$ conditions. All mean data are based on four stimulation cycles from each conditions. All cycles begin and end at BDC.

3.4.3. MTU Peak Force, Phase Dynamics, and Mechanical Power Output

MTU peak did not differ with respect to muscle stimulation driving frequency, ω_{drive} ($P=0.70$), or with age ($P=0.75$) (Fig 3A). Maximal peak MTU force approached $0.7 \times F_{\text{max}}$ in young and $0.55 \times F_{\text{max}}$ for a driving frequency of -40% and $-20\% \omega_0$ and tended to decrease to $0.45 \times F_{\text{max}}$ and $0.53 \times F_{\text{max}}$ in young and old, respectively.

MTU peak force phase decreased significantly with increasing ω_{drive} ($P<0.0001$), yet was not different across age ($P=0.11$) (Fig 3B). At lower ω_{drive} , peak force phase occurred $\sim 70\%$ of a cycle after minimum MTU length, or “bottom dead center” (BDC) across both ages. As ω_{drive} increased, peak force phase continued to decrease to $\sim 40\%$ of a cycle relative to BDC at $+40\% \omega_{\text{drive}}$.

Average net mechanical power output ($\bar{P}_{\text{mech}}^{\text{net}}$) of ~ 0 was observed across all frequencies in the MTU across both ages (Fig 3C). A net of zero indicated steady cyclic behavior similar to that of locomotion on level ground. Also, net zero output was the result of equal amount of average positive and negative mechanical power from the MTU. However, at lower stimulation frequencies, the net mechanical power output was slightly higher than 0 suggesting a more unstable system, and an increase in the positive amount of power generated. Both positive and negative mechanical power decreased as driving frequency increased.

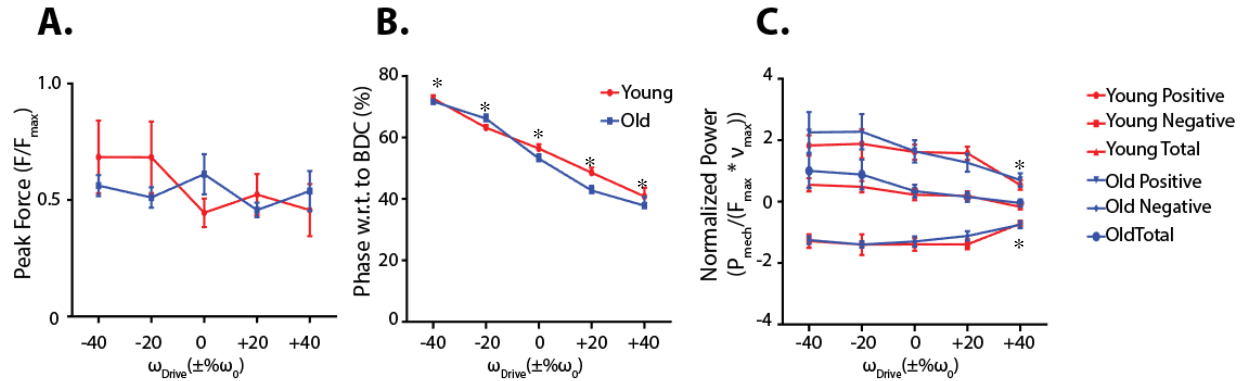


Figure 3. Mean \pm SE data for (A) normalized peak force, (B) peak force phase, and (C) MTU positive, negative, and net average mechanical power over a cycle of stimulation. All power units are reported as AU due to complexity of units. In all figures, conditions significantly different ($P < 0.05$) from other driving frequency conditions are indicated by *.

3.4.4. Operating Length and Velocity

MTU operating length and velocity tended to be more influenced by age than driving frequency (Fig 4). In young, shifting away from a driving frequency of resonance lead to operating a longer lengths (Fig 4A) and faster shortening velocities (Fig 4C), while decreasing the operating range for each. In general, however, the operating length ranges remain small between both young and old. In old, higher driving frequencies led to operating at shorter lengths (Fig 4B) and slower velocities (Fig 4D). Slower driving frequencies in old demonstrate little change in either operating point or range in length or velocity relative to driving at the resonant frequency. Between young and old, there was also a general shift of the active force-length curve.

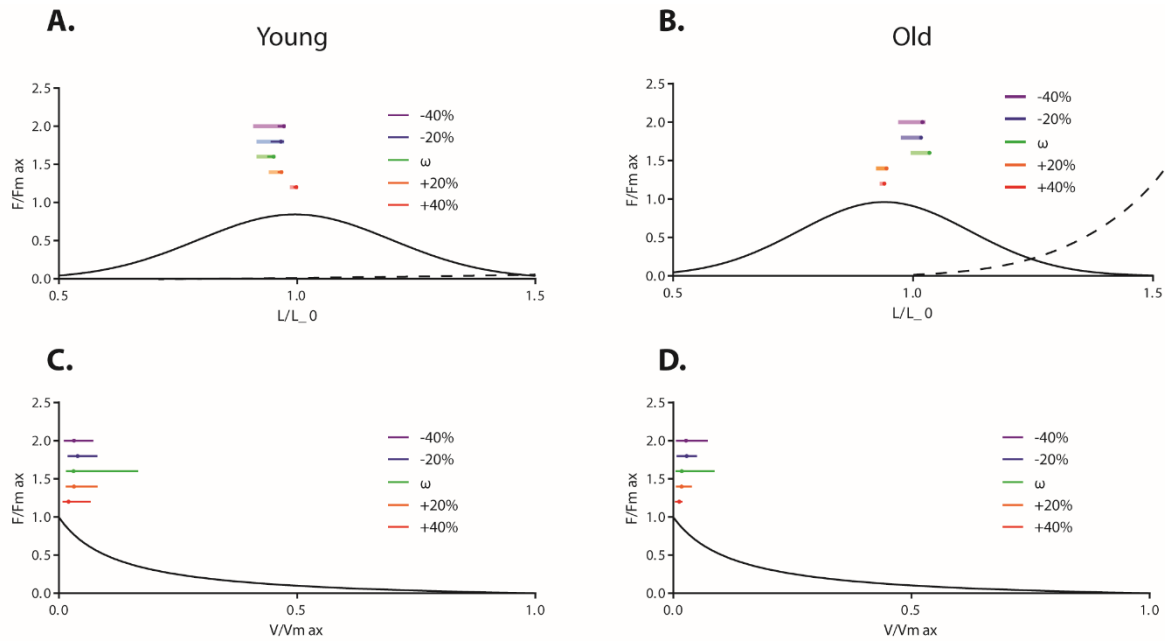


Figure 7. Operating length from (A) young and old (B), and operating velocity from young (C) and old (D) averaged across all viable experiments during stimulation. Means are labeled with (●) and ranges are labeled with bars from the active contraction. In (A) and (B), the length over the entire cycle is shown with translucent bars. Means are averaged across four stimulation cycles. Note the small operating ranges across both young and old conditions.

3.5. Discussion

In this study, we used both young and old MTUs to evaluate the changes that occur in structure and function during locomotion. Our general hypothesis that structural changes in the aged MTU would lead to detrimental functional outcomes was partially supported.

3.5.1. MTU active and passive properties with age

One specific hypothesis was that old MTUs would demonstrate increased stiffness leading to an increased resonant frequency. We discovered in the medial rat gastrocnemius that the tendon and muscle underwent small, insignificant changes to stiffness with advanced aging (Table 1), in contrary to previously reported studies.¹¹ Other studies have reported an increase in both stiffnesses for muscle and tendon, hypothesized to be the result of increased collagen deposition as muscle stem cells shift from a muscle-forming fate to a fibrogenic fate.^{11,30,31} The small changes

we observed demonstrated that old MTU tend towards more compliant tendons and stiffer muscles. These findings suggest that muscles may undergo this increased deposition of collagen, while the tendon may not replace or add additional collagen. These data add more to the ongoing debate of whether the tensile properties of tendons increase, decrease, or have no effect as a result of changing collagen properties.³²⁻³⁶ Furthermore, other studies have demonstrated that tendons can have different structural and material properties depending on their *in vivo* function.³⁷ Therefore, the discrepancy between our results and those of others may be the result of the activity of individual animals leading to different structural and material properties of each individual animal. Future studies should seek to monitor the activity of these animals as they age to better pair with the structure changes that may or may not occur.

These small changes in stiffness led to only minimal changes in the resonant frequency between young and old MTUs. In our previous modeling work (currently under review), changes in stiffness between the muscle and tendon result in contours along which the resonant frequency can change. The most extreme cases of resonant frequencies changing were due to muscle and tendon stiffnesses changing in the same way (i.e., muscle and tendon both becoming more stiff or more compliant). In cases where muscle and tendon stiffness are changed different to each other, the resonant frequency does not change, or only minimally. Therefore, this aspect of our hypothesis was not supported.

3.5.2. Overall System Dynamics

Another aspect of our hypothesis was that old MTUs would demonstrate decreased force, decreased length changes, and decreased power outputs when compared to young. While we also observed no change in the maximum isometric force (Table 1) or with different resonant frequencies (Fig 2ii, Fig 3A) with aging, the results suggest that aged MTU were trending towards

a reduction, similar to numerous other studies.^{11,38} Our lack of a significant difference may be the result of high variability between animals, or that the masses of the old animals were slightly larger than of those reported previously¹¹. Furthermore, across different driving frequencies, there was no difference to the change in maximal force produced (Fig 3A). This was in contrast to our previous work, where maximal force was reached when the system was driven at its own natural frequency.³⁹ These data may suggest that peak forces could be reached regardless of driving frequency. This result suggests that in this preparation, the driving frequency may not be as important in regulating the force output of the system.

With regard to length changes, old MTUs demonstrated small, decreased length changes compared to young (Fig 2iii), suggesting that old MTU become slightly more stiff, in agreement with our data collected from isometric testing (Table 1). Additionally, these differences become more pronounced at slower driving frequencies. This shift can be explained by the longer time between cycles. As young MTUs are slightly more compliant, they are able to undergo a longer range of length change over a wider period of time, yet due to being stiffer, old MTUs cannot make the same change in length in the same period of time. Furthermore, these smaller length changes resulted in smaller operating length ranges for old MTUs (Figs 4A and B). Since operating lengths were calculated based on regions where the stimulus was active, the length changes during this period (~50%-75% of the cycle) were nearly isometric, evidenced by the plateau-like regions of the length curves in the old MTUs (Fig 2iii). At higher stimulation frequencies, the old operating lengths got shorter and shifted toward to the ascending limb of the length tension curve. These reductions in operating lengths suggested by these results may protect the muscle from damage, as suggested by other studies.⁴⁰⁻⁴² As older muscles may be more prone to stretch-induced damage, this observation may be particularly beneficial.

These length changes, while small, occurred over a short period time, resulting in similar operating velocities between young and old (Figs 4C and D). Other studies have reported the same or slower velocities in old MTUs and muscles.^{11,43,44} Slower velocities in aged muscles is hypothesized to be the result of a loss of fast-type fibers, and preference to retain slow fibers.⁴⁵ Our results demonstrate almost no changes in operating velocity or v_{\max} between age groups. There was also no difference between operating velocity between driving frequencies. These results suggest that any changes to fiber type in the muscle were small. With these small changes in force, length, and velocity, power results were also only marginally affected. Furthermore, the influence of a dynamic load lead to more complex interactions between force, length, operating length and velocity, and stiffness, which may lead to a washing out effect of any differences.

In disagreement with our hypothesis, old MTUs did not demonstrate a change in power production compared to young. At slower driving frequencies, old MTUs tended towards an increase in the amount of positive power produced (Figs 2A and Biii, Fig 3C), but this increase was minimized at faster driving frequencies. In contrast to our previous work, power was not maximized at resonance²⁶, with instead the greatest amount of power occurring at $-40\% \omega_{\text{drive}}$. This increase in power is likely the result of the slightly increased stiffness of the old MTU and associated velocity change that occurs over a shorter period of time. Furthermore, young MTUs seemed more resistant to changes in the driving frequency, with virtually no change in the amount of power produced across trials. These data suggest that young MTUs are more robust to changes in driving frequency than old MTUs, yet the changes between young and old are small.

3.5.3. MTU Property Implications during Aging

While the changes between young and old MTUs were small, these small changes could have larger implications for the overall function of the animal. The increased stiffness in old MTUs

could lead to a reduced range of motion at the ankle, which provides the primary amount of work during locomotion.⁴⁶ This will in turn cause other MTUs at higher joints to perform more work to compensate.⁴⁷ In order to perform this added work, changes in the geometry of these muscles such as changes in pennation angle or fiber length would need to occur.⁴⁸ Additionally, as tendon is either lost or shortened due to age, the muscle must compensate for the lack of an elastic structure, leading to further increased power output.⁴⁹ These changes may help to explain why older individuals often walk with altered gait patterns.

Changes in the natural frequency can also significantly affect MTU dynamics both in this dataset and elsewhere²⁶, and can have substantive effects on the metabolic efficiency.²⁷ However, typical measures of metabolic efficiency consider whole body measures rather than single muscle estimates.¹ Our previous work demonstrated that investigation of the singular ankle MTU provides a reasonable approximation of observations in human studies.^{25,26} However the experiments performed here consider only isolated environments. In real-world environments, changes in elevation or ground composition can lead to proprioceptive (muscle spindle and golgi tendon) feedback that can allow the MTU to optimize its resonance frequency to that specific environment.⁵⁰ In young MTUs, the small changes between driving frequencies suggest a more robust system that may be more apt for handling these environmental changes. However, the relatively larger changes observed in the old MTU suggests that these old MTUs could be more negatively impacted by environmental changes. To our knowledge, we are the first to investigate the driving frequency effects in both young and old animals using this animal model.

The results of this study were highly variable, with old animals demonstrating small changes overall to the young. This high variability between the animals could be the result of the amount of activity performed across each individuals' lifespan. In more active humans, changes in muscle

and tendon stiffness can be smaller compared to those who are less active.⁵¹ A similar phenomenon may have occurred here with some animals being more active across the lifespan leading to smaller changes between the young animals. The discrepancy between numerous studies suggesting if MTUs get stiffer or more compliant with age could be a question of the response of the individual and not the group. Further studies should investigate this hypothesis to better reach an understanding of these age-related changes.

Of all the changes between young and old MTUs observed in this study, the stiffness changes observed may be the most consequential. While the overall MTU stiffness was not altered, the internal stiffnesses of the muscle and tendon were varied. This internal shifting of stiffnesses may explain help to explain the changes in function. For instance, the force of a given muscle can be described as a function of its max force output multiplied by its activation, force-velocity, and force-length properties, with the addition of passive contributions.¹⁹ Since activation was not varied throughout the experiment, the changes of force observed in the study can be most attributed to force-length and force-velocity changes. Indeed, the operating points between young and old varied greatly, likely due to the stiffness changes observed. These shifting force-length and – velocity points also help explain how the resonance between the two groups was not changed since these internal stiffness changes help to keep the overall function similar between groups. Therefore while the structural changes occur in these tissues, the overall change in function remains robust. These structural changes are the direct result of cellular changes in the tissue of both muscle and tendon with age. In muscle, muscle specific stem cells (satellite cells), responsible for muscle repair and regeneration, undergo a loss of function and injured muscle is instead outfitted with collagen or other connective proteins to fill the lost tissue.^{52,53} This increase in collagen can lead to an increased stiffness in muscle, similar to those observed here. In tendon, repair is almost non-

existent, yet increased crosslinks between collagen in tendon does appear with age, suggesting a further increase in stiffness.^{54,55} This effect was not observed in our data, perhaps as a result of tendon wasting instead of more crosslinks being formed. Future studies should investigate this cellular response to elucidate more sources of the structural changes observed in this and other studies.

3.6. Conclusions

In this study, we used an animal model to explore the effects of age on the MTU behavior during a model for hopping. Our results suggest that while changes were small, MTUs from older animals were stiffer leading to decreased length changes and causing subsequent increases in power output. These changes are likely to significantly impact the performance of the entire animal, requiring assistance from other MTUs in the animal. The small changes from these experiments may be the result of individual variation, where more active animals are better adapted and resemble characteristics similar to young MTUs.

3.7. References

1. Mian OS, Thom JM, Ardigo LP, Narici MV, Minetti AE. Metabolic cost, mechanical work, and efficiency during walking in young and older men. *Acta Physiol (Oxf)*. 2006;186(2):127-139. doi: APS1522 [pii].
2. Woo JS, Derleth C, Stratton JR, Levy WC. The influence of age, gender, and training on exercise efficiency. *J Am Coll Cardiol*. 2006;47(5):1049-1057. doi: S0735-1097(05)02863-9 [pii].
3. Cavagna GA, Legramandi MA, Peyre-Tartaruga LA. Old men running: Mechanical work and elastic bounce. *Proc Biol Sci*. 2008;275(1633):411-418. doi: Y349220312107868 [pii].
4. Keller K, Engelhardt M. Strength and muscle mass loss with aging process. age and strength loss. *Muscles Ligaments Tendons J*. 2014;3(4):346-350.
5. Ortega JD, Farley CT. Effects of aging on mechanical efficiency and muscle activation during level and uphill walking. *J Electromyogr Kinesiol*. 2015;25(1):193-198. doi: 10.1016/j.jelekin.2014.09.003 [doi].
6. Stearns-Reider KM, D'Amore A, Beezhold K, et al. Aging of the skeletal muscle extracellular matrix drives a stem cell fibrogenic conversion. *Aging Cell*. 2017;16(3):518-528. doi: 10.1111/acer.12578 [doi].
7. Mann CJ, Perdiguero E, Kharraz Y, et al. Aberrant repair and fibrosis development in skeletal muscle. *Skelet Muscle*. 2011;1(1):21-5040-1-21. doi: 10.1186/2044-5040-1-21 [doi].
8. Lacraz G, Rouleau AJ, Couture V, et al. Increased stiffness in aged skeletal muscle impairs muscle progenitor cell proliferative activity. *PLoS One*. 2015;10(8):e0136217. doi: 10.1371/journal.pone.0136217 [doi].
9. Narici MV, Maganaris CN. Adaptability of elderly human muscles and tendons to increased loading. *J Anat*. 2006;208(4):433-443. doi: JOA548 [pii].
10. Franz JR, Thelen DG. Depth-dependent variations in achilles tendon deformations with age are associated with reduced plantarflexor performance during walking. *J Appl Physiol (1985)*. 2015;119(3):242-249. doi: 10.1152/jappphysiol.00114.2015 [doi].
11. Danos N, Holt NC, Sawicki GS, Azizi E. Modeling age-related changes in muscle-tendon dynamics during cyclical contractions in the rat gastrocnemius. *J Appl Physiol (1985)*. 2016;jap.00396.2016. doi: 10.1152/jappphysiol.00396.2016 [doi].
12. Barber L, Barrett R, Lichtwark G. Validity and reliability of a simple ultrasound approach to measure medial gastrocnemius muscle length. *J Anat*. 2011;218(6):637-642. doi: 10.1111/j.1469-7580.2011.01365.x [doi].

13. Hodges PW, Pengel LH, Herbert RD, Gandevia SC. Measurement of muscle contraction with ultrasound imaging. *Muscle Nerve*. 2003;27(6):682-692. doi: 10.1002/mus.10375 [doi].
14. Buchanan TS, Lloyd DG, Manal K, Besier TF. Estimation of muscle forces and joint moments using a forward-inverse dynamics model. *Med Sci Sports Exerc*. 2005;37(11):1911-1916. doi: 00005768-200511000-00013 [pii].
15. Wilson GJ, Murphy AJ. The use of isometric tests of muscular function in athletic assessment. *Sports Med*. 1996;22(1):19-37.
16. Jacobs BY, Kloefkorn HE, Allen KD. Gait analysis methods for rodent models of osteoarthritis. *Curr Pain Headache Rep*. 2014;18(10):456-014-0456-x. doi: 10.1007/s11916-014-0456-x [doi].
17. Pardes AM, Beach ZM, Raja H, Rodriguez AB, Freedman BR, Soslowsky LJ. Aging leads to inferior achilles tendon mechanics and altered ankle function in rodents. *J Biomech*. 2017;60:30-38. doi: S0021-9290(17)30305-6 [pii].
18. MacIntosh BR, Esau SP, Holash RJ, Fletcher JR. Procedures for rat in situ skeletal muscle contractile properties. *J Vis Exp*. 2011;(56):e3167. doi(56):e3167. doi: 10.3791/3167 [doi].
19. Zajac FE. Muscle and tendon: Properties, models, scaling, and application to biomechanics and motor control. *Crit Rev Biomed Eng*. 1989;17(4):359-411.
20. Azizi E, Brainerd EL, Roberts TJ. Variable gearing in pennate muscles. *Proc Natl Acad Sci U S A*. 2008;105(5):1745-1750. doi: 10.1073/pnas.0709212105 [doi].
21. Azizi E, Roberts TJ. Biaxial strain and variable stiffness in aponeuroses. *J Physiol*. 2009;587(Pt 17):4309-4318. doi: 10.1113/jphysiol.2009.173690 [doi].
22. Josephson RK. Dissecting muscle power output. *J Exp Biol*. 1999;202(Pt 23):3369-3375.
23. Maganaris CN, Paul JP. Hysteresis measurements in intact human tendon. *J Biomech*. 2000;33(12):1723-1727. doi: S0021-9290(00)00130-5 [pii].
24. Winters JM, Stark L. Estimated mechanical properties of synergistic muscles involved in movements of a variety of human joints. *J Biomech*. 1988;21(12):1027-1041. doi: 0021-9290(88)90249-7 [pii].
25. Robertson BD, Farris DJ, Sawicki GS. More is not always better: Modeling the effects of elastic exoskeleton compliance on underlying ankle muscle-tendon dynamics. *Bioinspir Biomim*. 2014;9(4):046018-3182/9/4/046018. doi: 10.1088/1748-3182/9/4/046018 [doi].

26. Robertson BD, Sawicki GS. Unconstrained muscle-tendon workloops indicate resonance tuning as a mechanism for elastic limb behavior during terrestrial locomotion. *Proc Natl Acad Sci U S A*. 2015;112(43):E5891-8. doi: 10.1073/pnas.1500702112 [doi].
27. Dean JC, Kuo AD. Energetic costs of producing muscle work and force in a cyclical human bouncing task. *J Appl Physiol (1985)*. 2011;110(4):873-880. doi: 10.1152/jappphysiol.00505.2010 [doi].
28. Sawicki GS, Robertson BD, Azizi E, Roberts TJ. Timing matters: Tuning the mechanics of a muscle-tendon unit by adjusting stimulation phase during cyclic contractions. *J Exp Biol*. 2015;218(Pt 19):3150-3159. doi: 10.1242/jeb.121673 [doi].
29. Danos N, Holt NC, Sawicki GS, Azizi E. Modeling age-related changes in muscle-tendon dynamics during cyclical contractions in the rat gastrocnemius. *J Appl Physiol (1985)*. 2016;121(4):1004-1012. doi: 10.1152/jappphysiol.00396.2016 [doi].
30. Lieber RL, Ward SR. Cellular mechanisms of tissue fibrosis. 4. structural and functional consequences of skeletal muscle fibrosis. *Am J Physiol Cell Physiol*. 2013;305(3):C241-52. doi: 10.1152/ajpcell.00173.2013 [doi].
31. Blau HM, Cosgrove BD, Ho AT. The central role of muscle stem cells in regenerative failure with aging. *Nat Med*. 2015;21(8):854-862. doi: 10.1038/nm.3918 [doi].
32. Shadwick RE. Elastic energy storage in tendons: Mechanical differences related to function and age. *J Appl Physiol (1985)*. 1990;68(3):1033-1040. doi: 10.1152/jappl.1990.68.3.1033 [doi].
33. Blevins FT, Hecker AT, Bigler GT, Boland AL, Hayes WC. The effects of donor age and strain rate on the biomechanical properties of bone-patellar tendon-bone allografts. *Am J Sports Med*. 1994;22(3):328-333. doi: 10.1177/036354659402200306 [doi].
34. Narici MV, Maffulli N, Maganaris CN. Ageing of human muscles and tendons. *Disabil Rehabil*. 2008;30(20-22):1548-1554. doi: 10.1080/09638280701831058 [doi].
35. Baudry S, Lecoivre G, Duchateau J. Age-related changes in the behavior of the muscle-tendon unit of the gastrocnemius medialis during upright stance. *J Appl Physiol (1985)*. 2012;112(2):296-304. doi: 10.1152/jappphysiol.00913.2011 [doi].
36. Nakagawa Y, Hayashi K, Yamamoto N, Nagashima K. Age-related changes in biomechanical properties of the achilles tendon in rabbits. *Eur J Appl Physiol Occup Physiol*. 1996;73(1-2):7-10.
37. Birch HL. Tendon matrix composition and turnover in relation to functional requirements. *Int J Exp Pathol*. 2007;88(4):241-248. doi: IEP552 [pii].

38. Brooks SV, Faulkner JA. Contractile properties of skeletal muscles from young, adult and aged mice. *J Physiol*. 1988;404:71-82.
39. Robertson BD, Sawicki GS. Unconstrained muscle-tendon workloops indicate resonance tuning as a mechanism for elastic limb behavior during terrestrial locomotion. *Proc Natl Acad Sci U S A*. 2015;112(43):E5891-8. doi: 10.1073/pnas.1500702112 [doi].
40. Gosselin LE, Burton H. Impact of initial muscle length on force deficit following lengthening contractions in mammalian skeletal muscle. *Muscle Nerve*. 2002;25(6):822-827. doi: 10.1002/mus.10112 [doi].
41. Brooks SV, Faulkner JA. The magnitude of the initial injury induced by stretches of maximally activated muscle fibres of mice and rats increases in old age. *J Physiol*. 1996;497 (Pt 2)(Pt 2):573-580.
42. Brooks SV, Faulkner JA. Contraction-induced injury: Recovery of skeletal muscles in young and old mice. *Am J Physiol*. 1990;258(3 Pt 1):C436-42. doi: 10.1152/ajpcell.1990.258.3.C436 [doi].
43. Karamanidis K, Arampatzis A. Mechanical and morphological properties of different muscle-tendon units in the lower extremity and running mechanics: Effect of aging and physical activity. *J Exp Biol*. 2005;208(Pt 20):3907-3923. doi: 208/20/3907 [pii].
44. Gajdosik RL, Vander Linden DW, McNair PJ, et al. Viscoelastic properties of short calf muscle-tendon units of older women: Effects of slow and fast passive dorsiflexion stretches in vivo. *Eur J Appl Physiol*. 2005;95(2-3):131-139. doi: 10.1007/s00421-005-1394-4 [doi].
45. Miljkovic N, Lim JY, Miljkovic I, Frontera WR. Aging of skeletal muscle fibers. *Ann Rehabil Med*. 2015;39(2):155-162. doi: 10.5535/arm.2015.39.2.155 [doi].
46. Farris DJ, Sawicki GS. The mechanics and energetics of human walking and running: A joint level perspective. *J R Soc Interface*. 2012;9(66):110-118. doi: 10.1098/rsif.2011.0182 [doi].
47. DeVita P, Hortobagyi T. Age causes a redistribution of joint torques and powers during gait. *J Appl Physiol (1985)*. 2000;88(5):1804-1811.
48. Lichtwark GA, Wilson AM. Effects of series elasticity and activation conditions on muscle power output and efficiency. *J Exp Biol*. 2005;208(Pt 15):2845-2853. doi: 208/15/2845 [pii].
49. Roberts TJ. The integrated function of muscles and tendons during locomotion. *Comp Biochem Physiol A Mol Integr Physiol*. 2002;133(4):1087-1099. doi: S1095643302002441 [pii].

50. Raburn CE, Merritt KJ, Dean JC. Preferred movement patterns during a simple bouncing task. *J Exp Biol.* 2011;214(Pt 22):3768-3774. doi: 10.1242/jeb.058743 [doi].
51. Milanovic Z, Pantelic S, Trajkovic N, Sporis G, Kostic R, James N. Age-related decrease in physical activity and functional fitness among elderly men and women. *Clin Interv Aging.* 2013;8:549-556. doi: 10.2147/CIA.S44112 [doi].
52. Mays PK, McAnulty RJ, Campa JS, Laurent GJ. Age-related changes in collagen synthesis and degradation in rat tissues. importance of degradation of newly synthesized collagen in regulating collagen production. *Biochem J.* 1991;276 (Pt 2)(Pt 2):307-313.
53. Goldspink G, Fernandes K, Williams PE, Wells DJ. Age-related changes in collagen gene expression in the muscles of mdx dystrophic and normal mice. *Neuromuscul Disord.* 1994;4(3):183-191.
54. Tanaka S, Avigad G, Brodsky B, Eikenberry EF. Glycation induces expansion of the molecular packing of collagen. *J Mol Biol.* 1988;203(2):495-505. doi: 0022-2836(88)90015-0 [pii].
55. Ippolito E, Natali PG, Postacchini F, Accinni L, De Martino C. Morphological, immunochemical, and biochemical study of rabbit achilles tendon at various ages. *J Bone Joint Surg Am.* 1980;62(4):583-598.

CHAPTER 4: Optimizing a Cell Co-Culture System to Understand Bone-Muscle

Interactions

4.1. Abstract

Despite a good understanding of the mechanical interactions between bone and muscle, the biochemical interactions between the two are not well understood. Understanding these biochemical interactions could lead to new therapeutic options for musculoskeletal disorders. However, a good method for determining these biochemical interactions at the cellular level has yet to be investigated. Therefore, the objective of this study was to develop a viable co-culture system to investigate the biochemical interaction between muscle satellite cells (SCs) and bone marrow-derived mesenchymal stem cells (MSCs). Rat SCs and MSCs were either mono-cultured or co-cultured in Transwell® plates, subjected to different plate coatings and media formulations for 14 days, and biochemically and histologically analyzed for cell viability and cell differentiation. While plate coating did not influence cell viability or differentiation, the media provided to each cell type affected differentiation, with SCs preferring muscle-specific media, and MSCs preferring bone-specific media. The results suggest that when developing a co-culture system between SCs and MSCs, the media provided to each cell type is more important than the coating used. This study is the first to establish a viable co-culture technique to understand bone-muscle interactions. Further investigation of these interactions could lead to enhanced strategies or treatments for musculoskeletal diseases.

4.2. Introduction

Bone and muscle coupling consists of a complex system of mechanical and biochemical interactions.^{1,2} From a mechanical perspective, muscle's ability to generate force introduces axial, torsional, shear, and bending loads to the bone that can directly influence bone development during

growth and maintenance during aging.³⁻⁵ Greater muscle loading leads to increased bone mass, as described by the bone mechanostat paradigm⁶, which implies that as muscle function declines, so too does bone mass. Individuals with decreased bone mass (osteopenia) can often develop reduced muscle mass and function (sarcopenia),⁷ yet declines in muscle mass cannot fully explain the extent of osteopenia, nor can declines in bone mass fully explain the functional decline of muscle in sarcopenia.¹ To determine other contributing factors beyond mechanical interactions an emerging area of research has sought to understand the potential biochemical cues that underlie bone-muscle coupling.

Both bone and muscle secrete a variety of factors that can act on distant tissues in a classic endocrine fashion, including sending factors to each tissue.^{8,9} Bone can influence muscle through the secretion of osteocalcin, an osteoblast-specific protein that promotes bone formation but also prevents age-related loss of muscle mass and strength.^{10,11} Another protein from bone, prostaglandin E2, has been shown to enhance myotube proliferation.¹² Muscle influences bone through several factors including: (1) irisin, a hormone-like protein that promotes osteoblast differentiation¹³; (2) myostatin, a muscle inhibition protein that promotes osteoclastogenesis¹⁴; and (3) insulin-like growth factor 1 (IGF-1), which increases osteoblast activity.¹⁵ While several muscle-specific signaling factors have been shown to affect bone, bone-specific effects on muscle are less defined. Muscle flap studies have demonstrated that bone fractures heal more quickly and completely in the presence of muscle tissue,¹⁶ yet the underlying biochemical “crosstalk” between bone and muscle that is driving these changes is not well understood.

Bone-muscle interactions can be studied in several ways, including *in vivo* experiments, conditioned media experiments, and co-culture experiments. In an *in vivo* mouse experiment using a bone fracture model, researchers demonstrated that exogenous application of myostatin led to

increased muscle fibrosis and decreased bone callus size, suggesting a decrease in the ability of bone and muscle to heal.^{17,18} While this *in vivo* experiment showed the importance of biochemical bone-muscle interactions, these types of studies can be complex due to the need for specialized mouse models and application routes for exogenous factors, expensive, and require large subject numbers to ensure a well clustered data set. Therefore, development of *in vitro* experiments have become more prevalent due to their relative cost reduction and simplicity compared to *in vivo* experiments. Conditioned media experiments have demonstrated that conditioned media from osteocytes induce myogenic differentiation via the Wnt/ β -catenin pathway, and conditioned media from myocytes protect osteocytes from apoptosis.¹⁹ However, this type of experiment only examines the one-way response of a cell type to signals produced by another cell type²⁰ and does not capture the two-way interaction between cells as in the *in vivo* endocrine state. Additionally, conditioned media experiments in muscle cells often employ C2C12 satellite cells (SCs), a commonly used immortal cell line, which may not adequately represent the phenotype of *in vivo* SCs²¹ and cannot be used in studies of aging or genetic modifications. Direct co-culture experiments between skeletal muscle cells and bone-derived cells have demonstrated the ability for muscle cells to differentiate without bone cells also differentiating into muscle cells.²² However, determining which signaling factor comes from which cell type is difficult in direct co-culture, since the cell types and media cannot be separated for analysis. Developing an *in vitro* system with indirect co-culture, in which primary cells harvested are from live tissue and cultured separately yet allowed to communicate through a permeable barrier, may provide a better representation of *in vivo* bone-muscle crosstalk.

Previous cell culture studies have highlighted the importance of optimizing the cell culture environment to observe strong cell proliferation and differentiation.^{23,24} Without an appropriate

surface coating or media formulation, the cells of interest may not develop properly or demonstrate typical characteristics. An indirect co-culture system between bone-muscle has not yet been optimized. Therefore, the goal of this study was to determine the optimal culture conditions for an indirect co-culture system of primary SCs and bone marrow-derived mesenchymal stem cells (MSCs). Once optimized, this experimental design can be used in a variety of studies to improve understanding bone-muscle crosstalk.

4.3. Methods

4.3.1. Animals and cell isolation

The Institutional Animal Care and Use Committee at North Carolina State University approved all animal procedures. Three 6-week-old male brown rats (*Rattus Norvegicus*, Charles River, Wilmington, MA) were fed a normal diet and kept under a 12-hr light/12-hr dark cycle with free access to chow and water until euthanasia. After acclimation to the animal facility for one week, rats were euthanized by CO₂ inhalation, followed by immediate dissection to remove the gastrocnemius and tibialis anterior (TA) muscles and the tibia and femur from one leg. Rat bone MSCs were isolated from the tibia and femur using a method modified from Zhang and Chan²⁵. Briefly, the bones were placed in warm MSC-specific growth medium (MSCGM) consisting of alpha-MEM (Gibco, Gaithersburg, MD), 10% fetal bovine serum (Gemini Bio-Products, West Sacramento, CA), and 100 U/mL penicillin-100 µg/mL streptomycin (Gibco). The bone ends were removed, and the remaining segments were flushed with MSCGM to extract the marrow and isolate the MSCs. The MSCs were plated on a single 120-mm plastic plate (Corning, Tewksbury, MA) coated with 2% gelatin (Fisher Scientific, Hampton, NH) and cultured with MSCGM in a humidified atmosphere of 37°C and 5% CO₂. After 48 h, the nonadherent cells were washed out, and the cultures were expanded to passage 2.

SCs were extracted from the gastrocnemius and TA using a protocol from Danoviz and Yablonk-Reuveni²⁶. Briefly, the muscles were placed in warm SC-specific growth medium (SCGM) consisting of high glucose Dulbecco's MEM (Gibco), 20% fetal bovine serum (Gemini Bioproducts), 10% horse serum (Gibco), and 100 U/mL penicillin-100 µg/mL streptomycin (Gibco). Tendon, fat, blood vessels, and connective tissue were removed, and the remaining muscle was cut into small (~3 mm³) cubes. Muscle cubes were collected and added to a 1% Pronase solution (Pronase Protease, Millipore-Sigma, St. Louis, MO) in SCGM for one hour for digestion. The solution and remaining muscle were then collected and suspended in 10 mL of additional SCGM. The entire solution was subjected to mechanical trituration by passing the solution through a wide-bore pipette to liberate SCs. Finally, the triturated solution was passed through a cell strainer with a 70-µm pore size (Fisher Scientific), and SCs were collected and plated on a single 2% gelatin-coated 120-mm plate with SCGM in a humidified atmosphere of 37°C and 5% CO₂. After 48 h, the nonadherent cells were washed out, and the cultures were expanded to passage 2.

4.3.2. Co-culture validation and optimization

Numerous media formulations and culture surfaces were tested in both mono- and co-cultures of bone and muscle cells to develop an optimal co-culture procedure for both osteo- and myogenesis (Fig. 1). In mono-culture experiments, SCs and MSCs were each cultured at 20 x 10³ cells per well in a 12-well plate, with each condition run in triplicate per animal (9 wells total per condition). In co-culture experiments, SCs and MSCs were each cultured at 20 x 10³ cells per well in a 12-well Transwell[®] plate (Corning, Corning, NY), with SCs in the bottom well and MSCs in the insert, separated by the 0.4-µm pore membrane. First, to test the effects of media composition on cell proliferation and differentiation, MSCs, SCs, or a co-culture of MSCs and SCs were differentiated for 14 days in one of the following four media formulations: 1) myogenic media

(MM) containing high glucose Dulbecco's MEM (Gibco), 1% horse serum (Gibco), and 100 U/mL penicillin-100 µg/mL streptomycin (Gibco); 2) osteogenic media (OM) containing alpha-MEM (Gibco), 10% fetal bovine serum (Gibco), 50 mM ascorbic acid (Millipore-Sigma), 100 µM dexamethasone (Millipore-Sigma), 1 M β-glycerophosphate (Millipore-Sigma) and 100 U/mL penicillin-100 µg/mL streptomycin (Gibco); 3) a 50% MM:50% OM mixture; or 4) a 75% MM:25% OM mixture. For the co-cultures, these formulations were used in both the bottom well and insert. Second, to determine the optimal culture surface for MSC and SC proliferation and differentiation, MSCs, SCs, or a co-culture were cultured for 14 days in either OM (for MSCs) or MM (for SCs) in standard 12-well plates modified with one of the following four surface coatings: 2% gelatin (Millipore-Sigma), collagen I (Fisher Scientific), Matrigel® (Fisher Scientific), or nothing. For the co-cultures, MM was used in the bottom well, and OM was used in the insert.

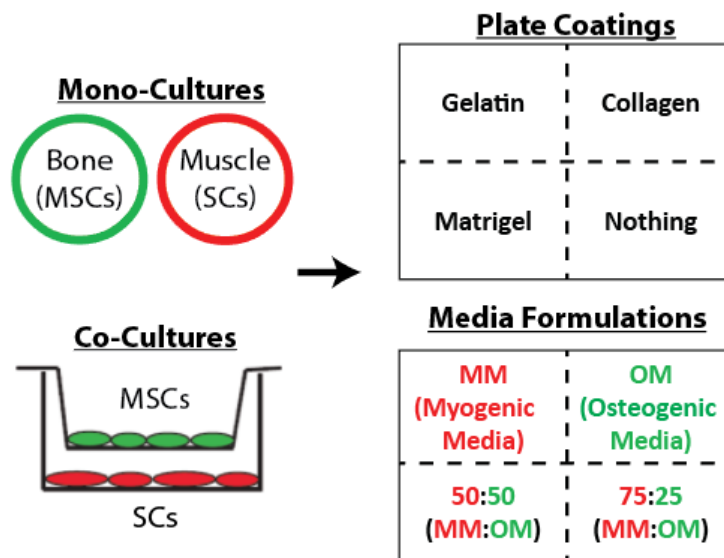


Figure 1. Experimental design. Bone (MSCs) and muscle (SCs) cells were plated in either mono-culture in 12-well plates or co-culture in a Transwell® system and tested with four media formulations and four plate coatings. MM=myogenic media, OM=osteogenic media.

4.3.3. Viability analyses

On differentiation days 3, 7, 10, and 14, an AlamarBlue[®] solution (ThermoFisher, Waltham, MA) was mixed into each well (90% media, 10% AlamarBlue[®]), and the cells were incubated at 37°C. After 3 h, the solution was collected, and absorbance readings were taken at 570 and 600 nm (Synergy H1 Biotek, Winooski, VT). For the co-cultures, the bottom well and insert of the Transwell[®] plates were analyzed separately. The percent reduction in AlamarBlue[®] level, a measure of proliferative ability, was determined from the absorbance reading according to the manufacturer's instructions.

4.3.4. Differentiation analysis

On differentiation day 14, wells were rinsed in phosphate buffered saline (PBS), fixed in 10% zinc-buffered formalin (VWR, Randor, PA) for 30 min, and then rinsed again with PBS. To assess mineral deposition for MSC differentiation, a 2% Alizarin Red S (Fisher) solution was applied to each sample for 5 min, rinsed with deionized water, and imaged using an iPhone 6S camera (Apple, Cupertino, CA) and EVOS XL light microscope (EVOS Life Technologies, Carlsbad, CA). Mineral deposition was quantified by solubilizing the Alizarin Red S stain with a 0.5 N HCl + 5% sodium dodecyl sulfate (SDS) solution for 30 minutes and then taking absorbance readings at 405 nm. Representative SC differentiation was determined by cell morphology with differentiated SCs exhibiting multi-nucleated and elongated cells.

4.3.5. Statistical analyses

Statistical analyses were performed with Prism (version 6.07; GraphPad Software, La Jolla, CA) using a significance level of $p < 0.05$. All results were averaged across the three rats and expressed in the form of mean \pm standard deviation. The effects of media formulation and culture surface were examined using two-way ANOVAs with culture type (Mono-SC, Mono-MSC, Co-

SC, Co-MSC) as one factor and either plate coating or media formulation as the second factor. Differences within each factor were evaluated with Tukey's post-hoc analyses.

4.4. Results

4.4.1 Viability results

Based on the alamarBlue[®] reduction results, neither plate coating nor media formulation affected MSC viability/proliferation at any time point (coating mono-culture: $p = 0.99$, coating co-culture: $p=0.99$, media mono-culture: $p=0.98$, media co-culture: $p=0.55$, Fig. 2). At day 14, cell viability remained stable across all samples. Similarly, SC viability was not affected by either plate coating or media formulation (coating mono-culture: $p = 0.99$, coating co-culture: $p=0.99$, media mono-culture: $p=0.92$, media co-culture: $p=0.54$, Fig. 3).

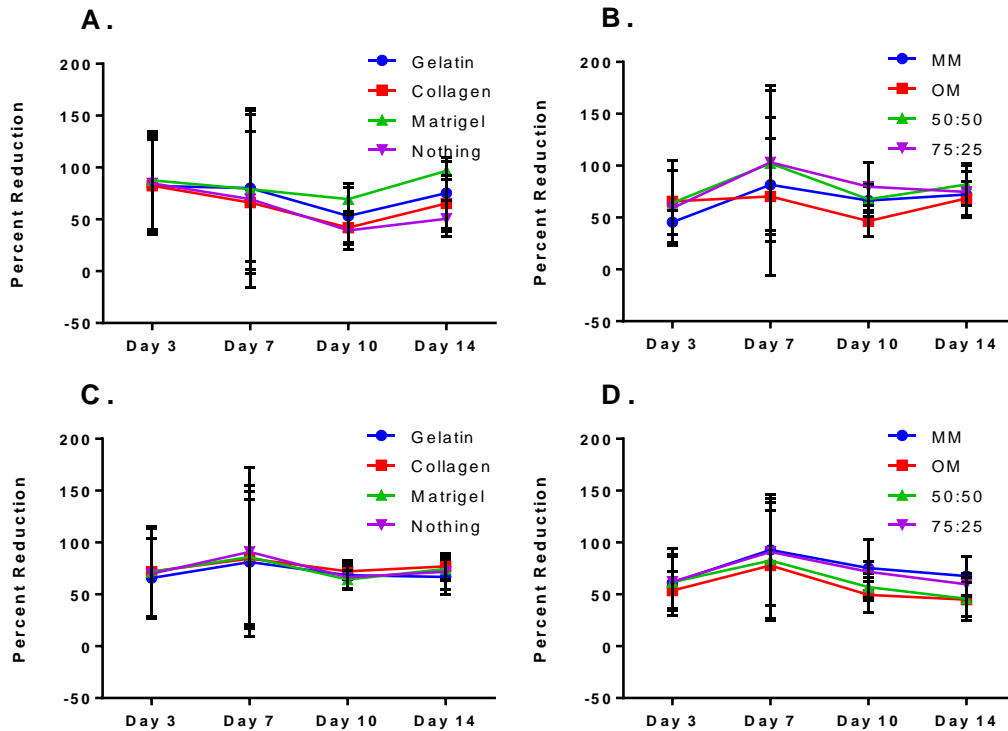


Figure 2. AlamarBlue percent reduction in MSCs. MSCs in mono-culture (A,B) or co-culture (C,D) with different plate coatings (A,C) and media formulations (B,D). Viability/proliferation was not affected by plate coating or media formulation. Data are mean \pm SD.

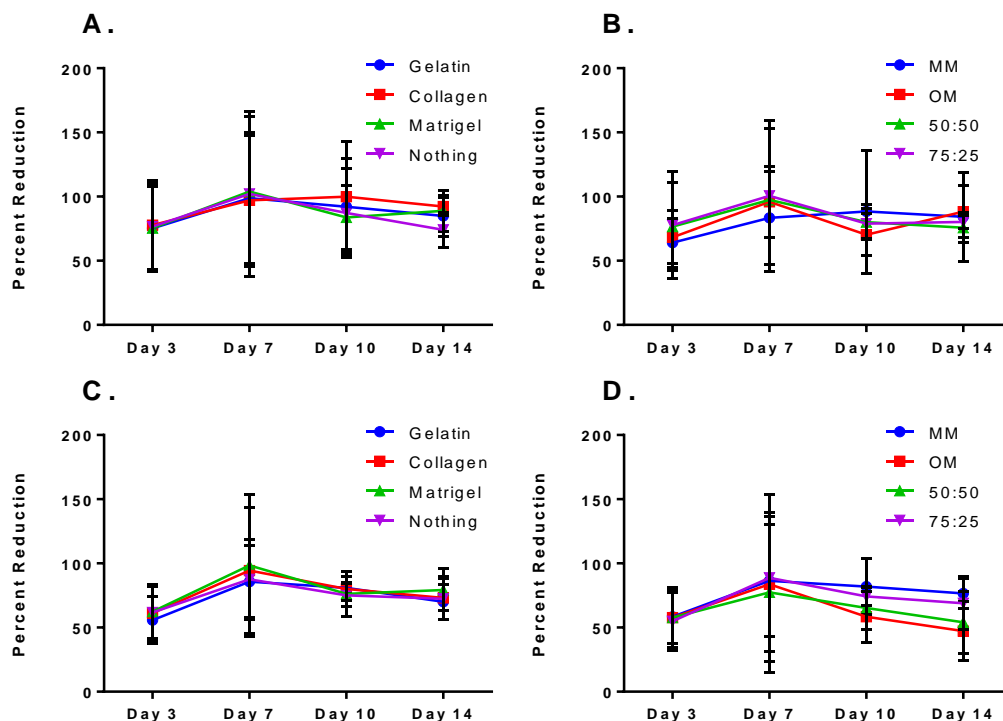


Figure 3. AlamarBlue percent reduction in SCs. SCs in mono-culture (A,B) or co-culture (C,D) with different plate coatings (A,C) and media formulations (B,D). Viability/proliferation was not affected by plate coating or media formulation. Data are mean \pm SD.

4.4.2. Differentiation results

Alizarin red S staining did not differ by plate coating, but it did differ among culture types (Fig. 4A). Mono-cultured MSCs demonstrated more staining, indicative of greater mineral deposition, than mono-cultured SCs ($p = 0.0036$) or co-cultured SCs ($p = 0.0029$), signifying that MSCs successfully differentiated to osteoblasts. While the alizarin red staining was not significantly different for co-cultured MSCs compared to both SC cultures, it was also not different compared to mono-cultured MSCs, suggesting that the co-cultured MSCs still mineralized, just not as much as mono-cultured MSCs. Media formulation had no effect on alizarin red staining (Fig. 4B). Although not statistically significant, mono-cultured MSCs generally had the greatest

amount of staining in OM media, with subsequent decreases when under the influence of mixed media. Surprisingly, co-cultured MSCs had similar alizarin red staining compared to SCs regardless of media. Qualitatively, based on images of the alizarin red staining, MSCs had greater mineral deposition than SCs, as expected. Furthermore, under different media formulations, MSCs demonstrated the most mineralization in OM (Fig. 5). As the amount of OM in the mixed media decreased, mineralization also decreased to levels similar to those seen in MM.

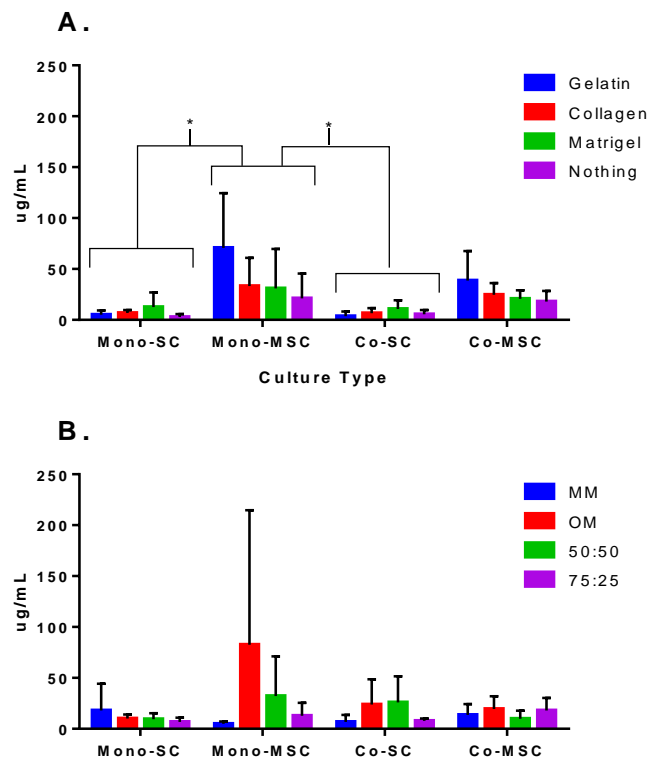


Figure 4. Alizarin red quantification. (A) Plate coating and (B) media formulation had no effect on AR quantification at 14 days post-differentiation. Regardless of coating, mono-cultured MSCs had more staining, indicative of more mineralization, than mono- or co-cultured SCs. Mono-cultured MSCs mineralized best in OM, as expected. Data are mean \pm SD. * $p < 0.05$.

Based on image assessments of SC morphology, SCs in MM had elongated cell shapes typical of early developing myotubes in both mono- and co-culture (Fig. 6). However, SCs in OM or mixed media had a cell shape that was less elongated and more fibroblastic in appearance. In media where FBS was still present, SCs often reached confluence and lifted off the plate by day 14. SCs did not

show a preference for a particular coating, with similar cell morphology across all plate coatings (data not shown).

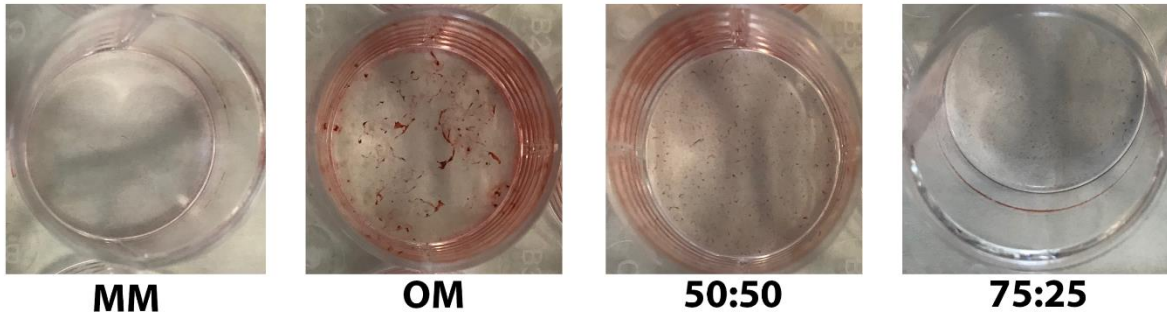


Figure 5. Representative alizarin red images of MSCs in mono-culture. At day 14, MSCs had the greatest mineral deposition in OM than in the other media formulations.

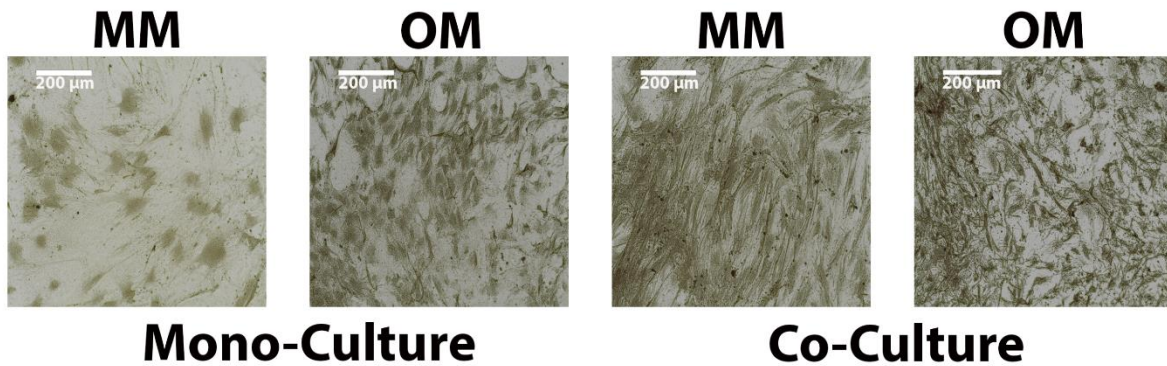


Figure 6. Representative images of differentiated SCs. At day 14, mono- and co-cultured SCs had an elongated shape typical of early developing myotubes in MM but were more fibroblastic in appearance in OM.

4.5. Discussion

Understanding bone-muscle interactions is becoming increasingly important for better understanding of musculoskeletal diseases. Here, we developed a co-culture system capable of allowing independent proliferation and differentiation of bone MSCs and muscle SCs. In developing this system, we determined the optimal conditions (culture surface and media formulation) that would enable the best viability and differentiation of MSCs and SCs. While culture surface had no effect on MSC or SC viability and differentiation, media formulation demonstrated marked effects on differentiation, with MSC-SC co-cultures performing best when

each cell type was plated with its own cell-specific media formulation (i.e., MSCs in OM and SCs in MM).

While utilizing co-cultures of two different cell types is not a unique approach^{20,23,27,28}, to our knowledge, a MSC-SC indirect co-culture has not previously been performed. Optimal conditions for a Transwell[®]-style co-culture approach are not well established, with other similar studies utilizing different cell types not discussing how the specific conditions were chosen. We chose a Transwell[®] system rather than a direct co-culture method due to the shared lineage of SCs and MSCs^{29,30} and the difficulty in separating these two cell types based on morphology. Additionally, bone morphogenetic proteins, secreted by bone-specific cells, can have the effect of slowing SC differentiation.³¹⁻³³ By separating the cell types and applying associated media, we can mitigate these direct contact effects.

The surface coating on which cells are cultured can be a critical component of regulating cellular behavior. In both bone-muscle, collagen type 1 is a component of extracellular matrix and can enhance viability in both SCs and MSCs^{5,34}, while also promoting osteogenesis in MSCs⁵. Gelatin was chosen as a cheaper option to collagen, and it can provide relatively greater cell adhesion. Matrigel[®] is a protein mixture secreted by mouse sarcoma cells and thus contains numerous structural proteins like laminin and collagen, as well as growth factors such as tumor growth factor beta and endothelial growth factor³⁵. This complex composition can allow for enhanced cellular proliferation and signaling behavior that may not arise with other coatings. In this study, plate coating did not affect cell viability or differentiation. Therefore, the importance of plate coating in these experiments may not be as critical unless growth factors are being investigated. In that case, Matrigel[®] should be avoided if looking at any of the growth factors in

its complex composition. Preliminary crosstalk data seems to support this assertion, as IGF-1 expression was greater with Matrigel[®] than with other coatings (Fig. 7).

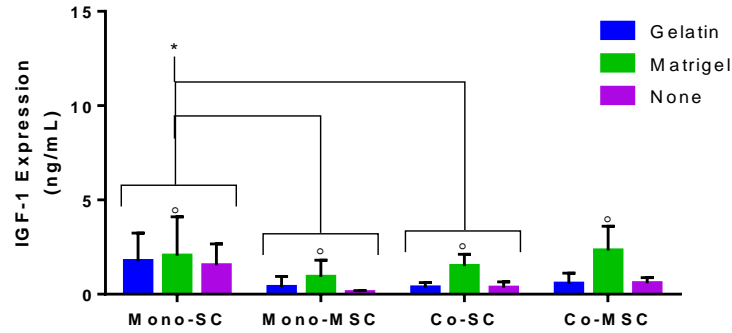


Figure 7. Preliminary bone-muscle crosstalk data. IGF-1 expression in conditioned media was greater in mono-cultured SCs than mono-cultured MSCs or co-cultured SCs (* $p < 0.05$ for group differences), and it was greater in Matrigel[®] than in other coatings ($^{\circ} p < 0.05$ for coating differences). Data are mean \pm SD.

The media chosen for these experiments played a larger role than did plate coating in the behavior of both SCs and MSCs. The MM formulation chosen for SCs is known to induce differentiation of SCs to myotubes^{36,37}. Similarly, the OM formulation chosen is known to induce differentiation of MSCs to osteoblasts³⁸. Because the media in the bottom well and insert get inevitably mixed in Transwell[®] systems, we opted to use mixed media formulations with different ratios of MM to OM to determine the effect on cell behavior. For cell viability, media had no effect in any culture type at any time point. Since OM, 50:50 OM:MM, and 75:25 OM:MM had FBS, proliferation was favored in SCs over differentiation resulting in highly confluent wells, or wells where cells lifted off the plate. This response is common in SCs where media with FBS is continually supplied.³⁹ Therefore, future co-culture studies should seek to minimize the amount of FBS when attempting to force SCs to grow to myotubes. For MSCs, mono-cultured MSCs in media other than OM showed declines in the amount of mineral produced. As the OM additives have reduced concentrations in other media formulations, differentiation was also reduced, and

MSCs tended to remain as undifferentiated MSCs. As with the SCs, MSCs also often became confluent by day 14, although they did not lift off the plate. Again, future co-cultures should attempt to reduce the dilution of OM to ensure the maximal amount of differentiation can occur in the MSCs.

Surprisingly, cell viability in co-culture did not differ significantly from that in mono-culture. We expected that co-cultured cells would synergistically enhance viability, since the crosstalk between cell types could lead to increased growth, as shown in other similar co-culture studies^{23,40,41}. In the work here, signaling changes may have regulated the growth of both SCs and MSCs such that neither proliferated more quickly than in mono-culture. Other studies have suggested that a functional ‘bone-muscle-unit’ may influence how both bone and muscle develop^{42,43}. Signaling factors can also regulate these changes in bone-muscle crosstalk². Further work is needed to determine these specific signaling pathways regulating MSC-SC interactions.

Co-culture was neither beneficial nor detrimental to cell viability, suggesting that this Transwell[®] method may be a stable method for investigating MSC-SC interactions. The decreased mineralization by co-cultured MSCs compared to mono-cultured MSCs, however, suggests that either the dilution of OM or signaling effects of SCs reduced differentiation of the MSCs. In plate coating experiments where SCs received MM and MSCs received OM, only a marginal decrease in mineralization of co-MSCs relative to mono-MSCs was observed, while media formulation experiments demonstrated mineralization of co-MSCs similar to those of SCs. Media mixing in co-culture can take a longer period of time⁴⁴, suggesting that the media formulation played more of a role in the reduction of mineralization than signaling effects from SCs. Taken together, this system is most effective when the media specific for each cell type is used and steps are taken to reduce the dilution of OM or the amount of FBS in MM.

4.6. References

1. Brotto M, Bonewald L. Bone and muscle: Interactions beyond mechanical. *Bone*. 2015;80:109-114. doi: 10.1016/j.bone.2015.02.010 [doi].
2. Brotto M, Johnson ML. Endocrine crosstalk between muscle and bone. *Curr Osteoporos Rep*. 2014;12(2):135-141. doi: 10.1007/s11914-014-0209-0 [doi].
3. Tieland M, Trouwborst I, Clark BC. Skeletal muscle performance and ageing. *J Cachexia Sarcopenia Muscle*. 2018;9(1):3-19. doi: 10.1002/jcsm.12238 [doi].
4. Russo CR. The effects of exercise on bone. basic concepts and implications for the prevention of fractures. *Clin Cases Miner Bone Metab*. 2009;6(3):223-228.
5. Boskey AL, Coleman R. Aging and bone. *J Dent Res*. 2010;89(12):1333-1348. doi: 10.1177/0022034510377791 [doi].
6. Frost HM. Wolff's law and bone's structural adaptations to mechanical usage: An overview for clinicians. *Angle Orthod*. 1994;64(3):175-188. doi: 10.1043/0003-3219(1994)0642.0.CO;2 [doi].
7. Reginster JY, Beaudart C, Buckinx F, Bruyere O. Osteoporosis and sarcopenia: Two diseases or one? *Curr Opin Clin Nutr Metab Care*. 2016;19(1):31-36. doi: 10.1097/MCO.0000000000000230 [doi].
8. Linkhart TA, Mohan S, Baylink DJ. Growth factors for bone growth and repair: IGF, TGF beta and BMP. *Bone*. 1996;19(1 Suppl):1S-12S. doi: S8756-3282(96)00138-X [pii].
9. Schwetz V, Pieber T, Obermayer-Pietsch B. The endocrine role of the skeleton: Background and clinical evidence. *Eur J Endocrinol*. 2012;166(6):959-967. doi: 10.1530/EJE-12-0030 [doi].
10. Mera P, Laue K, Ferron M, et al. Osteocalcin signaling in myofibers is necessary and sufficient for optimum adaptation to exercise. *Cell Metab*. 2017;25(1):218. doi: S1550-4131(16)30636-2 [pii].
11. Levinger I, Scott D, Nicholson GC, et al. Undercarboxylated osteocalcin, muscle strength and indices of bone health in older women. *Bone*. 2014;64:8-12. doi: 10.1016/j.bone.2014.03.008 [doi].
12. Mo C, Romero-Suarez S, Bonewald L, Johnson M, Brotto M. Prostaglandin E2: From clinical applications to its potential role in bone- muscle crosstalk and myogenic differentiation. *Recent Pat Biotechnol*. 2012;6(3):223-229. doi: BIOT-EPUB-20121022-3 [pii].

13. Colaianni G, Cuscito C, Mongelli T, et al. Irisin enhances osteoblast differentiation in vitro. *Int J Endocrinol*. 2014;2014:902186. doi: 10.1155/2014/902186 [doi].
14. Dankbar B, Fennen M, Brunert D, et al. Myostatin is a direct regulator of osteoclast differentiation and its inhibition reduces inflammatory joint destruction in mice. *Nat Med*. 2015;21(9):1085-1090. doi: 10.1038/nm.3917 [doi].
15. Bikle DD, Tahimic C, Chang W, Wang Y, Philippou A, Barton ER. Role of IGF-I signaling in muscle bone interactions. *Bone*. 2015;80:79-88. doi: 10.1016/j.bone.2015.04.036 [doi].
16. Harry LE, Sandison A, Paleolog EM, Hansen U, Pearse MF, Nanchahal J. Comparison of the healing of open tibial fractures covered with either muscle or fasciocutaneous tissue in a murine model. *J Orthop Res*. 2008;26(9):1238-1244. doi: 10.1002/jor.20649 [doi].
17. Elkasrawy M, Immel D, Wen X, Liu X, Liang LF, Hamrick MW. Immunolocalization of myostatin (GDF-8) following musculoskeletal injury and the effects of exogenous myostatin on muscle and bone healing. *J Histochem Cytochem*. 2012;60(1):22-30. doi: 10.1369/0022155411425389 [doi].
18. Kellum E, Starr H, Arounleut P, et al. Myostatin (GDF-8) deficiency increases fracture callus size, sox-5 expression, and callus bone volume. *Bone*. 2009;44(1):17-23. doi: 10.1016/j.bone.2008.08.126 [doi].
19. Huang J, Romero-Suarez S, Lara N, et al. Crosstalk between MLO-Y4 osteocytes and C2C12 muscle cells is mediated by the wnt/beta-catenin pathway. *JBMR Plus*. 2017;1(2):86-100. doi: 10.1002/jbm4.10015 [doi].
20. Holt DJ, Chamberlain LM, Grainger DW. Cell-cell signaling in co-cultures of macrophages and fibroblasts. *Biomaterials*. 2010;31(36):9382-9394. doi: 10.1016/j.biomaterials.2010.07.101 [doi].
21. Cornelison DD. Context matters: In vivo and in vitro influences on muscle satellite cell activity. *J Cell Biochem*. 2008;105(3):663-669. doi: 10.1002/jcb.21892 [doi].
22. Kulesza A, Burdzinska A, Szczepanska I, et al. The mutual interactions between mesenchymal stem cells and myoblasts in an autologous co-culture model. *PLoS One*. 2016;11(8):e0161693. doi: 10.1371/journal.pone.0161693 [doi].
23. Steward AJ, Cole JH, Ligler FS, Lobo EG. Mechanical and vascular cues synergistically enhance osteogenesis in human mesenchymal stem cells. *Tissue Eng Part A*. 2016;22(15-16):997-1005. doi: 10.1089/ten.TEA.2015.0533 [doi].
24. van der Valk J, Brunner D, De Smet K, et al. Optimization of chemically defined cell culture media--replacing fetal bovine serum in mammalian in vitro methods. *Toxicol In Vitro*. 2010;24(4):1053-1063. doi: 10.1016/j.tiv.2010.03.016 [doi].

25. Zhang L, Chan C. Isolation and enrichment of rat mesenchymal stem cells (MSCs) and separation of single-colony derived MSCs. *J Vis Exp.* 2010;(37). pii: 1852. doi(37):10.3791/1852. doi: 10.3791/1852 [doi].
26. Danoviz ME, Yablonka-Reuveni Z. Skeletal muscle satellite cells: Background and methods for isolation and analysis in a primary culture system. *Methods Mol Biol.* 2012;798:21-52. doi: 10.1007/978-1-61779-343-1_2 [doi].
27. Spector JA, Greenwald JA, Warren SM, et al. Co-culture of osteoblasts with immature dural cells causes an increased rate and degree of osteoblast differentiation. *Plast Reconstr Surg.* 2002;109(2):631-42; discussion 643-4.
28. Kubosch EJ, Heidt E, Bernstein A, Bottiger K, Schmal H. The trans-well coculture of human synovial mesenchymal stem cells with chondrocytes leads to self-organization, chondrogenic differentiation, and secretion of TGFbeta. *Stem Cell Res Ther.* 2016;7(1):64-016-0322-3. doi: 10.1186/s13287-016-0322-3 [doi].
29. Yin H, Price F, Rudnicki MA. Satellite cells and the muscle stem cell niche. *Physiol Rev.* 2013;93(1):23-67. doi: 10.1152/physrev.00043.2011 [doi].
30. Shefer G, Yablonka-Reuveni Z. Reflections on lineage potential of skeletal muscle satellite cells: Do they sometimes go MAD? *Crit Rev Eukaryot Gene Expr.* 2007;17(1):13-29. doi: 4df88ce75e22d4a8,75fe86467b43f70d [pii].
31. Friedrichs M, Wirsdoerfer F, Flohe SB, Schneider S, Wuelling M, Vortkamp A. BMP signaling balances proliferation and differentiation of muscle satellite cell descendants. *BMC Cell Biol.* 2011;12:26-2121-12-26. doi: 10.1186/1471-2121-12-26 [doi].
32. Asakura A, Komaki M, Rudnicki M. Muscle satellite cells are multipotential stem cells that exhibit myogenic, osteogenic, and adipogenic differentiation. *Differentiation.* 2001;68(4-5):245-253. doi: S0301-4681(09)60410-2 [pii].
33. Katagiri T, Yamaguchi A, Komaki M, et al. Bone morphogenetic protein-2 converts the differentiation pathway of C2C12 myoblasts into the osteoblast lineage. *J Cell Biol.* 1994;127(6 Pt 1):1755-1766.
34. Kragstrup TW, Kjaer M, Mackey AL. Structural, biochemical, cellular, and functional changes in skeletal muscle extracellular matrix with aging. *Scand J Med Sci Sports.* 2011;21(6):749-757. doi: 10.1111/j.1600-0838.2011.01377.x [doi].
35. Hughes CS, Postovit LM, Lajoie GA. Matrigel: A complex protein mixture required for optimal growth of cell culture. *Proteomics.* 2010;10(9):1886-1890. doi: 10.1002/pmic.200900758 [doi].
36. Yablonka-Reuveni Z. The skeletal muscle satellite cell: Still young and fascinating at 50. *J Histochem Cytochem.* 2011;59(12):1041-1059. doi: 10.1369/0022155411426780 [doi].

37. Danoviz ME, Yablonka-Reuveni Z. Skeletal muscle satellite cells: Background and methods for isolation and analysis in a primary culture system. *Methods Mol Biol.* 2012;798:21-52. doi: 10.1007/978-1-61779-343-1_2 [doi].
38. Jaiswal N, Haynesworth SE, Caplan AI, Bruder SP. Osteogenic differentiation of purified, culture-expanded human mesenchymal stem cells in vitro. *J Cell Biochem.* 1997;64(2):295-312. doi: 10.1002/(SICI)1097-4644(199702)64:23.0.CO;2-I [pii].
39. Lawson MA, Purslow PP. Differentiation of myoblasts in serum-free media: Effects of modified media are cell line-specific. *Cells Tissues Organs.* 2000;167(2-3):130-137. doi: 16776 [pii].
40. Strassburg S, Richardson SM, Freemont AJ, Hoyland JA. Co-culture induces mesenchymal stem cell differentiation and modulation of the degenerate human nucleus pulposus cell phenotype. *Regen Med.* 2010;5(5):701-711. doi: 10.2217/rme.10.59 [doi].
41. Joensuu K, Uusitalo L, Alm JJ, Aro HT, Hentunen TA, Heino TJ. Enhanced osteoblastic differentiation and bone formation in co-culture of human bone marrow mesenchymal stromal cells and peripheral blood mononuclear cells with exogenous VEGF. *Orthop Traumatol Surg Res.* 2015;101(3):381-386. doi: 10.1016/j.otsr.2015.01.014 [doi].
42. Schoenau E. From mechanostat theory to development of the "functional muscle-bone-unit". *J Musculoskelet Neuronal Interact.* 2005;5(3):232-238.
43. Fricke O, Schoenau E. The 'functional muscle-bone unit': Probing the relevance of mechanical signals for bone development in children and adolescents. *Growth Horm IGF Res.* 2007;17(1):1-9. doi: S1096-6374(06)00127-4 [pii].
44. Renaud J, Martinoli MG. Development of an insert co-culture system of two cellular types in the absence of cell-cell contact. *J Vis Exp.* 2016;(113). doi(113):10.3791/54356. doi: 10.3791/54356 [doi].

CHAPTER 5: Changes in Cellular Crosstalk between Skeletal Muscle Myoblasts and Bone Osteoblasts with Aging

5.1. Abstract

Musculoskeletal function declines with aging, resulting in an increased incidence of trips and falls. Both bone and muscle experience age-related losses in tissue mass that alter their mechanical interactions in a well characterized manner, but changes in the biochemical interactions between bone and muscle with aging are not well understood. Of note, insulin-like growth factor 1 (IGF-1), a potent growth factor for bone and muscle, can be negatively altered with aging and may help explain losses in these tissues. We recently developed a co-culture system for simultaneous growth of bone mesenchymal stem cells (MSCs) and muscle satellite cells (SCs) to investigate the biochemical crosstalk between the two cell types. Here, we utilized an aging rat model to study cellular changes between young and old rat MSCs and SCs, in particular whether 1) young MSCs and SCs have increased proliferation and differentiation compared to old MSCs and SCs; 2) young cells have increased IGF-1 and collagen expression as a measure of crosstalk compared to old cells; and 3) young cells can mitigate the aging phenotype of old cells in co-culture. Rat MSCs and SCs were either mono- or co-cultured in Transwell® plates, grown to confluence, and allowed to differentiate for 14 days. Across the 14 days, cell proliferation was measured, with differentiation and crosstalk measurements evaluated at 14 days. The results suggest that in both young and old, proliferation is greater in mono-cultures compared to co-cultures, yet age and cell type did not have a significant effect. Differentiation did not differ between young and old cells, yet MSCs and SCs demonstrated the greatest amount of differentiation in co-culture. Finally, age, cell type, and culture type did not have a significant effect on collagen or IGF-1 expression. These results suggest co-culture may have a controlling effect, with the two cell types acting together to

promote differentiation more than in mono-cultures, yet this response was not altered by age. In general, results for old cells had higher variability, suggesting that age-related changes are more lifestyle dependent. This study was the first to use this rat aging model to investigate changes between bone and skeletal muscle cells, however further investigations are required to determine what signaling changes occur in response to age. Determining these signaling changes could lead to new targets for mitigating the progression of aging.

5.2. Introduction

Musculoskeletal performance declines with aging, resulting in an increased incidence of trips and falls in the elderly.¹ These changes are compounded by concomitant losses in bone mass (osteopenia, osteoporosis) and skeletal muscle mass (sarcopenia),^{3,4} leading to high rates of fracture and muscle injury in the elderly population. Under the mechanostat paradigm, these detrimental muscle changes, which manifest in decreased muscle loading on the skeleton, will induce negative bone adaptation and bone loss.² Aged individuals with decreased bone mass (osteopenia) often also present with reduced muscle mass and function (sarcopenia).^{3,4} However, although elderly populations often experience both osteopenia and sarcopenia, age-related declines in either bone or muscle mass cannot fully explain the extent of functional declines in the other tissue, supporting the idea that bone-muscle interactions are not solely mechanical in nature. Indeed, the emergent thought is that biochemical interactions also play an important role in bone and muscle tissue health and function, in particular the direct communication between the two through paracrine signaling pathways, or cell-cell *crosstalk*.^{5,6} Improving our understanding of how bone-muscle crosstalk changes with aging could inform the development of targeted therapies to mitigate age-related losses in musculoskeletal function.

Age-related changes in biochemical signaling are well characterized for bone and muscle individually. In muscle, satellite cells (SCs) responsible for muscle repair have decreased activity from overuse, and signaling molecules such as inflammatory and growth factors are reduced.^{7,8} Similarly, bone loss associated with aging is the result of reduced functional ability of bone osteoblasts to produce new bone, as well as a loss of signaling factors.⁹

While these signaling changes have been investigated in either muscle or bone alone, the investigation of the signaling changes in tandem have been under characterized. The concurrent age-related changes in bone and muscle signaling are not fully understood, although the importance of this crosstalk has been established in several key studies. In elegant parabiosis studies, in which the vascular systems for young and old rat pairs were surgically merged, old rats experienced some muscle rejuvenation, including increased muscle mass and improved muscle fiber structure, although specific factors from the young rats stimulating this change remained unidentified.^{17,18} Further, *in vivo* studies demonstrated faster healing of bone fractures in the presence of muscle tissue,^{19,20} but again the specific crosstalk factors stimulating tissue repair were not investigated. Therefore, a more specific method is required to investigate the specific crosstalk changes. Our previous work optimized a co-culture system between SCs and bone mesenchymal stem cells (MSCs) to investigate the optimal growth conditions for each cell type. Utilization of this system could lead to better understanding of the crosstalk between muscle and bone.

One signaling target for investigation in both muscle and bone is insulin-like growth factor 1 (IGF-1). IGF-1 is a potent growth factor secreted by the liver in response to the secretion of growth hormone.¹⁰ However, IGF-1 has also been demonstrated to be released by both muscle and bone to be used in an autocrine or paracrine fashion.^{10,11} The downstream effects of IGF-1 result in protein synthesis such a collagen I to lead to increased muscle and bone mass.¹⁰ As a critical growth

factor for both muscle and bone, studies have demonstrated that reductions in IGF-1 lead to reductions in both muscle and bone mass,¹¹⁻¹³ and decreased the amount of collagen in these tissues.¹⁴⁻¹⁶ However, how IGF-1 is altered in the crosstalk between muscle and bone has not been investigated.

The purpose of this study was to characterize concurrent changes in bone and muscle cells and biochemical interactions with aging. Using our previously optimized co-culture system, we paired bone mesenchymal stem cells (MSCs) and muscle SCs from both young and old rats and examined cell viability, differentiation, and crosstalk using young-young, old-old, young-old, and old-young pairs. We hypothesized that in old cells, there would be decreased cell viability, a decrease in the differentiation of SCs and MSCs into their mature phenotypes, and a decrease in the amount of crosstalk, measured by IGF-1 and collagen I expression. Furthermore, we wanted to test the hypothesis that young factors could improve the aging phenotype as demonstrated by Conboy et al.¹⁸ By co-culturing young and old cells together we hypothesized that the young SCs or MSCs when cultured with the opposite old cell would be unchanged when compared to their regular young co-cultured with young cells. Additionally, the old cells (either SCs or MSCs) when cultured with young cells would see an increase in cell viability, cell differentiation, and cell crosstalk when compared to old cells co-cultured with other old cells.

5.3. Methods

5.3.1. Animals and cell isolation

The Institutional Animal Care and Use Committee at North Carolina State University approved all animal procedures. F344 x brown Norway F1 rat hybrids were used in this study as a model for aging, because they are commonly used in aging muscle function studies. Ten young (5-9 months old) and ten old (33-34 months old) F344 x brown Norway hybrid rats (National Institutes of

Aging, Bethesda, Maryland) were fed a normal diet and kept under a 12-hr light/12-hr dark cycle with free access to chow and water until euthanasia. After acclimation to the animal facility for one week, rats were euthanized by CO₂ inhalation, followed by immediate dissection to remove the gastrocnemius and tibialis anterior (TA) muscles and the tibia and femur from one leg. Rat bone MSCs were isolated from the tibia and femur using a method modified from Zhang and Chan.²¹ Briefly, the bones were placed in warm MSC-specific growth medium (MSCGM) consisting of alpha-MEM (Gibco, Gaithersburg, MD), 10% fetal bovine serum (Gemini Bio-Products, West Sacramento, CA), and 100 U/mL penicillin-100 µg/mL streptomycin (Gibco). The bone ends were removed, and the remaining segments were flushed with MSCGM to extract the marrow and isolate the MSCs. The MSCs were plated on a single 120-mm plastic plate (Corning, Tewksbury, MA) coated with 2% gelatin (Fisher Scientific, Hampton, NH) and cultured with MSCGM in a humidified atmosphere at 37°C with 5% CO₂. After 48 h, the nonadherent cells were washed out, and the cultures were expanded to passage 2.

SCs were extracted from the gastrocnemius and TA using a protocol from Danoviz and Yablouk-Reuveni.²² Briefly, the muscles were placed in warm SC-specific growth medium (SCGM) consisting of high glucose Dulbecco's MEM (Gibco), 20% fetal bovine serum (Gemini Bioproducts), 10% horse serum (Gibco), and 100 U/mL penicillin-100 µg/mL streptomycin (Gibco). Tendon, fat, blood vessels, and connective tissue were removed, and the remaining muscle was cut into small (~3 mm³) cubes. Muscle cubes were collected and added to a 1% Pronase solution (Pronase Protease, Millipore-Sigma, St. Louis, MO) in SCGM for one hour for digestion. The solution and remaining muscle were then collected and suspended in 10 mL of additional SCGM. The entire solution was subjected to mechanical trituration by passing the solution through a wide-bore pipette to liberate SCs. Finally, the triturated solution was passed through a cell

strainer with a 70- μm pore size (Fisher Scientific), and SCs were collected and plated on a single 2% gelatin-coated 120-mm plate with SCGM in a humidified atmosphere at 37°C with 5% CO₂. After 48 h, the nonadherent cells were washed out, and the cultures were expanded to passage 2.

5.3.2. Co-culture design

After passage 2, cells were plated in both mono- and co-culture (Fig. 1). In mono-culture experiments, SCs and MSCs were each cultured at 20×10^3 cells per well in a 12-well gelatin-coated plate, with each condition run in triplicate per animal. In co-culture experiments, SCs and MSCs were each cultured at 20×10^3 cells per well in a 12-well Transwell[®] gelatin-coated plate (Corning, Corning, NY), with SCs in the bottom well and MSCs in the insert, separated by the 0.4- μm pore membrane. Plates were allowed to grow to 50% confluence in SCGM for SCs and in MSCGM for MSCs. At 50% confluence, media was changed to myogenic media (MM) for SCs (containing high glucose Dulbecco's MEM (Gibco), 1% horse serum (Gibco), and 100 U/mL penicillin-100 $\mu\text{g}/\text{mL}$ streptomycin (Gibco)) and osteogenic media (OM) for MSCs (containing alpha-MEM (Gibco), 10% fetal bovine serum (Gibco), 50 mM ascorbic acid (Millipore-Sigma), 100 μM dexamethasone (Millipore-Sigma), 1 M β -glycerophosphate (Millipore-Sigma) and 100 U/mL penicillin-100 $\mu\text{g}/\text{mL}$ streptomycin (Gibco)) to allow differentiation to occur. Differentiation continued for 14 days, at which point outcome metrics (below) were assessed.

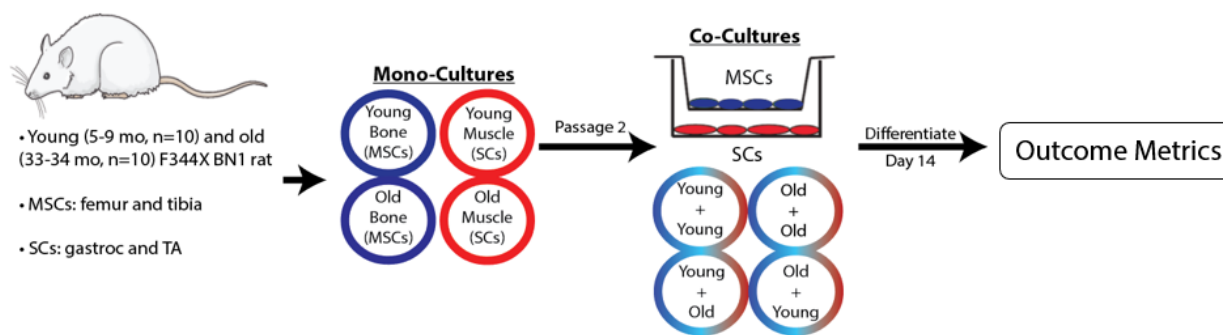


Figure 1. Study design. SCs and MSCs were isolated from rat tissue and cultivated in monoculture and co-culture and allowed to differentiate for 14 days. Outcome metrics (described below) were then assessed.

5.3.3. Cell proliferation

On differentiation days 0, 3, 7, 10, and 14, an alamarBlue[®] solution (ThermoFisher, Waltham, MA) was mixed into each well (90% media, 10% alamarBlue[®]), and the cells were incubated at 37°C. After 3 h, the solution was collected, and absorbance readings were taken at 570 and 600 nm (Synergy[™] H1M, BioTek Instruments, Inc., Winooski, VT). For the co-cultures, the bottom well and insert of the Transwell[®] plates were analyzed separately. The percent reduction in alamarBlue[®] level, a measure of proliferative ability, was determined from the absorbance reading according to the manufacturer's instructions.

5.3.4. Cell differentiation

On differentiation day 14, cells were rinsed with phosphate buffered saline (PBS), fixed in 10% zinc-buffered formalin (VWR, Randor, PA) for 30 min, and then rinsed again with PBS. To assess mineral deposition for MSC differentiation, a 2% Alizarin Red S (Fisher) solution was applied to each sample for 5 min, rinsed with deionized water, and imaged using an iPhone 6S camera (Apple, Cupertino, CA) and EVOS[®] XL light microscope (Life Technologies, Carlsbad, CA). Mineral deposition was quantified by solubilizing the Alizarin Red S stain with a 0.5 N HCl

+ 5% sodium dodecyl sulfate (SDS) solution for 30 min and then taking absorbance readings at 405 nm.

To assess SC differentiation, immunocytochemistry (ICC) procedures for skeletal myosin expression were performed. On differentiation day 14, cells were rinsed with DMEM, fixed in 10% zinc-buffered formalin for 10 min, and then rinsed with tris-buffered saline (TBS). A blocking solution of TBS with 2% normal goat serum (NGS) was applied to the cells and allowed to incubate at 4°C overnight. Cells were then allowed to warm to room temperature for 10 min. A rat-specific primary antibody for skeletal muscle myosin heavy chain (MA1-35718, ThermoFisher) was diluted 1:5 in TBS-NGS. Wells were rinsed with a TBS-0.05% Tween 20 (TW20, ThermoFisher) solution, and primary antibodies were applied. Cells were incubated for 1 h at room temperature, followed by an overnight incubation at 4°C in a humidified chamber with gentle shaking. Cells were again allowed to return to room temperature while the secondary antibody (AlexaFluor 584, A-21044, ThermoFisher) was diluted 1:10 in TBS-NGS. Cells were rinsed in TBS-TW20, and the secondary antibody was applied for 2 h at room temperature. Wells were aspirated and rinsed with TBS-TW20, and a diluted DAPI (ThermoFisher) solution was prepared (1 ug/mL diluted in TGS-NGS) and applied to the wells for 30 min at room temperature. Wells were rinsed with TBS-TW20 a final time and mounted with a drop of Vectashield (Vector Laboratories, Burlingame, CA) and a 25% glycerol solution in TBS. Cells were imaged (EVOS® FL Auto, Life Technologies, Carlsbad, CA), and area and integrated density of the fluorescent regions were measured. SC and MSC differentiation were also assessed qualitatively based on cell morphology, looking for multinucleated and elongated cells with SCs and a fibroblastic appearance and mineral nodules with MSCs.

5.3.5. Cellular crosstalk

Since IGF-1 aids growth in both bone and muscle, its expression was assessed in the conditioned media of both mono- and co-cultures at differentiation day 14 using an ELISA kit (ERIGF1, ThermoFisher), according to the manufacturer's instructions. A standard curve was produced, and samples expressing IGF-1 levels outside of the standards' range were omitted.

To assess the effect of aging on collagen production, ICC was performed to evaluate the amount of collagen deposited by the cells. The ICC protocol was the same as for the cellular differentiation analysis, except with a rat-specific collagen I primary antibody (PA1-36145, ThermoFisher) and a secondary antibody (A-11034, ThermoFisher) used at a 1:10 dilution in TBS-NGS.

5.3.6. Statistical analyses

Statistical analyses were performed with Prism (version 6.07; GraphPad Software, La Jolla, CA) using a significance level of 0.05. All results were averaged across the groups and expressed in the form of mean \pm standard error of the mean due to unbalanced samples. The effects of age (young, old) and cell type (Mono-SC, Mono-MSC, Co-SC, Co-MSC) were examined using two-way ANOVAs. In cases where differentiation day was considered, a two-way ANOVA was performed with repeated measures. Post-hoc pairwise comparisons within each factor were evaluated with Tukey tests if interactions were previously found to be significant.

5.4. Results

5.4.1. Cell viability

Percent reduction in alamarBlue[®] differed significantly by cell culture type at differentiation days 7, 10, and 14 ($p < 0.05$, Fig. 2), with mono-cultures demonstrating greater proliferation than co-cultures at these later time points, and with co-cultures demonstrating no difference between

young and old cell types. Young muscle (SCs) in mono-culture demonstrated greater proliferation at days 7, 10 and 14 of differentiation compared to young muscle paired with either young or old bone (MSCs) cells ($p < 0.05$, Fig. 2A). This pattern continued in young bone (Fig. 2B), old muscle (Fig. 2C) and old bone (Fig. 2D). Furthermore, no differences were found in proliferation between young and old co-cultures or mono-cultures (i.e., Ym vs Om, or YmYb vs OmYb).

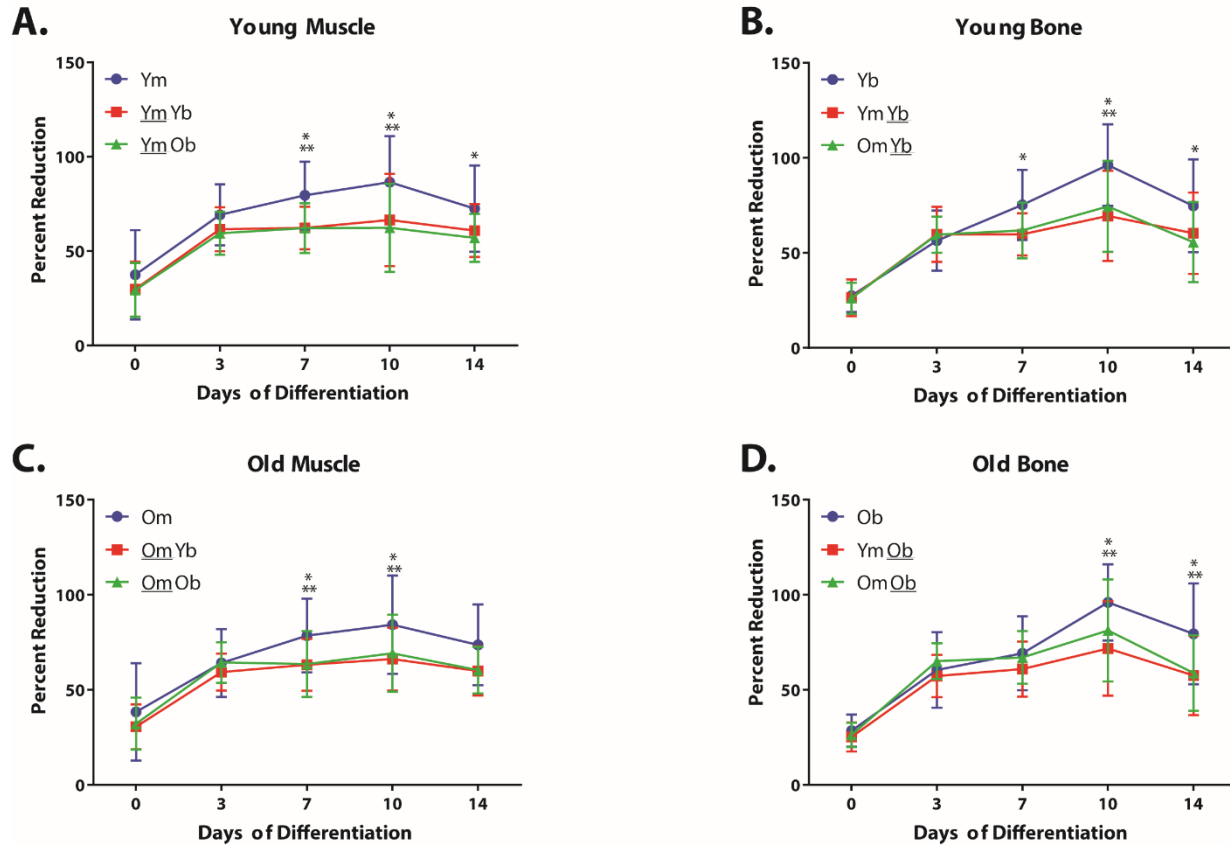


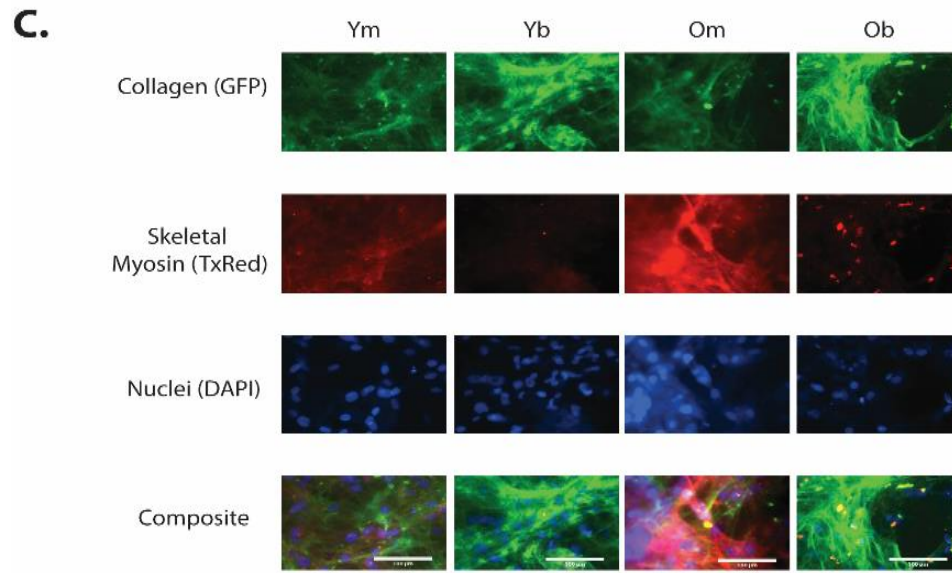
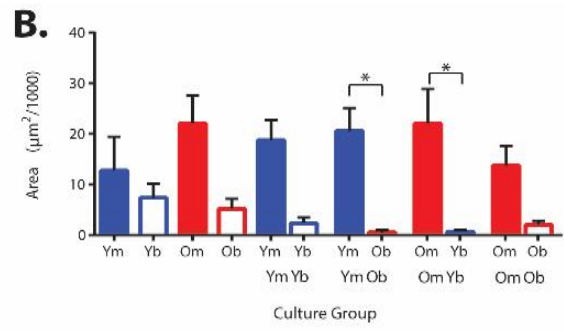
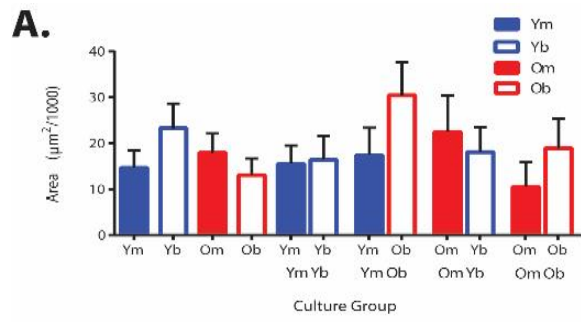
Figure 2. AlamarBlue® reduction across differentiation days for different cultures. Proliferative ability differed between some mono- and co-cultures during differentiation days 7-14 for A) young muscle, B) young bone, C) old muscle, and D) old bone. Data are mean \pm SEM. * $p < 0.05$ for mono-culture (blue) vs. co-culture (red). ** $p < 0.05$ for mono-culture (blue) vs. co-culture (green).

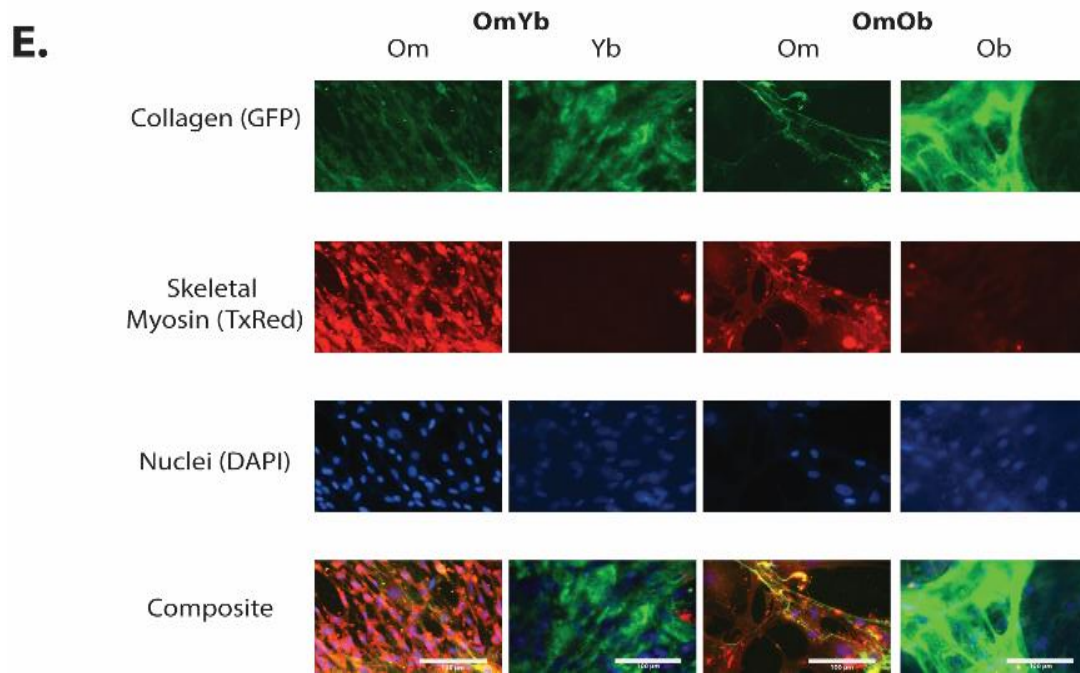
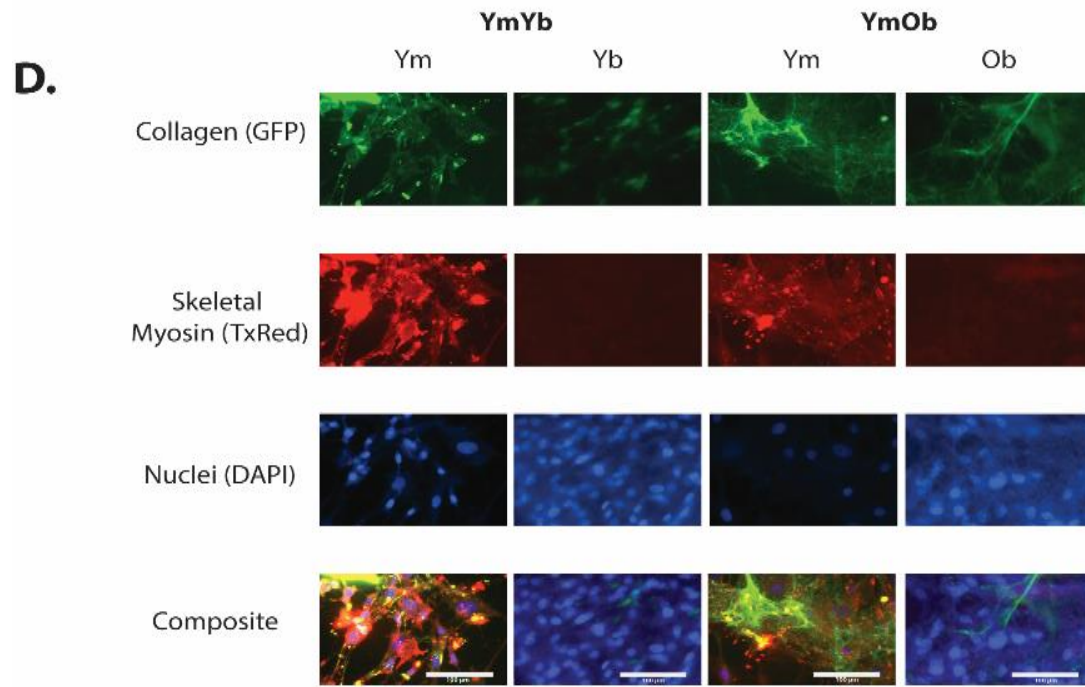
5.4.2. Collagen and Myosin Expression

Collagen immunostaining did not differ across cell or culture type (Fig. 3A). In general, differences in collagen expression between mono-cultures and co-cultures were small ($p > 0.05$), according to the amount of collagen staining in a given field. When these values were normalized

to intensity or number of cells in the area, there still was no difference. For myosin, the relative expression in muscle cells compared to that in bone cells was generally greater in co-culture than in mono-culture ($p < 0.05$, Fig. 3B), with no difference in the amount of myosin expressed between young and old cells, either in mono- or co-culture ($p > 0.05$). In mono-culture, myosin expression did not differ between muscle and bone cells regardless of age ($p > 0.05$). However, myosin expression in muscle cells seemed to trend higher than in bone cells. In co-culture, bone cells generally had little to no expression of myosin relative to their muscle cell counter-parts ($p < 0.05$). Age had no effect on the amount of myosin expressed in these co-cultures. Similarly, when controlling for intensity or number of cells within the field, these differences remained the same. Representative images of these condition are shown in Figures 3 C, D, and E.

Figure 3. Immunocytochemistry analysis of cultured cells. Collagen I expression (A) and skeletal myosin expression (B) after 14 days of differentiation. No differences in collagen expression were found across cell type or age, or in mono- vs. co-culture ($p < 0.05$). Myosin expression was typically increased in SCs in co-culture ($*, p < 0.05$) and tended to be increased compared to MSCs in mono-culture. Age had no effect between these conditions. Representative images from the various conditions are shown in (C), (D), and (E). Data are mean \pm SEM.





5.4.3. Mineralization

Alizarin red results in mono-culture showed that bone cells had or tended to have significantly more amounts of mineralization relative to muscle cells ($p < 0.05$), yet age did not have a significant effect ($p > 0.05$, Fig. 4A). In co-culture, however, all cell types and ages had very little mineralization ($p > 0.05$). Between mono- and co-cultures, mineralization was higher in bone cells in mono-culture than in co-culture. These data suggests that osteoblasts more successfully differentiated into osteoblasts in mono-culture than in co-culture.

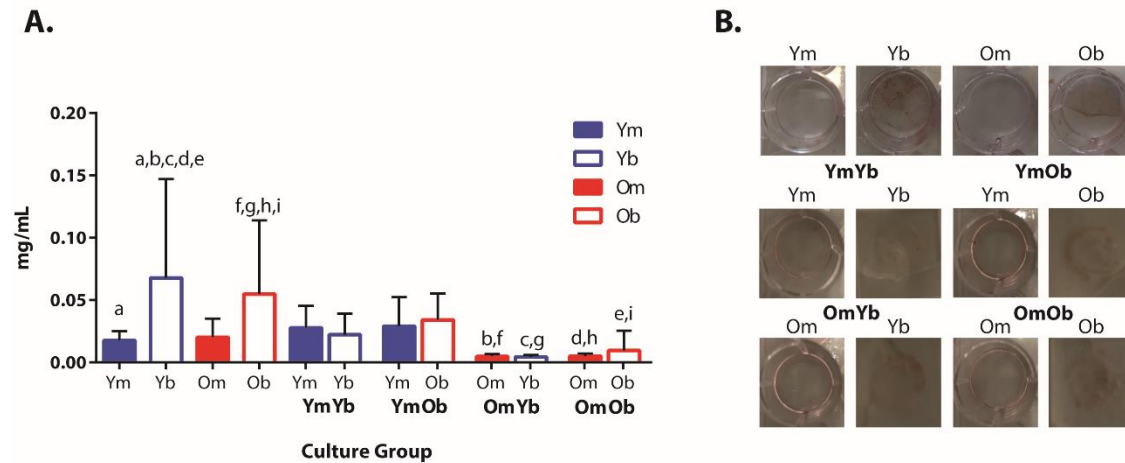


Figure 4. Alizarin red solubilization data from fixed cells. Solubilization results (A) and representative images (B). In mono-culture, MSCs tended to have or had a significantly greater amount of mineralization compared to SCs ($p < 0.05$). In co-culture, MSCs paired with old SCs had significantly less mineralization compared to their mono-culture equivalent ($p < 0.05$). MSCs paired with young SCs had similar amounts of mineralization compared to mono-culture ($p < 0.05$). Data are mean \pm SD. Bars with the same letter above them are significantly different.

5.4.4. Crosstalk

ELISA results for IGF-1 expression in conditioned media demonstrated no difference between cell or culture type (Fig. 5). In mono-culture, bone cells tended to have lower expression of IGF-1 compared to muscle cells, but these differences were not significant; young and old cells had similar IGF-1 expression in mono-culture. In co-culture, IGF-1 expression did not differ between cell types or between young and old cells. Furthermore, no differences were found in the amount

of expression between mono- and co-cultures. These results suggest that IGF-1 expression is not altered by communication between these two cell types in aging.

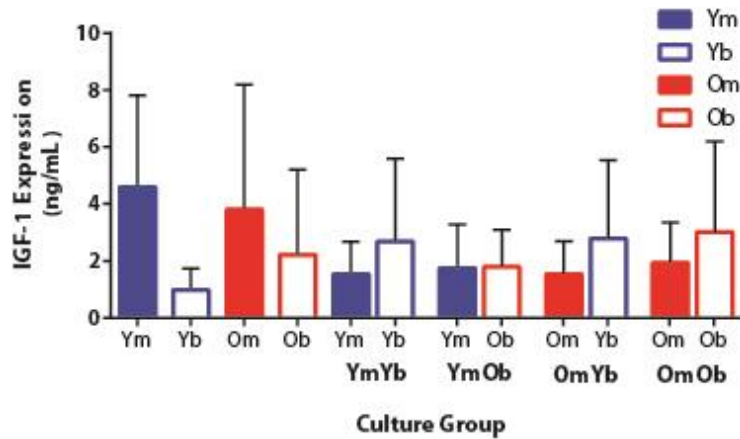


Figure 5. IGF-1 expression from conditioned media on day 14. IGF-1 expression did not differ by cell type, culture type, or age ($p > 0.05$). Data are mean \pm SEM.

5.5. Discussion

Understanding the bone-muscle interactions has become increasingly important to better understand musculoskeletal diseases. Understanding these interactions with regards to aging could lead to novel therapeutic options to improve aging outcomes. Here, we utilized a previously optimized co-culture system to investigate the bone-muscle interactions in both young and old cells. Our hypothesis was that, younger cells would generally demonstrate greater proliferation and differentiation compared to old cells. Furthermore, when placed in co-culture, young cells paired together would experience increased crosstalk between the cell types; young cells paired with old cells would be able to improve the old cells' proliferation, differentiation, and crosstalk; and old cells paired together would perform the worst in regards to proliferation, differentiation, and crosstalk. The results of these experiments demonstrated that our hypotheses were partially supported.

5.5.1. Cellular proliferation

Our specific hypothesis for cellular proliferation predicted that young cells would proliferate more than old cells. Additionally, as a secondary hypothesis, we predicted that cells in co-culture would undergo increased proliferation compared to the mono-cultured cells. Our alamarBlue[®] results suggested that there was no difference between young and old cells when undergoing proliferation contrary to our hypothesis. Furthermore, our secondary hypothesis was not supported in that monocultures overall demonstrated increased proliferative ability at later days of differentiation compared to co-cultures. Other studies investigating the proliferative potential between two cell types have demonstrated typically an increased proliferation response compared to monocultures.^{23,24} The differences between these finding and our own however, lie in the selection of animal model, cell type, and type of co-culture. In our case, we are the first to use this animal model of aging in a co-culture study between SCs and MSCs. The decreased proliferation found in our co-cultures may be the result of a regulatory effect between the two cell types in co-culture. This response may mimic those found in the *in vivo* state where bone-muscle interactions can regulate the growth of both tissue types.²⁵ More interestingly however, is that this regulatory effect was conserved across age in our data. Aging can hinder many aspects of the cellular lifecycle, with decreases in proliferation a common characteristic.²⁶⁻²⁸ Decreased proliferation was not observed in our old cell data and may be the result of a less severe phenotype in our cells that may be present in other studies. This less severe phenotype observed here continues through much of our data set.

5.5.2. Cellular differentiation

Another aspect of our hypothesis was that old SCs would demonstrate decreased differentiation (measured by skeletal myosin deposition) compared to young SCs and that SCs overall would

demonstrate an increased amount of myosin compared to MSCs. As a secondary hypothesis, we expected that co-cultured SCs would demonstrate more myosin deposition compared to monocultured SCs and that old SCs cultured with young MSCs would have an increased amount myosin compared to old SCs cultured with old MSCs. Old SCs can demonstrate a decrease in the amount of myosin as SCs become worn out, less proliferative, and instead more collagen or other fibrotic material is placed.^{29,30} Here, our hypotheses were only partially supported. In co-culture particularly, SCs had increase myosin content compared to MSCs, yet there was no change due to age. In monoculture, there was no change between myosin expression between SCs and MSCs, although SC myosin expression tending to be increased. These data suggest that in co-culture, MSCs may have a beneficial effect on the differentiation of SCs. Other studies utilizing co-culture have demonstrated that this beneficial response may often be the cases as cross-talk signals between the two cell types may enhance the differentiation.³¹ Taken together with the viability results, this suggests that instead of actively dividing, the co-culture conditions promoted differentiation of SCs. Continuing forward, a more morphological investigation of myoblast fusion could provide a more definitive explanation for differentiation changes as described by others previously. However, in regards to age, the lack of change between young and old further suggests that the old phenotype was less severe than those demonstrated by other studies, or that an increased variability within samples contributed to a lack of significant differences between conditions.

Surprisingly, MSC differentiation showed an opposite response compared to SCs. MSCs demonstrated increased mineral deposition, and by extension, increased differentiation in monocultures compared to co-cultures, with little effect of age. Our hypothesis suggested that MSCs would have improved mineralization in co-culture, with more mineralization in young cells,

neither of which were supported by our data. We believe there may be two cases why this response was observed: (1) SCs inhibited MSC differentiation or (2) media mixing between the two wells diluted differentiation media in MSC wells. In the first case, novel experiments exploring bone-muscle crosstalk have demonstrated that signaling factors from muscle such as myostatin and ciliary neurotrophic factor 1 (CNF-1) can inhibit osteoblast differentiation.^{32,33} These factors are secreted by muscle after sufficient growth in order to inhibit further muscle growth. In our preliminary studies and those of others, we have noticed that SCs can reach myoblast fusion as early at 10 days,³⁴⁻³⁶ whereas MSCs differentiation can take as long as 21 days in some studies^{37,38}. In this case, we suggest that SCs were reaching a more differentiated state more quickly than MSCs and may have secreted these inhibitory factors before MSCs could completely differentiate. We also found that growth of myoblasts occurred more quickly than MSCs and could result in monolayers lifting off the plate, precluding us from continuing to 21 days to see if MSCs could reach a more differentiated state. In the second case, the transwell setup required that each cell type receive their own differentiation media, yet the pores within the transwell did not stop mixing between the two wells. While another has reported that this mixing can take several days³⁹, and may not have been a factor in this study, we cannot exclude this possibility. In either case, the presence of significant mineralization in mono-cultures suggest that that the differences have arisen due to the co-culture setup itself. Furthermore, the lack of difference between young and old cultures continues to reinforce that the cells observed a less severe aging phenotype.

5.5.3. Cellular crosstalk

To investigate crosstalk, we investigated the role of IGF-1 in signaling between the two cell types, as well as collagen I expression in the two cell types. With age, muscle commonly loses its ability to repair and replace tissue effectively, and instead deposits collagen. Additionally, bone

experiences collagen loss resulting in an increased incidence of fractures and microcracks with age.⁹ IGF-1 is a potent growth factor of both muscle and bone, and can enhance collagen production. We hypothesized that with age, IGF-1 expression would be decreased, leading to decreases in collagen I deposition in both SCs and MSCs. In co-culture experiments, we hypothesized that old cells plated with young cells would behave more similarly to young cells and have similar IGF-1 and collagen I expression, but our results did not support these hypotheses. Instead, our results show that there was no change in IGF-1 expression (Fig. 5) and collagen expression (Fig. 3A) did not differ across the culture conditions, cell types, or age. Many studies have highlighted the role of crosstalk between muscle and bone and the importance of this crosstalk for the growth and development of both.⁵ In this study we focused on IGF-1 as it is an important mediator of growth and is often reduced with age.⁴⁰ However, IGF-1 has only been minimally investigated during bone-muscle crosstalk.

Our results with no age-related changes to IGF-1 expression were surprising, considering the differences in IGF-1 expression observed in several aging studies, but this discrepancy may result from the differences in study design. IGF-1 expression is frequently measured in serum samples⁴¹ or in whole tissue samples.⁴² While both bone and muscle can secrete and react to their own IGF-1 signals in an autocrine fashion, perhaps the IGF-1 expression in bone and muscle in an *in vivo* environment are enhanced by additional IGF-1 from the bloodstream and elsewhere. In the isolated *in vitro* environment used here, we found that IGF-1 is clearly secreted by bone and muscle but may only promote initial growth. Therefore, while we did not observe differences in IGF-1 expression associated with age or co-culture conditions in this isolated system, it cannot capture the system-wide IGF-1 signaling that occurs *in vivo*. Furthermore, IGF-1 is merely one bone-

muscle crosstalk factor that can be detrimentally affected by aging; studies of additional signaling factors could provide a more complete picture of age-related crosstalk changes *in vitro*.⁴³⁻⁴⁵

IGF-1 was also investigated due to its significant role in downstream collagen production. We anticipated diminished amounts of IGF-1 expression with aging would lead to decreased collagen deposition in old cells compared with young cells. In this context, the lack of differences in collagen I expression between cell types, ages, or culture types may not be so surprising. In bone, approximately 36% of its composition is collagen I, and this content decreases with age.^{46,47} Conversely, muscle has 2-6% collagen and content increases with age.^{48,49} However, collagen I deposition *in vitro* was not different between bone or muscle cells. Since collagen is deposited by mature cells, and given the early maturation stage of our cells, perhaps the differentiation time was not sufficient to allow significant collagen deposition. Furthermore, in co-culture, the lack of difference in collagen deposition may be indicative of a lack of influence of the crosstalk between the two cell types. While differences in IGF-1 expression or collagen deposition were not observed with co-culture, we cannot exclude the possibility that other signaling pathways or protein expression were not altered by crosstalk. Further studies are required to probe this possibility.

5.6. Conclusions

In summary, we demonstrated that co-culture of bone and muscle cells regulates proliferation more so than for cells grown in monoculture, yet age or cell type did not affect proliferation. Furthermore, differences in cellular differentiation or crosstalk were minimal with little to no effect of age, cell type, or culture condition on myosin expression, mineralization, IGF-1 expression, or collagen deposition. This study was the first to use the F344 x BN F1 hybrid rat in a study for cellular aging while also investigating the crosstalk between SCs and MSCs. The lack of differences between young and old cellular proliferation, differentiation, and crosstalk demonstrate

that this particular model may not be ideal for age-related cellular studies. However, the use of this model to successfully grow SCs and MSCs should provide evidence that further studies should seek to understand other aging changes across other cell types using this model. The use of a Transwell[®] co-culture system provides a framework with which to understand the individual contributions of each cell type, which cannot be isolated in direct co-culture models. Many potential bone-muscle crosstalk factors besides IGF-1 could be contributing to the concomitant age-related changes observed in bone and muscle *in vivo*, and future studies should focus either on developing *in vitro* systems that better mimic the *in vivo* aging environment and/or examining contributions of different signaling pathways to tissue aging. Overall, this study demonstrated that the intricate interactions between bone and muscle depends on a variety of cues, and advancing our understanding of these cues is essential for developing better models for mimicking aging and better treatments to mitigate functional musculoskeletal deficits with aging.

5.7. References

1. Lockhart TE, Smith JL, Woldstad JC. Effects of aging on the biomechanics of slips and falls. *Hum Factors*. 2005;47(4):708-729. doi: 10.1518/001872005775571014 [doi].
2. Fricke O, Schoenau E. The 'functional muscle-bone unit': Probing the relevance of mechanical signals for bone development in children and adolescents. *Growth Horm IGF Res*. 2007;17(1):1-9. doi: S1096-6374(06)00127-4 [pii].
3. Freemont AJ, Hoyland JA. Morphology, mechanisms and pathology of musculoskeletal ageing. *J Pathol*. 2007;211(2):252-259. doi: 10.1002/path.2097 [doi].
4. Marcell TJ. Sarcopenia: Causes, consequences, and preventions. *J Gerontol A Biol Sci Med Sci*. 2003;58(10):M911-6.
5. Brotto M, Bonewald L. Bone and muscle: Interactions beyond mechanical. *Bone*. 2015;80:109-114. doi: 10.1016/j.bone.2015.02.010 [doi].
6. Brotto M, Johnson ML. Endocrine crosstalk between muscle and bone. *Curr Osteoporos Rep*. 2014;12(2):135-141. doi: 10.1007/s11914-014-0209-0 [doi].
7. Brack AS, Conboy MJ, Roy S, et al. Increased wnt signaling during aging alters muscle stem cell fate and increases fibrosis. *Science*. 2007;317(5839):807-810. doi: 317/5839/807 [pii].
8. Yin H, Price F, Rudnicki MA. Satellite cells and the muscle stem cell niche. *Physiol Rev*. 2013;93(1):23-67. doi: 10.1152/physrev.00043.2011 [doi].
9. Boskey AL, Coleman R. Aging and bone. *J Dent Res*. 2010;89(12):1333-1348. doi: 10.1177/0022034510377791 [doi].
10. Bikle DD, Tahimic C, Chang W, Wang Y, Philippou A, Barton ER. Role of IGF-I signaling in muscle bone interactions. *Bone*. 2015;80:79-88. doi: 10.1016/j.bone.2015.04.036 [doi].
11. Wang Y, Nishida S, Elalieh HZ, Long RK, Halloran BP, Bikle DD. Role of IGF-I signaling in regulating osteoclastogenesis. *J Bone Miner Res*. 2006;21(9):1350-1358. doi: 10.1359/jbmr.060610 [doi].
12. Jaynes JB, Johnson JE, Buskin JN, Gartside CL, Hauschka SD. The muscle creatine kinase gene is regulated by multiple upstream elements, including a muscle-specific enhancer. *Mol Cell Biol*. 1988;8(1):62-70.
13. Wang Y, Cheng Z, Elalieh HZ, et al. IGF-1R signaling in chondrocytes modulates growth plate development by interacting with the PTHrP/ihh pathway. *J Bone Miner Res*. 2011;26(7):1437-1446. doi: 10.1002/jbmr.359 [doi].

14. Atti E, Boskey AL, Canalis E. Overexpression of IGF-binding protein 5 alters mineral and matrix properties in mouse femora: An infrared imaging study. *Calcif Tissue Int.* 2005;76(3):187-193. doi: 10.1007/s00223-004-0076-2 [doi].
15. Barton ER, Morris L, Musaro A, Rosenthal N, Sweeney HL. Muscle-specific expression of insulin-like growth factor I counters muscle decline in mdx mice. *J Cell Biol.* 2002;157(1):137-148. doi: 10.1083/jcb.200108071 [doi].
16. Velloso CP. Regulation of muscle mass by growth hormone and IGF-I. *Br J Pharmacol.* 2008;154(3):557-568. doi: 10.1038/bjp.2008.153 [doi].
17. Conboy MJ, Conboy IM, Rando TA. Heterochronic parabiosis: Historical perspective and methodological considerations for studies of aging and longevity. *Aging Cell.* 2013;12(3):525-530. doi: 10.1111/accel.12065 [doi].
18. Conboy IM, Conboy MJ, Wagers AJ, Girma ER, Weissman IL, Rando TA. Rejuvenation of aged progenitor cells by exposure to a young systemic environment. *Nature.* 2005;433(7027):760-764. doi: nature03260 [pii].
19. Fleming ME, Watson JT, Gaines RJ, O'Toole RV, Extremity War Injuries VII Reconstruction Panel. Evolution of orthopaedic reconstructive care. *J Am Acad Orthop Surg.* 2012;20 Suppl 1:S74-9. doi: 10.5435/JAAOS-20-08-S74 [doi].
20. Harry LE, Sandison A, Paleolog EM, Hansen U, Pearse MF, Nanchahal J. Comparison of the healing of open tibial fractures covered with either muscle or fasciocutaneous tissue in a murine model. *J Orthop Res.* 2008;26(9):1238-1244. doi: 10.1002/jor.20649 [doi].
21. Zhang L, Chan C. Isolation and enrichment of rat mesenchymal stem cells (MSCs) and separation of single-colony derived MSCs. *J Vis Exp.* 2010;(37). pii: 1852. doi(37):10.3791/1852. doi: 10.3791/1852 [doi].
22. Danoviz ME, Yablonka-Reuveni Z. Skeletal muscle satellite cells: Background and methods for isolation and analysis in a primary culture system. *Methods Mol Biol.* 2012;798:21-52. doi: 10.1007/978-1-61779-343-1_2 [doi].
23. Steward AJ, Cole JH, Ligler FS, Loba EG. Mechanical and vascular cues synergistically enhance osteogenesis in human mesenchymal stem cells. *Tissue Eng Part A.* 2016;22(15-16):997-1005. doi: 10.1089/ten.TEA.2015.0533 [doi].
24. Walenda T, Bork S, Horn P, et al. Co-culture with mesenchymal stromal cells increases proliferation and maintenance of haematopoietic progenitor cells. *J Cell Mol Med.* 2010;14(1-2):337-350. doi: 10.1111/j.1582-4934.2009.00776.x [doi].
25. Maurel DB, Jahn K, Lara-Castillo N. Muscle-bone crosstalk: Emerging opportunities for novel therapeutic approaches to treat musculoskeletal pathologies. *Biomedicines.* 2017;5(4):10.3390/biomedicines5040062. doi: E62 [pii].

26. Li Y, Charif N, Mainard D, Bensoussan D, Stoltz JF, de Isla N. Donor's age dependent proliferation decrease of human bone marrow mesenchymal stem cells is linked to diminished clonogenicity. *Biomed Mater Eng.* 2014;24(1 Suppl):47-52. doi: 10.3233/BME-140973 [doi].
27. Tsai WC, Chang HN, Yu TY, et al. Decreased proliferation of aging tenocytes is associated with down-regulation of cellular senescence-inhibited gene and up-regulation of p27. *J Orthop Res.* 2011;29(10):1598-1603. doi: 10.1002/jor.21418 [doi].
28. Harthan LB, McFarland DC, Velleman SG. Changes in proliferation, differentiation, fibroblast growth factor 2 responsiveness and expression of syndecan-4 and glypican-1 with turkey satellite cell age. *Dev Growth Differ.* 2013;55(5):622-634. doi: 10.1111/dgd.12069 [doi].
29. Thompson LV. Age-related muscle dysfunction. *Exp Gerontol.* 2009;44(1-2):106-111. doi: 10.1016/j.exger.2008.05.003 [doi].
30. Miljkovic N, Lim JY, Miljkovic I, Frontera WR. Aging of skeletal muscle fibers. *Ann Rehabil Med.* 2015;39(2):155-162. doi: 10.5535/arm.2015.39.2.155 [doi].
31. Plotnikov EY, Khryapenkova TG, Vasileva AK, et al. Cell-to-cell cross-talk between mesenchymal stem cells and cardiomyocytes in co-culture. *J Cell Mol Med.* 2008;12(5A):1622-1631. doi: JCMM205 [pii].
32. Johnson RW, White JD, Walker EC, Martin TJ, Sims NA. Myokines (muscle-derived cytokines and chemokines) including ciliary neurotrophic factor (CNTF) inhibit osteoblast differentiation. *Bone.* 2014;64:47-56. doi: 10.1016/j.bone.2014.03.053 [doi].
33. Qin Y, Peng Y, Zhao W, et al. Myostatin inhibits osteoblastic differentiation by suppressing osteocyte-derived exosomal microRNA-218: A novel mechanism in muscle-bone communication. *J Biol Chem.* 2017;292(26):11021-11033. doi: 10.1074/jbc.M116.770941 [doi].
34. Schuierer MM, Mann CJ, Bildsoe H, Huxley C, Hughes SM. Analyses of the differentiation potential of satellite cells from myoD^{-/-}, mdx, and PMP22 C22 mice. *BMC Musculoskelet Disord.* 2005;6:15-2474-6-15. doi: 1471-2474-6-15 [pii].
35. O'Connor MS, Carlson ME, Conboy IM. Differentiation rather than aging of muscle stem cells abolishes their telomerase activity. *Biotechnol Prog.* 2009;25(4):1130-1137. doi: 10.1002/btpr.223 [doi].
36. Gabillard JC, Sabin N, Paboeuf G. In vitro characterization of proliferation and differentiation of trout satellite cells. *Cell Tissue Res.* 2010;342(3):471-477. doi: 10.1007/s00441-010-1071-8 [doi].

37. Hanna H, Mir LM, Andre FM. In vitro osteoblastic differentiation of mesenchymal stem cells generates cell layers with distinct properties. *Stem Cell Res Ther.* 2018;9(1):203-018-0942-x. doi: 10.1186/s13287-018-0942-x [doi].
38. Zhang W, Yang N, Shi XM. Regulation of mesenchymal stem cell osteogenic differentiation by glucocorticoid-induced leucine zipper (GILZ). *J Biol Chem.* 2008;283(8):4723-4729. doi: M704147200 [pii].
39. Renaud J, Martinoli MG. Development of an insert co-culture system of two cellular types in the absence of cell-cell contact. *J Vis Exp.* 2016;(113). doi(113):10.3791/54356. doi: 10.3791/54356 [doi].
40. Balasubramanian P, Longo VD. Growth factors, aging and age-related diseases. *Growth Horm IGF Res.* 2016;28:66-68. doi: 10.1016/j.ghir.2016.01.001 [doi].
41. Gong Z, Kennedy O, Sun H, et al. Reductions in serum IGF-1 during aging impair health span. *Aging Cell.* 2014;13(3):408-418. doi: 10.1111/acer.12188 [doi].
42. Junnila RK, List EO, Berryman DE, Murrey JW, Kopchick JJ. The GH/IGF-1 axis in ageing and longevity. *Nat Rev Endocrinol.* 2013;9(6):366-376. doi: 10.1038/nrendo.2013.67 [doi].
43. Curtis E, Litwic A, Cooper C, Dennison E. Determinants of muscle and bone aging. *J Cell Physiol.* 2015;230(11):2618-2625. doi: 10.1002/jcp.25001 [doi].
44. Novotny SA, Warren GL, Hamrick MW. Aging and the muscle-bone relationship. *Physiology (Bethesda).* 2015;30(1):8-16. doi: 10.1152/physiol.00033.2014 [doi].
45. Hamrick MW. The skeletal muscle secretome: An emerging player in muscle-bone crosstalk. *Bonekey Rep.* 2012;1:60. doi: 10.1038/bonekey.2012.60 [doi].
46. Nyman JS, Roy A, Acuna RL, et al. Age-related effect on the concentration of collagen crosslinks in human osteonal and interstitial bone tissue. *Bone.* 2006;39(6):1210-1217. doi: S8756-3282(06)00580-1 [pii].
47. Young MF. Bone matrix proteins: Their function, regulation, and relationship to osteoporosis. *Osteoporos Int.* 2003;14 Suppl 3:S35-42. doi: 10.1007/s00198-002-1342-7 [doi].
48. Gillies AR, Lieber RL. Structure and function of the skeletal muscle extracellular matrix. *Muscle Nerve.* 2011;44(3):318-331. doi: 10.1002/mus.22094 [doi].
49. Lacraz G, Rouleau AJ, Couture V, et al. Increased stiffness in aged skeletal muscle impairs muscle progenitor cell proliferative activity. *PLoS One.* 2015;10(8):e0136217. doi: 10.1371/journal.pone.0136217 [doi].

CHAPTER 6: General Conclusions and Future Directions

6.1. Introduction

The work presented herein demonstrates a novel approach to understanding musculoskeletal changes with age by using a whole tissue-level functional study examining muscle-tendon unit (MTU) mechanics in tandem with a cellular-level study examining bone-muscle crosstalk. Both studies were performed using the same animals, thus enabling a more wholistic look at musculoskeletal aging across multiple length scales than done in previous studies. Of note, however, was that the results from the aging animal studies (Chapters 3 and 5) demonstrated small age-related changes and high variability in both tissue and cellular metrics. The high variability contributed greatly to the inability to detect statistical significance in the studies, yet it suggests that musculoskeletal aging may proceed in a more subject-specific manner.

6.2. Tissue-level functional outcomes

As discussed in Chapters 1-3, a large discrepancy exists in the functional response of MTUs with aging. The data set generated here suggests a conclusion similar to some studies that old MTUs have an increased muscle stiffness and a decreased tendon stiffness. In this particular animal model, these muscle and tendon changes offset each other somewhat, providing a robustness to the system that resisted large changes in MTU function. These experimental results agreed with our modeling results in Chapter 2, as this internal change of stiffness led to a resonant frequency very similar to that of a young system. The model predicted our experimental results of small functional changes when resonant frequencies remain similar. Literature suggests that the resonant frequency of an ankle task can be self-selected in response to changing environments or conditions to “tune” the system.¹ Therefore, when tendons become more compliant, resonant frequency should decrease, and aged individuals would be expected to lower movement frequency to

maintain their tuned condition. However, the increased stiffness of muscle raises the entire stiffness of the MTU to levels more closely matching the young condition. The change in internal stiffnesses alter the force-length characteristics of the MTU, forcing the MTU to undergo smaller operating lengths. These changes in aged MTUs help to explain the shuffled gait patterns of elderly individuals², where unchanged resonant frequencies yet smaller length changes dictate that the individual has to move with smaller, quicker steps to compensate. If other joints are considered, other MTUs may compensate for these ankle-related changes leading to increased work performed at the hip.²

Aging studies often overlook the lifestyle of the individual before and during the aging process. For instance, sedentary lifestyles where MTU activation is minimal demonstrate an increase amount of muscle wasting compared to more active counterparts.^{3,4} Muscle wasting alone can lead to decreased force production due to a loss of cross-sectional area³, but lost muscle tissue may be replaced by fibrous proteins and lead to increased stiffness.^{5,6} These processes can be attenuated by resistive load training and exercise. A study examining plantar flexors demonstrated that strength training over a 3 month duration increases the cross-sectional area by as much as 17%, with improved functional outcomes compared to untrained controls.⁷ The old animals in our study demonstrated a higher variability in body mass and MTU mass compared to the young animals, suggesting that the cage activity of these animals over their lifespans may have contributed more to the stiffness changes of the MTU than aging alone. Other confounding factors that have not been explored here can also alter MTU stiffness and play a role in the function of aged MTUs, such as altered proprioceptive feedback, traumatic injury, and altered MTU geometry. However, awareness of and controlling for these factors in future studies could be paramount to reducing variability in aging experiments.

6.3. Cellular crosstalk outcomes

Our results from Chapter 5 were surprising, in that very few differences were observed between young and old cells from either bone or muscle. Perhaps most interesting was the lack of difference in crosstalk measurements across the study. Our initial hypothesis that IGF-1 signaling would drive collagen deposition and subsequently lead to increased collagen deposition in muscle and decreased in bone was not supported. However, these results may be less surprising when considered along with the small stiffness differences at the tissue level discussed in Chapter 3. Previous studies have shown that signaling pathways are altered differently in aging between the two tissues, leading to increased collagen deposition in aged muscle⁸ and decreased deposition in aged bone⁹. While IGF-1 signaling has a number of downstream targets, one of the most prominent is the production of collagen.¹⁰ IGF-1 is known to decrease in muscle with aging, suggesting that collagen deposition should also decrease, yet studies suggests that this is not the case.¹¹ Perhaps one of the several other potent signaling factors, such as tumor growth factor beta (TGF- β)¹² or the interleukin family¹³, which are increased with age and can induce collagen deposition, are involved. On the other hand, if these other signaling factors can induce collagen deposition with age, then bone should also have increased collagen deposition. However, these observations are not typically observed in aged, since remodeling in aging is generally shifted toward relatively more resorption than formation and thus more collagen degradation.⁹ In summary, while IGF-1 was a good single choice for observing crosstalk changes between muscle and bone, various other potential factors exist that can impact collagen deposition and subsequent stiffness changes in these tissues at the cellular level.

As with the functional muscle data set, the results of the cell culture work were also highly variable, particularly for metrics in the older cells. While large variability is common in cell culture

work,¹⁴ lifestyle differences between individual animals likely also contributed by regulating different signaling mechanisms that greatly reduced the aging phenotype. Studies have shown the importance of simple lifestyle changes and the large downstream effects these can have on regulating genome expression and protein expression.¹⁵ While these animals were in highly controlled environments, we cannot discount the possibility that even small changes in cage activity or nutrition throughout the lifecycle may have contributed to the increased variability in cellular responses with aging.

6.4. Future directions and final thoughts

While the studies herein were novel and provided key insights into the highly variable and seemingly individualistic nature of bone and muscle aging, some key future directions will help us better understand aging effects on the musculoskeletal system. In the tissue function studies, monitoring cage activity by either running wheel use¹⁶ or motion cameras¹⁷ has been a common practice and could provide insight into activity differences that may influence the aging response. In particular, controlling for these individual metrics in tissue functional data may provide better measurements than typical body mass or muscle mass normalizations. Unfortunately, data sets of this type would be both logistically and technically expensive, requiring years of upkeep to monitor the lifecycle of these animals, as well as sophisticated analysis to determine significant differences.

In cell culture studies, the particular co-culture setup used here was novel in that it allowed the individual contributions of each cell type to be isolated, yet reaching full differentiation potential in both cell types proved difficult. Future studies should differentiate each cell type completely before combining them in co-culture to ensure cells have reach a more mature state, which may better reflect *in vivo* conditions. Additionally, while IGF-1 was an interesting target, assessing the potential of various other signaling factors could identify ones that play a role in mediating bone-

muscle crosstalk with aging. The use of recent “-omics” technologies, such as proteomics or metabolomics, would allow for high-throughput data acquisition of entire families of signaling factors that were not examined in the studies herein.¹⁸ Furthermore, while the quantity of collagen I was investigated and was not different among groups, the quality of deposited collagen has not been addressed. Differences in collagen crosslinks or amount of advanced glycation end products (AGEs) could speak to the quality of collagen in each cell culture. Since AGEs accumulate with advancing age, they could be deposited more in the old cell cultures, even though the collagen amount was not different.

Finally, while one novel aspect of this study was that all data were acquired from the same set of animals, the opportunity to better bridge the tissue- and cell-level studies cannot be avoided. Histology on the tissue itself could provide a snapshot of the amount of collagen in the tissue *in vivo*, which may be different than the amount that is deposited by cells *in vitro*. While this technique would not assess the potential “rescuing” effect addressed by the young/old co-culture design, these results could help better link functional outcomes from the cell and tissue studies.

Additional study designs could also be used to build off the studies herein that were not addressed (i.e., pharmacological intervention, parabiosis studies, etc.), which could provide insight into the mechanisms underlying the stiffness changes observed between young and old animals. Nevertheless, by highlighting the relationships between tissue and cell structural changes, this work provides a framework for more cross-disciplinary studies that may lead to designs of new clinical interventions. While some of these technologies may exist for humans (e.g., ankle-foot orthoses or exoskeletons to alter stiffness, pharmacological agents to assist collagen deposition or reabsorption), whether these technologies can help mitigate age-related pathologies remains to be seen.

6.5. References

1. Raburn CE, Merritt KJ, Dean JC. Preferred movement patterns during a simple bouncing task. *J Exp Biol.* 2011;214(Pt 22):3768-3774. doi: 10.1242/jeb.058743 [doi].
2. DeVita P, Hortobagyi T. Age causes a redistribution of joint torques and powers during gait. *J Appl Physiol (1985).* 2000;88(5):1804-1811.
3. Narici MV, Maganaris CN. Adaptability of elderly human muscles and tendons to increased loading. *J Anat.* 2006;208(4):433-443. doi: JOA548 [pii].
4. Narici MV, Maffulli N, Maganaris CN. Ageing of human muscles and tendons. *Disabil Rehabil.* 2008;30(20-22):1548-1554. doi: 10.1080/09638280701831058 [doi].
5. Brack AS, Conboy MJ, Roy S, et al. Increased wnt signaling during aging alters muscle stem cell fate and increases fibrosis. *Science.* 2007;317(5839):807-810. doi: 317/5839/807 [pii].
6. Lacraz G, Rouleau AJ, Couture V, et al. Increased stiffness in aged skeletal muscle impairs muscle progenitor cell proliferative activity. *PLoS One.* 2015;10(8):e0136217. doi: 10.1371/journal.pone.0136217 [doi].
7. Ferri A, Scaglioni G, Pousson M, Capodaglio P, Van Hoecke J, Narici MV. Strength and power changes of the human plantar flexors and knee extensors in response to resistance training in old age. *Acta Physiol Scand.* 2003;177(1):69-78. doi: 1050 [pii].
8. Goldspink G, Fernandes K, Williams PE, Wells DJ. Age-related changes in collagen gene expression in the muscles of mdx dystrophic and normal mice. *Neuromuscul Disord.* 1994;4(3):183-191.
9. Boskey AL, Coleman R. Aging and bone. *J Dent Res.* 2010;89(12):1333-1348. doi: 10.1177/0022034510377791 [doi].
10. Blackstock CD, Higashi Y, Sukhanov S, et al. Insulin-like growth factor-1 increases synthesis of collagen type I via induction of the mRNA-binding protein LARP6 expression and binding to the 5' stem-loop of COL1a1 and COL1a2 mRNA. *J Biol Chem.* 2014;289(11):7264-7274. doi: 10.1074/jbc.M113.518951 [doi].
11. Miljkovic N, Lim JY, Miljkovic I, Frontera WR. Aging of skeletal muscle fibers. *Ann Rehabil Med.* 2015;39(2):155-162. doi: 10.5535/arm.2015.39.2.155 [doi].
12. Mendias CL, Gumucio JP, Davis ME, Bromley CW, Davis CS, Brooks SV. Transforming growth factor-beta induces skeletal muscle atrophy and fibrosis through the induction of atrogen-1 and scleraxis. *Muscle Nerve.* 2012;45(1):55-59. doi: 10.1002/mus.22232 [doi].

13. Wynn TA. Cellular and molecular mechanisms of fibrosis. *J Pathol.* 2008;214(2):199-210. doi: 10.1002/path.2277 [doi].
14. Mannello F, Tonti GA. Concise review: No breakthroughs for human mesenchymal and embryonic stem cell culture: Conditioned medium, feeder layer, or feeder-free; medium with fetal calf serum, human serum, or enriched plasma; serum-free, serum replacement nonconditioned medium, or ad hoc formula? all that glitters is not gold! *Stem Cells.* 2007;25(7):1603-1609. doi: 2007-0127 [pii].
15. Alegria-Torres JA, Baccarelli A, Bollati V. Epigenetics and lifestyle. *Epigenomics.* 2011;3(3):267-277. doi: 10.2217/epi.11.22 [doi].
16. Novak CM, Burghardt PR, Levine JA. The use of a running wheel to measure activity in rodents: Relationship to energy balance, general activity, and reward. *Neurosci Biobehav Rev.* 2012;36(3):1001-1014. doi: 10.1016/j.neubiorev.2011.12.012 [doi].
17. Redfern WS, Tse K, Grant C, et al. Automated recording of home cage activity and temperature of individual rats housed in social groups: The rodent big brother project. *PLoS One.* 2017;12(9):e0181068. doi: 10.1371/journal.pone.0181068 [doi].
18. Griffin TJ, Seth G, Xie H, Bandhakavi S, Hu WS. Advancing mammalian cell culture engineering using genome-scale technologies. *Trends Biotechnol.* 2007;25(9):401-408. doi: S0167-7799(07)00184-9 [pii].